



Global sea-level budget 1993–present

WCRP Global Sea Level Budget Group

A full list of authors and their affiliations appears at the end of the paper.

Correspondence: Anny Cazenave (anny.cazenave@legos.obs-mip.fr)

Received: 13 April 2018 – Discussion started: 15 May 2018

Revised: 31 July 2018 – Accepted: 1 August 2018 – Published: 28 August 2018

Abstract. Global mean sea level is an integral of changes occurring in the climate system in response to unforced climate variability as well as natural and anthropogenic forcing factors. Its temporal evolution allows changes (e.g., acceleration) to be detected in one or more components. Study of the sea-level budget provides constraints on missing or poorly known contributions, such as the unsurveyed deep ocean or the still uncertain land water component. In the context of the World Climate Research Programme Grand Challenge entitled “Regional Sea Level and Coastal Impacts”, an international effort involving the sea-level community worldwide has been recently initiated with the objective of assessing the various datasets used to estimate components of the sea-level budget during the altimetry era (1993 to present). These datasets are based on the combination of a broad range of space-based and in situ observations, model estimates, and algorithms. Evaluating their quality, quantifying uncertainties and identifying sources of discrepancies between component estimates is extremely useful for various applications in climate research. This effort involves several tens of scientists from about 50 research teams/institutions worldwide (www.wcrp-climate.org/grand-challenges/gc-sea-level, last access: 22 August 2018). The results presented in this paper are a synthesis of the first assessment performed during 2017–2018. We present estimates of the altimetry-based global mean sea level (average rate of $3.1 \pm 0.3 \text{ mm yr}^{-1}$ and acceleration of 0.1 mm yr^{-2} over 1993–present), as well as of the different components of the sea-level budget (<http://doi.org/10.17882/54854>, last access: 22 August 2018). We further examine closure of the sea-level budget, comparing the observed global mean sea level with the sum of components. Ocean thermal expansion, glaciers, Greenland and Antarctica contribute 42 %, 21 %, 15 % and 8 % to the global mean sea level over the 1993–present period. We also study the sea-level budget over 2005–present, using GRACE-based ocean mass estimates instead of the sum of individual mass components. Our results demonstrate that the global mean sea level can be closed to within 0.3 mm yr^{-1} (1σ). Substantial uncertainty remains for the land water storage component, as shown when examining individual mass contributions to sea level.

1 Introduction

Global warming has already several visible consequences, in particular an increase in the Earth’s mean surface temperature and ocean heat content (Rhein et al., 2013; IPCC, 2013), melting of sea ice, loss of mass of glaciers (Gardner et al., 2013), and ice mass loss from the Greenland and Antarctica ice sheets (Rignot et al., 2011a; Shepherd et al., 2012). On average over the last 50 years, about 93 % of heat excess accumulated in the climate system because of greenhouse gas emissions has been stored in the ocean, and the remaining 7 % has been warming the atmosphere and con-

tinents, and melting sea and land ice (von Schuckmann et al., 2016). Because of ocean warming and land ice mass loss, sea level rises. Since the end of the last deglaciation about 3000 years ago, sea level remained nearly constant (e.g., Lambeck, 2002; Lambeck et al., 2010; Kemp et al., 2011). However, direct observations from in situ tide gauges available since the mid-to-late 19th century show that the 20th century global mean sea level has started to rise again at a rate of 1.2 to 1.9 mm yr^{-1} (Church and White, 2011; Jevrejeva et al., 2014; Hay et al., 2015; Dangendorf et al., 2017). Since the early 1990s sea-level rise (SLR) is measured by high-precision altimeter satellites and the rate has

increased to $\sim 3 \text{ mm yr}^{-1}$ on average (Legeais et al., 2018; Nerem et al., 2018).

Accurate assessment of present-day global mean sea-level variations and its components (ocean thermal expansion, ice sheet mass loss, glaciers mass change, changes in land water storage, etc.) is important for many reasons. The global mean sea level is an integral of changes occurring in the Earth's climate system in response to unforced climate variability as well as natural and anthropogenic forcing factors, e.g., net contribution of ocean warming, land ice mass loss and changes in water storage in continental river basins. Temporal changes in the components are directly reflected in the global mean sea-level curve. If accurate enough, study of the sea-level budget provides constraints on missing or poorly known contributions, e.g., the deep ocean undersampled by current observing systems, or still uncertain changes in water storage on land due to human activities (e.g., groundwater depletion in aquifers). Global mean sea level corrected for ocean mass change in principle allows one to independently estimate temporal changes in total ocean heat content, from which the Earth's energy imbalance can be deduced (von Schuckmann et al., 2016). The sea level and/or ocean mass budget approach can also be used to constrain models of glacial isostatic adjustment (GIA). The GIA phenomenon has a significant impact on the interpretation of GRACE-based space gravimetry data over the oceans (for ocean mass change) and over Antarctica (for ice sheet mass balance). However, there is still no complete consensus on best estimates, a result of uncertainties in deglaciation models and mantle viscosity structure. Finally, observed changes in the global mean sea level and its components are fundamental for validating climate models used for projections.

In the context of the Grand Challenge entitled “Regional Sea Level and Coastal Impacts” of the World Climate Research Programme (WCRP), an international effort involving the sea-level community worldwide has been recently initiated with the objective of assessing the sea-level budget during the altimetry era (1993 to present). To estimate the different components of the sea-level budget, different datasets are used. These are based on the combination of a broad range of space-based and in situ observations. Evaluating their quality, quantifying their uncertainties and identifying the sources of discrepancies between component estimates, including the altimetry-based sea-level time series, are extremely useful for various applications in climate research.

Several previous studies have addressed the sea-level budget over different time spans and using different datasets. For example, Munk (2002) found that the 20th century sea-level rise could not be closed with the data available at that time and showed that if the missing contribution were due to polar ice melt, this would be in conflict with external astronomical constraints. The enigma has been resolved in two ways. Firstly, an improved theory of rotational stability of the Earth (Mitrovica et al., 2006) effectively removed the constraints proposed by Munk (2002) and allows a polar ice

sheet contribution to 20th century sea-level rise of as much as $\sim 1.1 \text{ mm yr}^{-1}$, with about 0.8 mm yr^{-1} beginning in the 20th century. In addition, more recent studies by Gregory et al. (2013) and Slangen et al. (2017), combining observations with model estimates, showed that it was possible to effectively close the 20th century sea-level budget within uncertainties, particularly over the altimetry era (e.g., Cazenave et al., 2009; Leuliette and Willis, 2011; Church and White, 2011; Llovel et al., 2014; Chambers et al., 2017; Dieng et al., 2017; X. Chen et al., 2017; Nerem et al., 2018). Assessments of the published literature have also been performed in past IPCC (Intergovernmental Panel on Climate Change) reports (e.g., Church et al., 2013). Building on these previous works, here we intend to provide a collective update of the global mean sea-level budget, involving the many groups worldwide interested in present-day sea-level rise and its components. We focus on observations rather than model-based estimates and consider the high-precision altimetry era starting in 1993. This era includes the period since the mid-2000s in which new observing systems, like the Argo float project (Roemmich et al., 2012) and the GRACE space gravimetry mission (Tapley et al., 2004a, b), provide improved datasets of high value for such a study. Only the global mean budget is considered here. Regional budget will be the focus of a future assessment.

Section 2 describes for each component of the sea-level budget equation the different datasets used to estimate the corresponding contribution to sea level, discusses associated errors and provides trend estimates for the two periods. Section 3 addresses the mass and sea-level budgets over the study periods. A discussion is provided in Sect. 4, followed by a conclusion.

2 Methods and data

In this section, we briefly present the global mean sea-level budget (Sect. 2.1) and then provide, for each term of the budget equation, an assessment of the most up-to-date published results. Multiple organizations and research groups routinely generate the basic measurements as well as the derived datasets and products used to study the sea-level budget. Sections 2.2 to 2.7 summarize the measurements and methodologies used to derive observed sea level, as well as steric and mass components. In most cases, we focus on observations but in some instances (e.g., for GIA corrections applied to the data), model-based estimates are the only available information.

2.1 Sea-level budget equation

Global mean sea level (GMSL) change as a function of time t is usually expressed by the sea-level budget equation:

$$\text{GMSL}(t) = \text{GMSL}(t)_{\text{steric}} + \text{GMSL}(t)_{\text{ocean mass}}, \quad (1)$$

where $\text{GMSL}(t)_{\text{steric}}$ refers to the contributions of ocean thermal expansion and salinity to sea-level change, and $\text{GMSL}(t)_{\text{ocean mass}}$ refers to the change in mass of the oceans. Due to water conservation in the climate system, the ocean mass term (also noted as $M(t)_{\text{ocean}}$) can further be expressed as follows:

$$\begin{aligned} M(t)_{\text{ocean}} + M(t)_{\text{glaciers}} + M(t)_{\text{Greenland}} + M(t)_{\text{Antarctica}} \\ + M(t)_{\text{TWS}} + M(t)_{\text{WV}} + M(t)_{\text{Snow}} \\ + \text{uncertainty} = 0, \end{aligned} \quad (2)$$

where $M(t)_{\text{glaciers}}$, $M(t)_{\text{Greenland}}$, $M(t)_{\text{Antarctica}}$, $M(t)_{\text{TWS}}$, $M(t)_{\text{WV}}$ and $M(t)_{\text{Snow}}$ represent temporal changes in mass of glaciers, Greenland and Antarctica ice sheets, terrestrial water storage (TWS), atmospheric water vapor (WV), and snow mass changes. The uncertainty is a result of uncertainties in all of the estimates. For the altimetry era, many studies have investigated closure of the sea-level budget and potentially missing mass terms, for example, permafrost melting.

From Eq. (2), we deduce the following:

$$\begin{aligned} \text{GMSL}(t)_{\text{ocean mass}} = -[M(t)_{\text{glaciers}} + M(t)_{\text{Greenland}} \\ + M(t)_{\text{Antarctica}} + M(t)_{\text{TWS}} + M(t)_{\text{WV}} + M(t)_{\text{Snow}} \\ + \text{missing mass terms}] \end{aligned} \quad (3)$$

In the next subsections, we successively discuss the different terms of the budget (Eqs. 1 and 2) and how they are estimated from observations. We do not consider the atmospheric water vapor and snow components, assumed to be small. Two periods are considered: (1) 1993–present (i.e., the entire altimetry era) and (2) 2005–present (i.e., the period covered by both Argo and GRACE).

2.2 Altimetry-based global mean sea level over 1993–present

The launch of the TOPEX/Poseidon (T/P) altimeter satellite in 1992 led to a new paradigm for measuring sea level from space, providing for the first time precise and globally distributed sea-level measurements at 10-day intervals. At the time of the launch of T/P, the measurements were not expected to have sufficient accuracy for measuring GMSL changes. However, as the radial orbit error decreased from ~ 10 cm at launch to ~ 1 cm presently, and other instrumental and geophysical corrections applied to altimetry system improved (e.g., Stammer and Cazenave, 2018), several groups regularly provided an altimetry-based GMSL time series (e.g., Nerem et al., 2010; Church et al., 2011; Ablain et al., 2015; Legeais et al., 2018). The initial T/P GMSL time

series was extended with the launch of Jason-1 (2001), Jason-2 (2008) and Jason-3 (2016). By design, each of these missions has an overlap period with the previous one in order to intercompare the sea-level measurements and estimate instrument biases (e.g., Nerem et al., 2010; Ablain et al., 2015). This has allowed the construction of an uninterrupted GMSL time series that is currently 25 years long.

2.2.1 Global mean sea-level datasets

Six groups (AVISO/CNES, SL_cci/ESA, University of Colorado, CSIRO, NASA/GSFC, NOAA) provide altimetry-based GMSL time series. All of them use 1 Hz altimetry measurements derived from T/P, Jason-1, Jason-2 and Jason-3 as reference missions. These missions provide the most accurate long-term stability at global and regional scales (Ablain et al., 2009, 2017a), and are all on the same historical T/P ground track. This allows computation of a long-term record of the GMSL from 1993 to present. In addition, complementary missions (ERS-1, ERS-2, Envisat, Geosat Follow-on, CryoSat-2, SARAL/AltiKa and Sentinel-3A) provide increased spatial resolution and coverage of high-latitude ocean areas, pole-ward of 66° N–S latitude (e.g., the European Space Agency/ESA Climate Change Initiative/CCI sea-level dataset; Legeais et al., 2018).

The above groups adopt different approaches when processing satellite altimetry data. The most important differences concern the geophysical corrections needed to account for various physical phenomena such as atmospheric propagation delays, sea state bias, ocean tides, and the ocean response to atmospheric wind and pressure forcing. Other differences come from data editing, methods to spatially average individual measurements during orbital cycles and links between successive missions (Masters et al., 2012; Henry et al., 2014).

Overall, the quality of the different GMSL time series is similar. Long-term trends agree well to within 6% of the signal, approximately 0.2 mm yr^{-1} (see Fig. 1) within the GMSL trend uncertainty range ($\sim 0.3 \text{ mm yr}^{-1}$; see next section). The largest differences are observed at interannual timescales and during the first years (before 1999; see below). Here we use an ensemble mean GMSL based on averaging all individual GMSL time series.

2.2.2 Global mean sea-level uncertainties and TOPEX-A drift

Based on an assessment of all sources or uncertainties affecting satellite altimetry (Ablain et al., 2017a), the GMSL trend uncertainty (90% confidence interval) is estimated as 0.3 to 0.4 mm yr^{-1} over the whole altimetry era (1993–2017). The main contribution to the uncertainty is the wet tropospheric correction with a drift uncertainty in the range of 0.2 – 0.3 mm yr^{-1} (Legeais et al., 2018) over a 10-year period. To a lesser extent, the orbit error (Couhert et al., 2015; Escudier

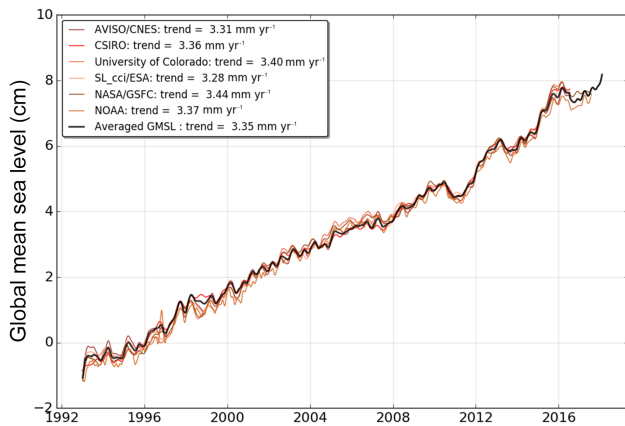


Figure 1. Evolution of GMSL time series from six different groups' (AVISO/CNES, SL_cci/ESA, University of Colorado, CSIRO, NASA/GSFC, NOAA) products. Annual signals are removed and 6-month smoothing applied. All GMSL time series are centered in 1993 with zero mean. A GIA correction of -0.3 mm yr^{-1} has been subtracted from each dataset.

et al., 2018) and the altimeter parameters' (range, σ_0 and significant wave height – SWH) instability (Ablain et al., 2012) also contribute to the GMSL trend uncertainty, at the level of 0.1 mm yr^{-1} . Furthermore, imperfect links between successive altimetry missions lead to another trend uncertainty of about 0.15 mm yr^{-1} over the 1993–2017 period (Zawadzki and Ablain, 2016).

Uncertainties are higher during the first decade (1993–2002), when T/P measurements display larger errors at climatic scales. For instance, the orbit solutions are much more uncertain due to gravity field solutions calculated without GRACE data. Furthermore, the switch from TOPEX-A to TOPEX-B in February 1999 (with no overlap between the two instrumental observations) leads to an error of $\sim 3 \text{ mm}$ in the GMSL time series (Escudier et al., 2018).

However, the most significant error that affects the first 6 years (January 1993 to February 1999) of the T/P GMSL measurements is due to an instrumental drift of the TOPEX-A altimeter, not included in the formal uncertainty estimates discussed above. This effect on the GMSL time series was recently highlighted via comparisons with tide gauges (Valadeau et al., 2012; Watson et al., 2015; X. Chen et al., 2017; Ablain et al., 2017b), via a sea-level budget approach (i.e., comparison with the sum of mass and steric components; Dieng et al., 2017) and by comparing with Poseidon-1 measurements (Lionel Zawadzki, personal communication, 2017). In a recent study, Beckley et al. (2017) asserted that the corresponding error on the 1993–1998 GMSL resulted from incorrect onboard calibration parameters.

All approaches conclude that during the period January 1993 to February 1999, the altimetry-based GMSL was overestimated. TOPEX-A drift correction was estimated to be close to 1.5 mm yr^{-1} (in terms of sea-level trend) with an

uncertainty of ± 0.5 to $\pm 1.0 \text{ mm yr}^{-1}$ (Watson et al., 2015; X. Chen et al., 2017; Dieng et al., 2017). Beckley et al. (2017) proposed to not apply the suspect onboard calibration correction on TOPEX-A measurements. The impact of this approach is similar to the TOPEX-A drift correction estimated by Dieng et al. (2017) and Ablain et al. (2017b). In the latter study, accurate comparison between TOPEX-A-based GMSL and tide gauge measurements leads to a drift correction of about -1.0 mm yr^{-1} between January 1993 and July 1995, and $+3.0 \text{ mm yr}^{-1}$ between August 1995 and February 1999, with an uncertainty of 1.0 mm yr^{-1} (with a 68 % confidence level, see Table 1).

2.2.3 Global mean sea-level variations

The ensemble mean GMSL rate after correcting for the TOPEX-A drift (for all of the proposed corrections) amounts to 3.1 mm yr^{-1} over 1993–2017 (Fig. 2). This corresponds to a mean sea-level rise of about 7.5 cm over the whole altimetry period. More importantly, the GMSL curve shows a net acceleration, estimated to be at 0.08 mm yr^{-2} (X. Chen et al., 2017; Dieng et al., 2017) and $0.084 \pm 0.025 \text{ mm yr}^{-2}$ (Nerem et al., 2018) (note Watson et al., 2015 found a smaller acceleration after correcting for the instrumental bias over a shorter period up to the end of 2014.). GMSL trends calculated over 10-year moving windows illustrate this acceleration (Fig. 3). GMSL trends are close to 2.5 mm yr^{-1} over 1993–2002 and 3.0 mm yr^{-1} over 1996–2005. After a slightly smaller trend over 2002–2011, the 2008–2017 trend reaches 4.2 mm yr^{-1} . Uncertainties (90 % confidence interval) associated with these 10-year trends regularly decrease through time from 1.3 mm yr^{-1} over 1993–2002 (corresponding to T/P data) to 0.65 mm yr^{-1} for 2008–2017 (corresponding to Jason-2 and Jason-3 data).

Removing the trend from the GMSL time series highlights interannual variations (not shown). Their magnitudes depend on the period ($+3 \text{ mm}$ in 1998–1999, -5 mm in 2011–2012 and $+10 \text{ mm}$ in 2015–2016) and are well correlated in time with El Niño and La Niña events (Nerem et al., 2010, 2018; Cazenave et al., 2014). However, substantial differences (of 1–3 mm) exist between the six detrended GMSL time series. This issue needs further investigation.

For the sea-level budget assessment (Sect. 3), we will use the ensemble mean GMSL time series corrected for the TOPEX-A drift using the Ablain et al. (2017b) correction.

2.2.4 Comparison with tide gauges

Prior to 1992, global sea-level rise estimates relied on the tide gauge measurements, and it is worth mentioning past attempts to produce global sea-level reconstructions utilizing these measurements (e.g., Gornitz et al., 1982; Barnett, 1984; Douglas, 1991, 1997, 2001). Here we focus on global sea-level reconstructions that overlap with satellite altimetry data over a substantial common time span. Some of

Table 1. TOPEX-A GMSL drift corrections proposed by different studies.

TOPEX-A drift correction	to be subtracted from the first 6 years (Jan 1993 to Feb 1999) of the uncorrected GMSL record
Watson et al. (2015)	$1.5 \pm 0.5 \text{ mm yr}^{-1}$ over Jan 1993–Feb 1999
X. Chen et al. (2017), Dieng et al. (2017)	$1.5 \pm 0.5 \text{ mm yr}^{-1}$ over Jan 1993–Feb 1999
Beckley et al. (2017)	No onboard calibration applied
Ablain et al. (2017b)	$-1.0 \pm 1.0 \text{ mm yr}^{-1}$ over Jan 1993–Jul 1995 $+3.0 \pm 1.0 \text{ mm yr}^{-1}$ over Aug 1995–Feb 1999

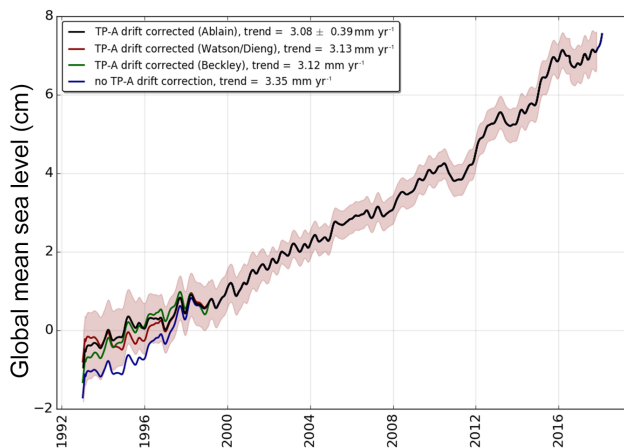


Figure 2. Evolution of ensemble mean GMSL time series (average of the six GMSL products from AVISO/CNES, SL_cci/ESA, University of Colorado, CSIRO, NASA/GSFC and NOAA). On the black, red and green curves, the TOPEX-A drift correction is applied respectively based on Ablain et al. (2017b), Watson et al. (2015) and Dieng et al. (2017), and Beckley et al. (2017). Annual signal removed and 6-month smoothing applied; GIA correction also applied. Uncertainties (90% confidence interval) of correlated errors over a 1-year period are superimposed for each individual measurement (shaded area).

these reconstructions rely on tide gauge data only (Jevrejeva et al., 2006, 2014; Merrifield et al., 2009; Wenzel and Schroter, 2010; Ray and Douglas, 2011; Hamlington et al., 2011; Spada and Galassi, 2012; Thompson and Merrifield, 2014; Dangendorf et al., 2017; Frederikse et al., 2017). In addition, there are reconstructions that jointly use satellite altimetry, tide gauge records (Church and White, 2006, 2011) and reconstructions, which combine tide gauge records with ocean models (Meyssignac et al., 2011) or physics-based and model-derived geometries of the contributing processes (Hay et al., 2015).

For the period since 1993, with most of the world coastlines densely sampled, the rates of sea-level rise from all tide-gauge-based reconstructions and estimates from satellite altimetry agree within their specific uncertainties,

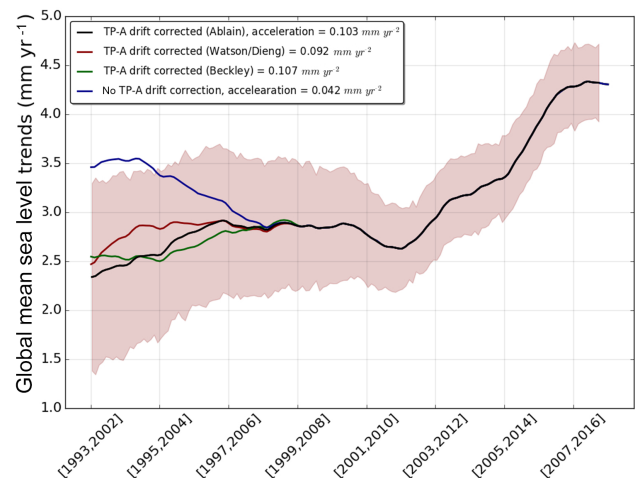


Figure 3. Ensemble mean GMSL trends calculated over 10-year moving windows. On the black, red and green curves, the TOPEX-A drift correction is applied respectively based on Ablain et al. (2017b), Watson et al. (2015) and Dieng et al. (2017), and Beckley et al. (2017). Uncorrected GMSL trends are shown by the blue curve. The shaded area represents trend uncertainty over 10-year periods (90% confidence interval).

e.g., rates of $3.0 \pm 0.7 \text{ mm yr}^{-1}$ (Hay et al. 2015), $2.8 \pm 0.5 \text{ mm yr}^{-1}$ (Church and White, 2011; Rhein et al., 2013), $3.1 \pm 0.6 \text{ mm yr}^{-1}$ (Jevrejeva et al., 2014), $3.1 \pm 1.4 \text{ mm yr}^{-1}$ (Dangendorf et al., 2017) and the estimate from satellite altimetry $3.2 \pm 0.4 \text{ mm yr}^{-1}$ (Nerem et al., 2010; Rhein et al., 2013). However, classical tide-gauge-based reconstructions still tend to overestimate the interannual to decadal variability of global mean sea level (e.g., Calafat et al., 2014; Dangendorf et al., 2015; Natarov et al., 2017) compared to global mean sea level from satellite altimetry, due to limited and uneven spatial sampling of the global ocean afforded by the tide gauge network. Sea-level rise being non uniform, spatial variability of sea-level measured at tide gauges is evidenced by 2-D reconstruction methods. The most widely used approach is the use of empirical orthogonal functions (EOFs) calibrated with the satellite altimetry data (e.g., Church and

White, 2006). Alternatively, Choblet et al. (2014) implemented a Bayesian inference method based on a Voronoi tessellation of the Earth's surface to reconstruct sea level during the 20th century. Considerable uncertainties remain, however, in long-term assessments due to poorly sampled ocean basins such as the South Atlantic, or regions which are significantly influenced by open-ocean circulation (e.g., subtropical North Atlantic) (Frederikse et al., 2017). Uncertainties involved in specifying vertical land motion corrections at tide gauges also impact tide gauge reconstructions (Jevrejeva et al., 2014; Wöppelmann and Marcos, 2016; Hamlington et al., 2016). Frederikse et al. (2017) also recently demonstrated that both global mean sea level reconstructed from tide gauges and the sum of steric and mass contributors show a good agreement with altimetry estimates for the overlapping period 1993–2014.

2.3 Steric sea level

Steric sea-level variations result from temperature- (T) and salinity- (S) related density changes in sea water associated with volume expansion and contraction. These are referred to as thermosteric and halosteric components. Despite clear detection of regional salinity changes and the dominance of the salinity effect on density changes at high latitudes (Rhein et al., 2013), the halosteric contribution to present-day global mean steric sea-level rise is negligible, as the ocean's total salt content is essentially constant over multidecadal timescales (Gregory and Lowe, 2000). Hence, in this study, we essentially consider the thermosteric sea-level component.

Averaged over the 20th century, ocean thermal expansion associated with ocean warming has been the largest contribution to global mean sea-level rise (Church et al., 2013). This remains true for the altimetry period starting in the year 1993 (e.g., X. Chen et al., 2017; Dieng et al., 2017; Nerem et al., 2018). But total land ice mass loss (from glaciers, Greenland and Antarctica) during this period now dominates the sea-level budget (see Sect. 3).

Until the mid-2000s, the majority of ocean temperature data were retrieved from shipboard measurements. These include vertical temperature profiles along research cruise tracks from the surface sometimes all the way down to the bottom layer (e.g., Purkey and Johnson, 2010) and upper-ocean broad-scale measurements from ships of opportunity (Abraham et al., 2013). These upper-ocean in situ temperature measurements, however, are limited to the upper 700 m depth due to common use of expandable bathythermographs (XBTs). Although the coverage has been improved through time, large regions characterized by difficult meteorological conditions remained under-sampled, in particular the southern hemispheric oceans and the Arctic area.

2.3.1 Thermosteric datasets

Over the altimetry era, several research groups have produced gridded time series of temperature data for different depth levels, based on XBTs (with additional data from mechanical bathythermographs – MBTs – and conductivity–temperature–depth – CTD – devices and moorings) and Argo float measurements. The temperature data have further been used to provide thermosteric sea-level products. These differ because of different strategies adopted for data editing, temporal and spatial data gaps filling, mapping methods, baseline climatology, and instrument bias corrections (in particular the time-to-depth correction for XBT data, Boyer et al., 2016).

The global ocean in situ observing system has been dramatically improved through the implementation of the international Argo program of autonomous floats, delivering a unique insight into the interior ocean from the surface down to 2000 m depth of the ice-free global ocean (Roemmich et al., 2012; Riser et al., 2016). More than 80 % of initially planned full deployment of Argo float program was achieved during the year 2005, with quasi global coverage of the ice-free ocean by the start of 2006. At present, more than 3800 floats provide systematic T and S data, with quasi (60° S–60° N latitude) global coverage down to 2000 m depth. A full overview on in situ ocean temperature measurements is given for example in Abraham et al. (2013).

In this section, we consider a set of 11 direct (in situ) estimates, publicly available over the entire altimetry era, to review global mean thermosteric sea-level rise and, ultimately, to construct an ensemble mean time series. These datasets are as follows:

1. CORA = Coriolis Ocean database for ReAnalysis, Copernicus Service, France (marine.copernicus.eu/), product name: INSITU_GLO_TS_OA_REP_OBSERVATIONS_013_002_b;
2. CSIRO (RSOI) = Commonwealth Scientific and Industrial Research Organisation/Reduced-Space Optimal Interpolation, Australia;
3. ACECRC/IMAS-UTAS = Antarctic Climate and Ecosystem Cooperative Research Centre/Institute for Marine and Antarctic Studies-University of Tasmania, Australia (http://www.cmar.csiro.au/sealevel/thermal_expansion_ocean_heat_timeseries.html);
4. ICCES = International Center for Climate and Environment Sciences, Institute of Atmospheric Physics, China (<http://ddl.escience.cn/f/PKFR>);
5. ICDC = Integrated Climate Data Center, University of Hamburg, Germany;
6. IPRC = International Pacific Research Center, University of Hawaii, USA (<http://apdrc.soest.hawaii>).

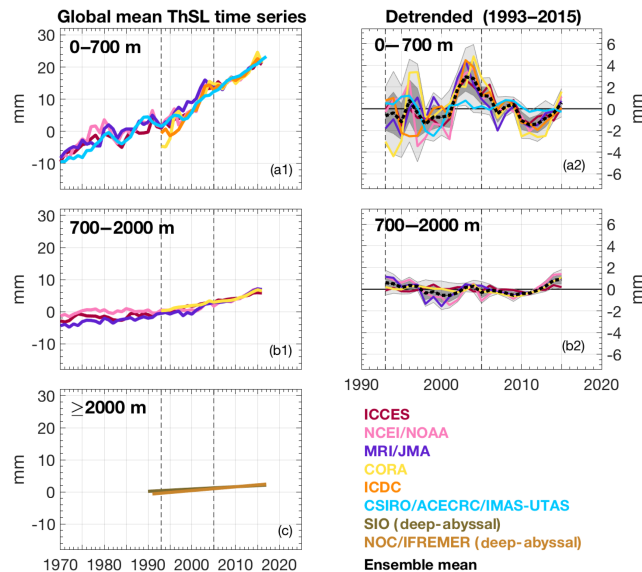


Figure 4. Left panels: annual mean global mean thermosteric anomaly time series since 1970, from various research groups (color) and for three depth integrations: 0–700 m (top), 700–2000 m (middle) and below 2000 m (bottom). Vertical dashed lines are plotted along 1993 and 2005. For comparison, all time series were offset arbitrarily. Right panels: respective linearly detrended time series for 1993–2015. Black bold dashed line is the ensemble mean and gray shadow bar the ensemble spread (1 standard deviation). Units are millimeters.

edu/projects/Argo/data/gridded/On_standard_levels/index-1.html;

7. JAMSTEC = Japan Agency for Marine-Earth Science and Technology, Japan (ftp://ftp2.jamstec.go.jp/pub/argo/MOAA_GPV/Glb_PRS/OI/);
8. MRI/JMA = Meteorological Research Institute/Japan Meteorological Agency, Japan ([https://climate.mri-jma.go.jp/~ishii.wcrp/](https://climate.mri-jma.go.jp/~ishii/wcrp/));
9. NCEI/NOAA = National Centers for Environmental Information/National Oceanic and Atmospheric Administration, USA;
10. SIO = Scripps Institution of Oceanography, USA; Deep-abysal: <https://cchdo.ucsd.edu/>;
11. SIO = Scripps Institution of Oceanography, USA; Deep-abysal: <https://cchdo.ucsd.edu/> (for the abyssal ocean).

Their characteristics are presented in Table 2.

2.3.2 Individual estimates

All in situ estimates compiled in this study show a steady rise in global mean thermosteric sea level, independent of depth integration and decadal or multidecadal periods (Figs. 4 and

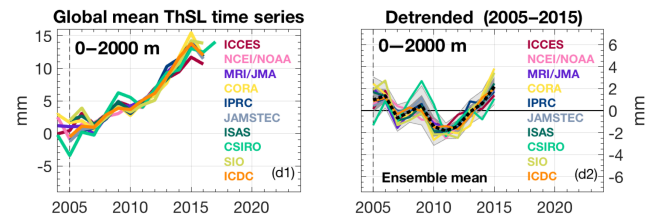


Figure 5. Left panel: annual mean global mean thermosteric anomaly time series since 2004, from various research groups (color) in the upper 2000 m. A vertical dashed line is plotted along 2005. For comparison, all time series were offset arbitrarily. Right panel: respective linearly detrended time series for 2005–2015. Black bold dashed line is the ensemble mean and gray shadow bar the ensemble spread (1 standard deviation). Units are millimeters.

5, left panels). As the deep-abysal ocean estimate only illustrates the updated version of the linear trend from Purkey and Johnson (2010) for 1990–2010 extrapolated to 2016, it does not have any variability superimposed.

Interannual to decadal variability during the altimeter era (since 1993) is similar for both 0–700 and 700–2000 m, with larger amplitude in the upper ocean (Figs. 4 and 5, right panels). For the 0–700 m, there is an apparent change in amplitude before and after the Argo era (since 2005), mostly due to a maximum (2–4 mm) around 2001–2004, except for one estimate. Higher amplitude and larger spread in variability between estimates before the Argo era is a symptom of the much sparser in situ coverage of the global ocean. Interannual variability over the Argo era (Figs. 4 and 5, right panels) is mainly modulated by El Niño–Southern Oscillation (ENSO) phases in the upper 500 m of the ocean, particularly for the Pacific, the largest ocean basin (Roemmich and Gilson, 2011; Roemmich et al., 2016; Johnson and Birnbaum, 2017).

In terms of depth contribution, on average, the upper 300 m explains the same percentage (almost 70 %) of the 0–700 m linear rate over both altimetry and Argo eras, but the contribution from the 0–700 to 0–2000 m varies: about 75 % for 1993–2016 and 65 % for 2005–2016. Thus, the 700–2000 m contribution increases by 10 % during the Argo decade, when the number of observations within 700–2000 m has significantly increased.

2.3.3 Ensemble mean thermosteric sea level

Given that the global mean thermosteric sea-level anomaly estimates compiled for this study are not necessarily referenced to the same baseline climatology, they cannot be directly averaged together to create an ensemble mean. To circumvent this limitation, we created an ensemble mean in three steps, as explained below.

Firstly, we detrended the individual time series by removing a linear trend for 1993–2016 and averaged together to obtain an “ensemble mean variability time series”. Sec-

Table 2. Compilation of available in situ datasets from different originators and/or contributors. The table indicates the time span covered by the data, the depth of integration, as well as the temporal resolution and latitude coverage.

Product/institution	Period	Depth integration (m)				Temporal resolution/latitudinal range	Reference
		0–700	700–2000	0–2000	≥ 2000		
1 CORA	1993–2016	Y	Y	Y	–	Monthly 60° S–60° N	http://marine.copernicus.eu/services-portfolio/access-to-products/
2 CSIRO (RSOI)	2004–2017	Y/E (0–300)	Y/E	Y/E	–	Monthly 65° S–65° N	Roemmich et al. (2015), Wijffels et al. (2016)
3 CSIRO/ACECRC/IMAS-UTAS	1970–2017	Y/E (0–300)	–	–	–	Yearly (3-year running mean) 65° S–65° N	Domingues et al. (2008), Church et al. (2011)
4 ICCES	1970–2016	Y/E (0–300)	Y/E	Y/E	–	Yearly 89° S–89° N	Cheng et al. (2017)
5 ICDC	1993–2016	Y (1993)	–	Y (2005)	–	Monthly	Gouretski and Koltermann (2007)
6 IPRC	2005–2016	–	–	Y	–	Monthly	http://apdr.csoest.hawaii.edu/projects/argo (last access: 22 August 2018)
7 JAMSTEC	2005–2016	–	–	Y	–	Monthly	Hosoda et al. (2008)
8 MRI/JMA	1970–2016 (rel. to 1961–1990 averages)	Y/E (0–300)	Y/E	Y/E	–	Yearly 89° S–89° N	Ishii et al. (2009, 2017)
9 NCEI/NOAA	1970–2016	Y/E	Y/E	Y/E	–	Yearly 89° S–89° N	Levitus et al. (2012)
10 SIO	2005–2016	–	–	Y	–	Monthly	Roemmich and Gilson (2009)
11 SIO (Deep–abyssal)	1990–2010 (as of Jan 2018)	–	–	–	Y/E	Linear trend 89° S–89° N, as an aggregation of 32 deep ocean basins	Purkey and Johnson (2010)

only, we averaged together the corresponding linear trends of the individual estimates to obtain an “ensemble mean linear rate”. Thirdly, we combined this “ensemble mean linear rate” with the “ensemble mean variability time series” to obtain the final ensemble mean time series. We applied the same steps for the Argo era (2005–2016).

To maximize the number of individual estimates used in the final full-depth ensemble mean time series, the three steps above were actually divided into depth integrations and then summed. For the Argo era, we summed 0–2000 m (nine estimates) and ≥ 2000 m (one estimate). For the altimetry era, we summed 0–700 m (six estimates), 700–2000 (four esti-

mates) and ≥ 2000 m (one estimate), although there is no statistical difference if the calculation was only based on the sum of 0–2000 m (4 estimates) and ≥ 2000 m (1 estimate). There is also no statistical difference between the full-depth ensemble mean time series created for the Altimeter and Argo eras during their overlapping years (since 2005).

Figure 6 shows the full-depth ensemble mean time series over 1993–2015 and 2005–2015. It reveals a global mean thermosteric sea-level rise of about 30 mm over 1993–2016 (24 years) or about 18 mm over 2005–2016 (12 years), with a record high in 2015. These thermosteric changes are equiv-

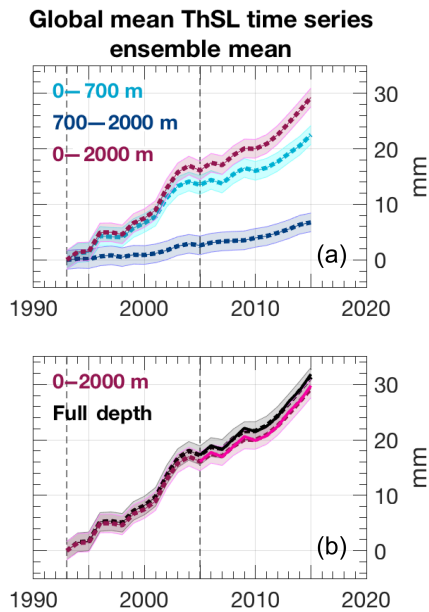


Figure 6. Ensemble mean time series for global mean thermosteric anomaly, for three depth integrations (a) and for 0–2000 m and full depth (b). In the bottom panel, dashed lines are for the 1993–2015 period whereas solid lines are for 2005–2015. Error bars represent the ensemble spread (standard deviation). Units are millimeters.

alent to a linear rate of 1.32 ± 0.4 and 1.31 ± 0.4 mm yr^{-1} respectively.

Figure 7 shows thermosteric sea-level trends for each of the datasets used over the 1993–2015 (a) and 2005–2015 (b) time spans and different depth ranges (including full depth), as well as associated ensemble mean trends. The full depth ensemble mean trend amounts to 1.3 ± 0.4 mm yr^{-1} over 2005–2015. It is similar to the 1993–2015 ensemble mean trend, suggesting negligible acceleration of the thermosteric component over the altimetry era.

2.4 Glaciers

Glaciers have strongly contributed to sea-level rise during the 20th century – around 40% – and will continue to be an important part of the projected sea-level change during the 21st century – around 30% (Kaser et al., 2006; Church et al., 2013; Gardner et al., 2013; Marzeion et al., 2014; Zemp et al., 2015; Huss and Hock, 2015). Because glaciers are time-integrated dynamic systems, a response lag of at least 10 years to a few hundred years is observed between changes in climate forcing and glacier shape, mainly depending on glacier length and slope (Johannesson et al., 1989; Bahr et al., 1998). Today, glaciers are globally (a notable exception is the Karakoram–Kunlun Shan region, e.g., Brun et al., 2017) in a strong disequilibrium with the current climate and are losing mass, due essentially to the global warming in the second half of the 20th century (Marzeion et al., 2018).

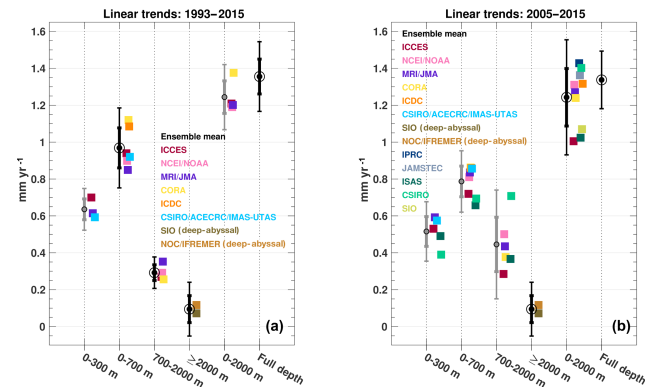


Figure 7. Linear rates of global mean thermosteric sea level for depth integrations (x axis), individual estimates and ensemble means, over 1993–2015 (a) and 2005–2015 (b). Ensemble mean rates with a black circle were used in the estimation of the time series described in Sect. 2.3.4. Error bars are standard deviation due to spread of the estimates except for ≥ 2000 m. Units are millimeters per year.

Global glacier mass changes are derived from in situ measurements of glacier mass changes or glacier length changes. Remote sensing methods measure elevation changes over entire glaciers based on differencing digital elevation models (DEMs) from satellite imagery between two epochs (or at points from repeat altimetry), surface flow velocities for determination of mass fluxes and glacier mass changes from space-based gravimetry. Mass balance modeling driven by climate observations is also used (Marzeion et al., 2017, provide a review of these different methods).

Glacier contribution to sea level is primarily the result of their surface mass balance and dynamic adjustment, plus iceberg discharge and frontal ablation (below sea level) in the case of marine-terminating glaciers. The sum of worldwide glacier mass balances does not correspond to the total glacier contribution to sea-level change for the following reasons:

- Glacier ice below sea level does not contribute to sea-level change, apart from a small lowering when replacing ice with seawater of a higher density. Total volume of glacier ice below sea level is estimated to be 10–60 mm sea-level equivalent (SLE, Huss and Farinotti, 2012; Haeberli and Linsbauer, 2013; Huss and Hock, 2015).
- There is incomplete transfer of melting ice from glaciers to the ocean: meltwater stored in lakes or wetlands, meltwater intercepted by natural processes and human activities (e.g., drainage to lakes and aquifers in endorheic basins, impoundment in reservoirs, agriculture use of freshwater, Loriaux and Casassa, 2013; Käab et al., 2015).

Despite considerable progress in observing methods and spatial coverage (Marzeion et al., 2017), estimating glacier con-

tribution to sea-level change remains challenging due to the following reasons:

- The number of regularly observed glaciers (in the field) remains very low (0.25 % of the 200 000 glaciers of the world have at least one observation and only 37 glaciers have multidecade-long observations, Zemp et al., 2015).
- Uncertainty of the total glacier ice mass remains high (Fig. 8, Grinsted, 2013; Pfeffer et al., 2014; Farinotti et al., 2017; Frey et al. 2014).
- Uncertainties in glacier inventories and DEMs are not negligible. Sources of uncertainties include debris-covered glaciers, disappearance of small glaciers, positional uncertainties, wrongly mapped seasonal snow, rock glaciers, voids and artifacts in DEMs (Paul et al., 2004; Bahr and Radić, 2012).
- Uncertainties of satellite retrieval algorithms from space-based gravimetry and regional DEM differencing are still high, especially for global estimates (Gardner et al., 2013; Marzeion et al., 2017; Chambers et al., 2017).
- Uncertainties of global glacier modeling (e.g., initial conditions, model assumptions and simplifications, local climate conditions; Marzeion et al., 2012).
- Knowledge about some processes governing mass balance (e.g., wind redistribution and metamorphism, sublimation, refreezing, basal melting) and dynamic processes (e.g., basal hydrology, fracturing, surging) remains limited (Farinotti et al., 2017).

An annual assessment of glacier contribution to sea-level change is difficult to perform from ground-based or space-based observations apart from space-based gravimetry, due to the sparse and irregular observation of glaciers, and the difficulty of accurately assessing the annual mass balance variability. Global annual averages are highly uncertain because of the sparse coverage, but successive annual balances are uncorrelated and therefore averages over several years are known with greater confidence.

2.4.1 Glacier datasets

The following datasets are considered, with a focus on the trends of annual mass changes:

1. update of Gardner et al. (2013) (Reager et al., 2016), from satellite gravimetry and altimetry, and glaciological records, called G16;
2. update of Marzeion et al. (2012) (Marzeion et al., 2017), from global glacier modeling and mass balance observations, called M17;
3. update of Cogley (2009) (Marzeion et al., 2017), from geodetic and direct mass-balance measurements, called C17;

4. update of Leclercq et al. (2011) (Marzeion et al., 2017), from glacier length changes, called L17;

5. average of GRACE-based estimates of Marzeion et al. (2017), from spatial gravimetry measurements, called M17-G.

In general it is not possible to align measurements of glacier mass balance with the calendar. Most in situ measurements are for glaciological years that extend between successive annual minima of the glacier mass at the end of the summer melt season. Geodetic measurements have start and end dates several years apart and are distributed irregularly through the calendar year; some are corrected to align with annual mass minima but most are not. Consequently, measurements discussed here for 1993–2016 (the altimetry era) and 2005–2016 (the GRACE and Argo era) are offset by up to a few months from the nominal calendar years.

Peripheral glaciers around the Greenland and Antarctic ice sheets are not treated in detail in this section (see Sects. 2.5 and 2.6 for mass-change estimates that combine the peripheral glaciers with the Greenland ice sheet and Antarctic ice sheet respectively). This is primarily because of the lack of observations (especially ground-based measurements) and also because of the high spatial variability of mass balance in those regions, and the slightly different climate (e.g., precipitation regime) and processes (e.g., refreezing). In the past, these regions have often been neglected. However, Radić and Hock (2010) estimated the total ice mass of peripheral glaciers around Greenland and Antarctica as 191 ± 70 mm SLE, with an actual contribution to sea-level rise of around 0.23 ± 0.04 mm yr⁻¹ (Radić and Hock, 2011). Gardner et al. (2013) found a contribution from Greenland and Antarctic peripheral glaciers equal to 0.12 ± 0.05 mm yr⁻¹.

Note that some new or updated datasets for peripheral glaciers surrounding polar ice sheets are under development and will hopefully be available in coming years in order to incorporate Greenland and Antarctic peripheral glaciers in the estimates of global glacier mass changes.

2.4.2 Methods

No globally complete observational dataset exists for glacier mass changes (except GRACE estimates; see below). Any calculation of the global glacier contribution to sea-level change has to rely on spatial interpolation or extrapolation or both, or to consider limited knowledge of responses to climate change (due to the heterogeneous spatial distribution of glaciers around the world). Consequently, most observational methods to derive glacier sea-level contribution must extend local observations (in situ or satellite) to a larger region. Thanks to the recent global glacier outline inventory (Randolph Glacier Inventory – RGI – first release in 2012) as well as global climate observations, glacier modeling can now also be used to estimate the contribution of glaciers to

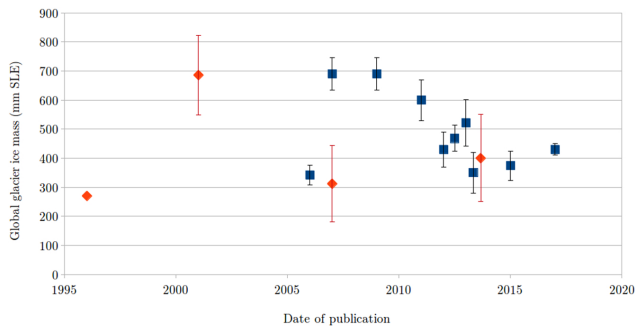


Figure 8. Evolution of global glacier ice mass estimates from different studies published over the past 2 decades, based on different observations and methods. The red marks correspond to IPCC reports. We clearly see the most recent publications lead to less scattered results. Note that Antarctica and Greenland peripheral glaciers are taken into account in this figure.

sea level (Marzeion et al., 2012; Huss and Hock, 2015; Mausson et al., 2018). Still, those global modeling methods need to globalize local observations and glacier processes which require fundamental assumptions and simplifications. Only GRACE-based gravimetric estimates are global but they suffer from large uncertainties in retrieval algorithms (signal leakage from hydrology, GIA correction) and coarse spatial resolution, not resolving smaller glaciated mountain ranges or those peripheral to the Greenland ice sheet.

The DEM differencing method is not yet global, but regional, and can hopefully in the near future be applied globally. This method needs also to convert elevation changes to mass changes (using assumptions on snow and ice densities). In contrast, very detailed glacier surface mass balance and glacier dynamic models are today far from being applicable globally, mainly due to the lack of crucial observations (e.g., meteorological data, glacier surface velocity and thickness) and of computational power for the more demanding theoretical models. However, somewhat simplified approaches are currently being developed to make the best use of the steadily increasing datasets. Modeling-based estimates suffer also from the large spread in estimates of the actual global glacier ice mass (Fig. 8). The mean value is 469 ± 146 mm SLE, with recent studies converging towards a range of values between 400 and 500 mm SLE global glacier ice mass. But as mentioned above, a part of this ice mass will not contribute to sea level.

2.4.3 Results (trends)

Table 3 presents most recent estimates of trends in global glacier mass balances.

The ensemble mean contribution of glaciers to sea-level rise for the time period 1993–2016 is 0.65 ± 0.051 mm yr⁻¹ SLE and 0.74 ± 0.18 mm yr⁻¹ for the time period 2005–2016 (uncertainties are averaged). Different studies refer to dif-

Table 3. Glacier contribution to sea level; all data are in millimeters per year of SLE.

	1993–2016 mm yr ⁻¹ SLE	2005–2016 mm yr ⁻¹ SLE
G16		0.70 ± 0.070^a
M17	0.68 ± 0.032	0.80 ± 0.048
C17	0.63 ± 0.070	0.75 ± 0.070^b
L17		0.84 ± 0.640^c
M17-G		0.61 ± 0.070^d

^a The time period of G16 is 2002–2014. ^b The time period of C17 is 2003–2009. ^c The time period of L17 is 2003–2009. ^d The time period of M17-G is 2002/2005–2013/2015 because this value is an average of different estimates.

ferent time periods. However, because of the probable low variability of global annual glacier changes, compared to other components of the sea-level budget, averaging trends for slightly different time periods is appropriate.

The main source of uncertainty is that the vast majority of glaciers are unmeasured, which makes interpolation or extrapolation necessary, whether for in situ or satellite measurements, as well as for glacier modeling. Other main contributions to uncertainty in the ensemble mean stem from methodological differences, such as the downscaling of atmospheric forcing required for glacier modeling, the separation of glacier mass change to other mass change in the spatial gravimetry signal and the derivation of observational estimates of mass change from different raw measurements (e.g., length and volume changes, mass balance measurements, and geodetic methods), all with their specific uncertainties.

2.5 Greenland

Ice sheets are the largest potential source of future sea-level rise and represent the largest uncertainty in projections of future sea level. Almost all land ice ($\sim 99.5\%$) is locked in the ice sheets, with a volume in sea-level equivalent (SLE) terms of 7.4 m for Greenland and 58.3 m for Antarctica. It has been estimated that approximately 25% to 30% of the total land ice contribution to sea-level rise over the last decade came from the Greenland ice sheet (e.g., Dieng et al., 2017; Box and Colgan, 2017).

There are three main methods that can be used to estimate the mass balance of the Greenland ice sheet: (1) measurement of changes in elevation of the ice surface over time (dh/dt) either from imagery or altimetry; (2) the mass budget or input–output method (IOM), which involves estimating the difference between the surface mass balance and ice discharge; and (3) consideration of the redistribution of mass via gravity anomaly measurements, which only became viable with the launch of GRACE in 2002. Uncertainties due to the GIA correction are small in Greenland compared

Table 4. Datasets considered in the Greenland mass balance assessment, as well as covered time span and type of observations.

Reference	Time period	Method
Update from Barletta et al. (2013)	2003–2016	GRACE
Groh and Horwath (2016)	2003–2015	GRACE
Update from Luthcke et al. (2013)	2003–2015	GRACE
Update from Sasgen et al. (2012)	2003–2016	GRACE
Update from Schrama et al. (2014)	2003–2016	GRACE
Update from van den Broeke et al. (2016)	1993–2016	Input–output method (IOM)
Wiese et al. (2016a, b)	2003–2016	GRACE
Update from Wouters et al. (2008)	2003–2016	GRACE

to Antarctica: on the order of $\pm 20 \text{ Gt yr}^{-1}$ mass equivalent (Khan et al., 2016). Prior to 2003, mass trends are reliant on IOM and altimetry. Both techniques have limited sampling in time and/or space for parts of the satellite era (1992–2002) and errors for this earlier period are, therefore, higher (van den Broeke et al., 2016; Hurkmans et al., 2014).

The consistency between the three methods mentioned above was demonstrated for Greenland by Sasgen et al. (2012) for the period 2003–2009. Ice-sheet-wide estimates showed excellent agreement although there was less consistency at a basin scale. We have, therefore, high confidence and relatively low uncertainties in the mass rates for the Greenland ice sheet in the satellite era (see also Bamber et al., 2018).

2.5.1 Datasets considered for the assessment

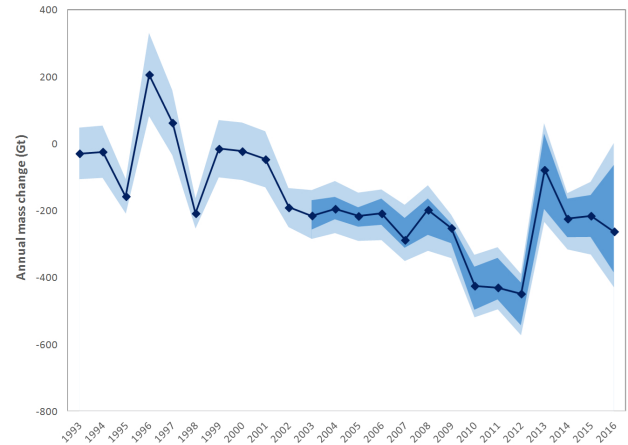
This assessment of sea-level budget contribution from the Greenland ice sheet considers the datasets shown in Table 4.

2.5.2 Methods and analyses

All but one of these datasets are based on GRACE data and therefore provide annual time series from ~ 2002 onwards. The one exception uses IOM (van Den Broeke et al., 2016) to give an annual mass time series for a longer time period (1993 onwards).

Notwithstanding this, each group has chosen their own approach to estimate mass balance from GRACE observations. As the aim of this global sea-level budget assessment is to compile existing results (rather than undertake new analyses), we have not imposed a specific methodology. Instead, we asked for the contributed datasets to reflect each group's 'best estimate' of annual trends for Greenland using the method(s) they have published.

Greenland contains glaciers and ice caps (GIC) around the margins of the main ice sheet, often referred to as peripheral GIC (PGIC), which are a significant proportion of the total mass imbalance (circa 15–20 %) (Bolch et al., 2013). Some studies consider the mass balance of the ice sheets and the PGIC separately but there has been, in general, no consistency in the treatment of PGIC and many studies do not

**Figure 9.** Greenland annual mass change from 1993 to 2016. The medium blue region shows the range of estimates from the datasets listed in Table 1. The lighter blue region shows the range of estimates when stated errors are included, to provide upper and lower bounds. The dark blue line shows the mean mass trend.

specify if they are included or excluded from the total. The GRACE satellites have an approximate spatial resolution of 300 km and the large number of studies that use GRACE, by default, include all land ice within the domain of interest. For this reason, the results below for Greenland mass trends all include PGIC.

From these datasets, for each year from 1993 to 2015 (and 2016 where available), we have calculated an average change in mass (calculated as the weighted mean based on the stated error value for each year) and an error term. Prior to 2003, the results are based on just one dataset (van den Broeke et al., 2016).

2.5.3 Results

There is generally a good level of agreement between the datasets (Fig. 9), and taken together they provide an average estimate of 171 Gt yr^{-1} of ice mass loss (or sea-level budget contribution) from Greenland for the period 1993 to 2016, increasing to 272 Gt yr^{-1} for the period 2005 to 2016 (Table 5).

All the datasets illustrate the previously documented accelerating mass loss up to 2012 (Rignot et al., 2011a; Velicogna, 2009). In 2012, the ice sheet experienced exceptional surface melting reaching as far as the summit (Nghiem et al., 2012) and a record mass loss, since at least 1958, of over 400 Gt (van Den Broeke et al., 2016). The following years, however, show a reduced loss (not more than 270 Gt in any year). Inclusion of the years since 2012 in the 2005–2016 trend estimate reduces the overall rate of mass loss acceleration and its statistical significance. There is greater divergence in the GRACE time series for 2016. We associate this with the degradation of the satellites as they came to

Table 5. Annual time series of Greenland mass change (GT yr^{-1} , negative values mean decreasing mass). The Δ mass is calculated as the weighted mean based on the stated error value for each year. The error for each year is calculated as the mean of all stated 1σ errors divided by \sqrt{N} where N is the number of datasets available for that year, assuming that the errors are uncorrelated. The standard deviation (σ) is also given to illustrate the level of agreement between datasets for each year when multiple datasets are available (2003 onwards).

Year	Δ mass (Gt yr^{-1})	Error (Gt yr^{-1})	σ (Gt)
1993	−30	76	
1994	−25	77	
1995	−159	51	
1996	205	123	
1997	61	97	
1998	−209	45	
1999	−16	85	
2000	−24	85	
2001	−48	83	
2002	−192	58	
2003	−216	13	28
2004	−196	12	24
2005	−218	13	21
2006	−210	12	29
2007	−289	10	31
2008	−199	11	39
2009	−253	11	21
2010	−426	9	42
2011	−431	9	47
2012	−450	10	41
2013	−80	13	76
2014	−225	13	38
2015	−217	13	48
2016	−263	23	123
Average estimate 1993–2015	−167	54	
Average estimate 1993–2016	−171	53	
Average estimate 2005–2015	−272	11	
Average estimate 2005–2016	−272	13	

wards the end of their mission. For 2005–2012, it might be inferred that there is a secular trend towards greater mass loss and from 2010 to 2012 the value is relatively constant. Interannual variability in mass balance of the ice sheet is driven, primarily, by the surface mass balance (i.e., atmospheric weather) and it is apparent that the magnitude of this year-to-year variability can be large: it exceeded 360 Gt (or 1 mm sea-level equivalent) between 2012 and 2013. Caution is required, therefore, in extrapolating trends from a short record such as this.

2.6 Antarctica

The annual turnover of mass of Antarctica is about 2200 Gt yr^{-1} (over 6 mm yr^{-1} of SLE), 5 times larger than in Greenland (Wessem et al., 2017). In contrast to Greenland, ice and snow melt have a negligible influence on Antarctica's mass balance, which is therefore completely controlled by the balance between snowfall accumulation in the drainage basins and ice discharge along the periphery. The continent is also 7 times larger than Greenland, which makes satellite techniques absolutely essential to survey the continent. Interannual variations in accumulation are large in Antarctica, showing decadal to multidecadal variability, so that many years of data are required to extract trends, and missions limited to only a few years may produce misleading results (e.g., Rignot et al., 2011a, b).

As in Greenland, the estimation of the mass balance has employed a variety of techniques, including (1) the gravity method with GRACE since April 2002 until the end of the mission in late 2016; (2) the IOM method using a series of Landsat and synthetic-aperture radar (SAR) satellites for measuring ice motion along the periphery (Rignot et al., 2011a, b), ice thickness from airborne depth radar sounders such as Operation IceBridge (Leuschen, 2014a), and reconstructions of surface mass balance using regional atmospheric climate models constrained by re-analysis data (RACMO, MAR and others); and (3) a radar or laser altimetry method which mixes various satellite altimeters and correct ice elevation changes with density changes from firm models. The largest uncertainty in the GRACE estimate in Antarctica is the GIA, which is larger than in Greenland, and a large fraction of the observed signal. The IOM method compares two large numbers with large uncertainties to estimate the mass balance as the difference. In order to detect an imbalance at the 10 % level, surface mass balance and ice discharge need to be estimated with a precision typically of 5 to 7 %. The altimetry method is limited to areas of shallow slope; hence, it is difficult to use in the Antarctic Peninsula and in the deep interior of the Antarctic continent due to unknown variations of the penetration depth of the signal in snow and firn. The only method that expresses the partitioning of the mass balance between surface processes and dynamic processes is the IOM method (e.g., Rignot et al., 2011a). The gravity method is an integrand method which does not suffer from the limitations of surface mass balance models but is limited in spatial resolution (e.g., Velicogna et al., 2014). The altimetry method provides independent evidence of changes in ice dynamics, e.g., by revealing rapid ice thinning along the ice streams and glaciers revealed by ice motion maps, as opposed to large-scale variations reflecting a variability in surface mass balance (McMillan et al., 2014).

All these techniques have improved in quality over time and have accumulated a decade to several decades of observations, so that we are now able to assess the mass balance of the Antarctic continent using methods with reasonably low

uncertainties and multiple lines of evidence as the methods are largely independent, which increases confidence in the results (see recent publication by the IMBIE Team, 2018). There is broad agreement in the mass loss from the Antarctic Peninsula and West Antarctica; most residual uncertainties are associated with East Antarctica as the signal is relatively small compared to the uncertainties, although most estimates tend to indicate a low contribution to sea level (e.g., Shepherd et al., 2012).

2.6.1 Datasets considered for the assessment

This assessment considers the datasets shown in Table 6.

In Table 6, the negative trend estimate by Zwally et al. (2016) is not added. It is worth noting that including it would only slightly reduce the ensemble mean trend.

2.6.2 Methods and analyses

The datasets used in this assessment are Antarctica mass balance time series generated using different approaches. Two estimates are a joint inversion of GRACE, altimetry and GPS data (Martín-Español et al., 2016) as well as GRACE and CryoSat data (Forsberg et al., 2017). Two methods are mascon solutions obtained from the GRACE intersatellite range-rate measurements over equal-area spherical caps covering the Earth's surface (Luthcke et al., 2013; Wiese et al., 2016b), three estimates use the GRACE spherical harmonics solutions (Velicogna et al., 2014; Wiese et al., 2016b; Wouters et al., 2013) and one uses gridded GRACE products (Sasgen et al., 2013).

All GRACE time series were provided as monthly time series (except for the one using the Martín-Español et al., 2016, method, which was provided as annual estimates). In addition, different groups use different GIA corrections, therefore the spread of the trend solutions also represents the error associated with the GIA correction which, in Antarctica, is the largest source of uncertainty. Sasgen et al. (2013) used their own GIA solution (Sasgen et al., 2017), as did Martín-Español et al. (2016); Luthcke et al. (2013), Velicogna et al. (2014), and Groh and Horwath (2016) used IJ05-R2 (Ivins et al., 2013). Wouter et al. (2013) used Whitehouse et al. (2012), and Wiese et al. (2016b) used A et al. (2013). In addition, Groh and Horwath (2016) did not include the peripheral glaciers and ice caps, while all other estimates do.

Table 6 shows the Antarctic contribution to sea level during 2005–2015 from the different GRACE solutions, and for the input and output method. There is a single IOM-based dataset that provides trends for the period 1993–2015 (update of Rignot et al., 2011a). For the period 2005–2015, we calculated the annual sea-level contribution from Antarctica using GRACE and IOM estimates (Table 7).

As we are interested in evaluating the long-term trend and interannual variability of the Antarctic contribution to sea level, for each GRACE dataset available in monthly time se-

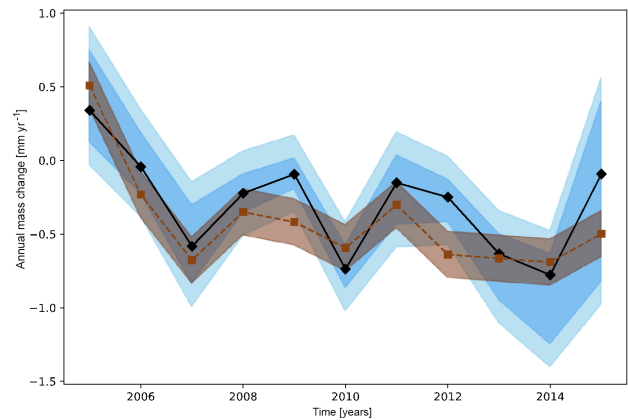


Figure 10. Antarctic annual sea-level contribution during 2005 to 2015. The black squares are the mean annual sea level calculated using the GRACE datasets listed in Table 6. The darker blue band shows the range of estimates from the datasets. The light blue band accounts for the error in the different GRACE estimates. The brown squares are the annual sea-level contribution calculated using the input–output method (updated from Rignot et al., 2011a); the light brown band is the associated error.

ries, we first removed the annual and subannual components of the signal by applying a 13-month averaging filter and we then used the smoothed time series to calculate annual mass change. Figure 10 shows the annual sea-level contribution from Antarctica calculated from the GRACE-derived estimates and for the input–output method. The GRACE mean annual estimates are calculated as the mean of the annual contributions from the different groups, and the associated error calculated as the sum of the spread of the annual estimates and the mean annual error.

2.6.3 Results

There is generally broad agreement between the GRACE datasets (Fig. 10), as most of the differences between GRACE estimates are caused by differences in the GIA correction. We find a reasonable agreement between GRACE and the IOM estimates although the IOM estimates indicate higher losses. Taken together, these estimates yield an average of 0.42 mm yr^{-1} sea-level budget contribution from Antarctica for the period 2005 to 2015 (Table 7) and 0.25 mm yr^{-1} sea level for the time period 1993–2005, where the latter value is based on IOM only.

All the datasets illustrate the previously documented accelerating mass loss of Antarctica (Rignot et al., 2011a, b; Velicogna, 2009). In 2005–2010, the ice sheet experienced ice mass loss driven by an increase in mass loss in the Amundsen Sea sector of West Antarctica (Mouginot et al., 2014). The following years showed a reduced increase in mass loss, as colder ocean conditions prevailed in the Amundsen Sea embayment sector of West Antarctica in 2012–2013 which reduced the melting of the ice shelves in

Table 6. Datasets considered in this assessment of the Antarctica mass change, and associated trends for the 2005–2015 and 1993–2015 expressed in millimeters per year of SLE. Positive values mean positive contribution to sea level (i.e., sea-level rise).

Reference	Method	2005–2015	1993–2015
		trend (mm yr ⁻¹) SLE	trend (mm yr ⁻¹) SLE
Update from Martín-Español et al. (2016)	Joint inversion	0.43 ± 0.07	–
Update from Forsberg et al. (2017)	GRACE–altimetry–GPS	0.31 ± 0.02	–
	GRACE–CryoSat		
Update from Groh and Horwath (2016)	GRACE	0.32 ± 0.11	–
Update from Luthcke et al. (2013)	GRACE	0.36 ± 0.06	–
Update from Sasgen et al. (2013)	GRACE	0.47 ± 0.07	–
Update from Velicogna et al. (2014)	GRACE	0.33 ± 0.08	–
Update from Wiese et al. (2016b)	GRACE	0.39 ± 0.02	–
Update from Wouters et al. (2013)	GRACE	0.41 ± 0.05	–
Update from Rignot et al. (2011b)	Input–output method (IOM)	0.46 ± 0.05	0.25 ± 0.1
Update from Schrama et al. (2014); version 1	GRACE	0.47 ± 0.03	
	ICE6G GIA model		
Update from Schrama et al. (2014); version 2	GRACE	0.33 ± 0.03	
	Updated GIA models		

Table 7. Annual sea-level contribution from Antarctica during 2005–2015 from GRACE and input–output method (IOM) calculated as described above and expressed in millimeters per year of SLE. Also shown is the mean of the estimate from the two methods; associated errors are the mean of the two estimated errors. Positive values mean positive contribution to sea level (i.e., sea-level rise).

Year	GRACE	IOM	Mean
	(mm yr ⁻¹) SLE	(mm yr ⁻¹) SLE	(mm yr ⁻¹) SLE
2005	−0.34 ± 0.47	−0.51 ± 0.16	−0.42 ± 0.31
2006	0.04 ± 0.36	0.23 ± 0.16	0.14 ± 0.26
2007	0.58 ± 0.42	0.68 ± 0.16	0.63 ± 0.29
2008	0.22 ± 0.29	0.35 ± 0.16	0.29 ± 0.22
2009	0.09 ± 0.26	0.42 ± 0.16	0.26 ± 0.21
2010	0.74 ± 0.30	0.59 ± 0.16	0.67 ± 0.23
2011	0.15 ± 0.39	0.30 ± 0.16	0.23 ± 0.27
2012	0.25 ± 0.30	0.64 ± 0.16	0.44 ± 0.23
2013	0.63 ± 0.38	0.67 ± 0.16	0.65 ± 0.27
2014	0.78 ± 0.46	0.69 ± 0.16	0.73 ± 0.31
2015	0.09 ± 0.77	0.50 ± 0.16	0.29 ± 0.46
Average estimate 2005–2015	0.38 ± 0.06	0.46 ± 0.05	0.42 ± 0.06

front of the glaciers (Dutrieux et al., 2014). Divergence in the GRACE time series is observed after 2015 due to the degradation of the satellites towards the end of the mission.

The large interannual variability in mass balance in 2005–2015, characteristic of Antarctica, nearly masks out the trend in mass loss, which is more apparent in the longer time series than in short time series. The longer record highlights the pronounced decadal variability in ice sheet mass balance in Antarctica, demonstrating the need for multidecadal

time series in Antarctica, which have been obtained only by IOM and altimetry. The interannual variability in mass balance is driven almost entirely by surface mass balance processes. The mass loss of Antarctica, about 200 Gt yr⁻¹ in recent years, is only about 10 % of its annual turnover of mass (2200 Gt yr⁻¹), in contrast with Greenland where the mass loss has been growing rapidly to nearly 100 % of the annual turnover of mass. This comparison illustrates the challenge of detecting mass balance changes in Antarctica, but at the same time, that satellite techniques and their interpretation have made tremendous progress over the last 10 years, producing realistic and consistent estimates of the mass using a number of independent methods (Bamber et al., 2018; the IMBIE Team, 2018).

2.7 Terrestrial water storage

Human transformations of the Earth's surface have impacted the terrestrial water balance, including continental patterns of river flow and water exchange between land, atmosphere and ocean, ultimately affecting global sea level. For instance, massive impoundment of water in man-made reservoirs has reduced the direct outflow of water to the sea through rivers, while groundwater abstractions, wetland and lake storage losses, deforestation, and other land use changes have caused changes to the terrestrial water balance, including changing evapotranspiration over land, leading to net changes in land–ocean exchanges (Chao et al., 2008; Wada et al., 2012a, b; Konikow, 2011; Church et al., 2013; Döll et al., 2014a, b). Overall, the combined effects of direct anthropogenic processes have reduced land water storage, increasing the rate of sea-level rise by 0.3–0.5 mm yr⁻¹ during recent decades (Church et al., 2013; Gregory et al., 2013; Wada et al.,

2016). Additionally, recent work has shown that climate-driven changes in water stores can perturb the rate of sea-level change over interannual to decadal timescales, making global land mass budget closure sensitive to varying observational periods (Cazenave et al., 2014; Dieng et al., 2015a; Reager et al., 2016; Rietbroek et al., 2016). Here we discuss each of the major component contributions from land, with a summary in Table 8, and estimate the net terrestrial water storage contribution to sea level.

2.7.1 Direct anthropogenic changes in terrestrial water storage

Water impoundment behind dams

Wada et al. (2016) built on work by Chao et al. (2008) to combine multiple global reservoir storage datasets in pursuit of a quality-controlled global reservoir database. The result is a list of 48 064 reservoirs that have a combined total capacity of 7968 km³. The time history of growth of the total global reservoir capacity reflects the history of the human activity in dam building. Applying assumptions from Chao et al. (2008), Wada et al. (2016) estimated that humans have impounded a total of 10 416 km³ of water behind dams, accounting for a cumulative 29 mm drop in global mean sea level. From 1950 to 2000 when global dam-building activity was at its highest, impoundment contributed to the average rate of sea-level change at -0.51 mm yr^{-1} . This was an important process in comparison to other natural and anthropogenic sources of sea-level change over the past century, but has now largely slowed due to a global decrease in dam-building activity.

Global groundwater depletion

Groundwater currently represents the largest secular trend component to the land water storage budget. The rate of groundwater depletion (GWD) and its contribution to sea level has been subject to debate (Gregory et al., 2013; Taylor et al., 2013). In the IPCC AR4 (Solomon et al., 2007), the contribution of nonfrozen terrestrial waters (including GWD) to sea-level variation was not considered due to its perceived uncertainty (Wada et al., 2016). Observations from GRACE opened a path to monitor total water storage changes, including groundwater in data-scarce regions (Strassberg et al., 2007; Rodell et al., 2009; Tiwari et al., 2009; Jacob et al., 2012; Shamsudduha et al., 2012; Voss et al., 2013). Some studies have also applied global hydrological models in combination with the GRACE data (see Wada et al., 2016, for a review).

Earlier estimates of GWD contribution to sea level range from 0.075 to 0.30 mm yr⁻¹ (Sahagian et al., 1994; Gornitz, 1995, 2001; Foster and Loucks, 2006). More recently, Wada et al. (2012b), using hydrological modeling, estimated that the contribution of GWD to global sea level increased from 0.035 (± 0.009) to 0.57 (± 0.09) mm yr⁻¹ during the

20th century and projected that it would further increase to 0.82 (± 0.13) mm yr⁻¹ by 2050. Döll et al. (2014b) used hydrological modeling, well observations and GRACE satellite gravity anomalies to estimate a 2000–2009 global GWD of 113 km³ yr⁻¹ (0.314 mm yr⁻¹ SLE). This value represents the impact of human groundwater withdrawals only and does not consider the effect of climate variability on groundwater storage. A study by Konikow (2011) estimated global GWD to be 145 (± 39) km³ yr⁻¹ ($0.41 \pm 0.1 \text{ mm yr}^{-1}$ SLE) during 1991–2008 based on measurements of changes in groundwater storage from in situ observations, calibrated groundwater modeling, GRACE satellite data and extrapolation to unobserved aquifers.

An assumption of most existing global estimates of GWD impacts on sea-level change is that nearly 100 % of the GWD ends up in the ocean. However, groundwater pumping can also perturb regional climate due to land–atmosphere interactions (Lo and Famiglietti, 2013). A recent study by Wada et al. (2016) used a coupled land–atmosphere model simulation to track the fate of water pumped from underground and found it more likely that $\sim 80 \%$ of the GWD ends up in the ocean over the long term, while 20 % re-infiltrates and remains in land storage. They estimated an updated contribution of GWD to global sea-level rise ranging from 0.02 (± 0.004) mm yr⁻¹ in 1900 to 0.27 (± 0.04) mm yr⁻¹ in 2000 (Fig. 11). This indicates that previous studies had likely overestimated the cumulative contribution of GWD to global SLR during the 20th century and early 21st century by 5–10 mm.

Land cover and land-use change

Humans have altered a large part of the land surface, replacing about 40 % of natural vegetation by anthropogenic land cover such as crop fields or pasture. Such land cover change can affect terrestrial hydrology by changing the infiltration-to-runoff ratio and can impact subsurface water dynamics by modifying recharge and increasing groundwater storage (Scanlon et al., 2007). The combined effects of anthropogenic land cover changes on land water storage can be quite complex. Using a combined hydrological and water resource model, Bosmans et al. (2017) estimated that land cover change between 1850 and 2000 has contributed to a discharge increase of 1058 km³ yr⁻¹, on the same order of magnitude as the effect of human water use. These recent model results suggest that land-use change is an important topic for further investigation in the future. So far, this contribution remains highly uncertain.

Deforestation and afforestation

At present, large losses in tropical forests and moderate gains in temperate-boreal forests result in a net reduction of global forest cover (FAO, 2015; Keenan et al., 2015; MacDicken, 2015; Sloan and Sayer, 2015). Net deforestation releases carbon and water stored in both biotic tissues and

soil, which leads to sea-level rise through three primary processes: deforestation-induced runoff increases (Gornitz et al., 1997), carbon loss-related decay and plant storage loss, and complex climate feedbacks (Butt et al., 2011; Chagnon and Bras, 2005; Nobre et al., 2009; Shukla et al., 1990; Spracklen et al., 2012). Due to these three causes, and if uncertainties from the land–atmospheric coupling are excluded, a summary by Wada et al. (2016) suggests that the current net global deforestation leads to an upper-bound contribution of $\sim 0.035 \text{ mm yr}^{-1}$ SLE.

Wetland degradation

Wetland degradation contributes to sea level primarily through (i) direct water drainage or removal from standing inundation, soil moisture and plant storage, and (ii) water release from vegetation decay and peat combustion. Wada et al. (2016) consider a recent wetland loss rate of 0.565 \% yr^{-1} since 1990 (Davidson, 2014) and a present global wetland area of 371 mha averaged from three databases: Matthews natural wetlands (Matthews and Fung, 1987), ISLSCP (Darras, 1999), and DISCover (Belward et al., 1999; Lovel and Belward, 1997). They assume a uniform 1 m depth of water in wetlands (Milly et al., 2010), to estimate a contribution of recent global wetland drainage to sea level of 0.067 mm yr^{-1} . Wada et al. (2016) apply a wetland area and loss rate as used for assessing wetland water drainage, to determine that the annual reduction of wetland carbon stock since 1990, if completely emitted, releases water equivalent to $0.003\text{--}0.007 \text{ mm yr}^{-1}$ SLE. Integrating the impacts of wetland drainage, oxidation and peat combustion, Wada et al. (2016) suggest that the recent global wetland degradation results in an upper bound of 0.074 mm yr^{-1} SLE.

Lake storage changes

Lakes store the greatest mass of liquid water on the terrestrial surface (Oki and Kanae, 2006), yet, because of their “dynamic” nature (Sheng et al., 2016; Wang et al., 2012), their overall contribution to sea level remains uncertain. In the past century, perhaps the greatest contributor in global lake storage was the Caspian Sea (Milly et al., 2010), where the water level exhibits substantial oscillations attributed to meteorological, geological, and anthropogenic factors (Ozyavas et al., 2010; Chen et al., 2017a). Assuming the lake level variation kept pace with groundwater changes (Sahagian et al., 1994), the overall contribution of the Caspian Sea, including both surface and groundwater storage variations through 2014, has been about 0.03 mm yr^{-1} SLE since 1900, $0.075 (\pm 0.002) \text{ mm yr}^{-1}$ since 1995 and $0.109 (\pm 0.004) \text{ mm yr}^{-1}$ since 2002. Additionally, between 1960 and 1990, the water storage in the Aral Sea Basin declined at a striking rate of $64 \text{ km}^3 \text{ yr}^{-1}$, equivalent to 0.18 mm yr^{-1} SLE (Sahagian, 2000; Sahagian et al., 1994; Vörösmarty and Sahagian, 2000) due mostly to upstream water diversion for irrigation (Perera,

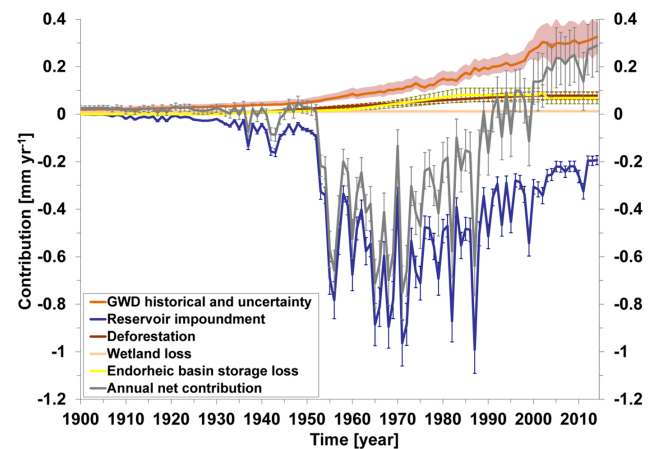


Figure 11. Time series of the estimated annual contribution of terrestrial water storage change to global sea level over the period 1900–2014 (rates in millimeters per year of SLE) (modified from Wada et al., 2016).

1993), which was modeled by Pokhrel et al. (2012) to be $\sim 500 \text{ km}^3$ during 1951–2000, equivalent to 0.03 mm yr^{-1} SLE. Dramatic decline in the Aral Sea continued in recent decades, with an annual rate of $6.043 (\pm 0.082) \text{ km}^3 \text{ yr}^{-1}$ measured from 2002 to 2014 (Schwatke et al., 2015). Assuming that groundwater drainage has kept pace with lake level reduction (Sahagian et al., 1994), the Aral Sea has contributed $0.0358 (\pm 0.0003) \text{ mm yr}^{-1}$ to the recent sea-level rise.

Water cycle variability

Natural changes in the interannual to decadal cycling of water can have a large effect on the apparent rate of sea-level change over decadal and shorter time periods (Milly et al., 2003; Lettenmaier and Milly, 2009; Llovel et al., 2010). For instance, ENSO-driven modulations of the global water cycle can be important in decadal-scale sea-level budgets and can mask underlying secular trends in sea level (Fasullo et al., 2013; Cazenave et al., 2014; Nerem et al., 2018).

Sea-level variability due to climate-driven hydrology represents a super-imposed variability on the secular rates of global mean sea-level rise. While this term can be large and is important in the interpretation of the sea-level record, it is arguably the most difficult term in the land water budget to quantify.

2.7.2 Net terrestrial water storage

GRACE-based estimates

Measurements of non-ice-sheet continental land mass from GRACE satellite gravity have been presented in several recent studies (Jensen et al., 2013; Rietbroek et al., 2016; Reager et al., 2016; Scanlon et al., 2018) and can be used to

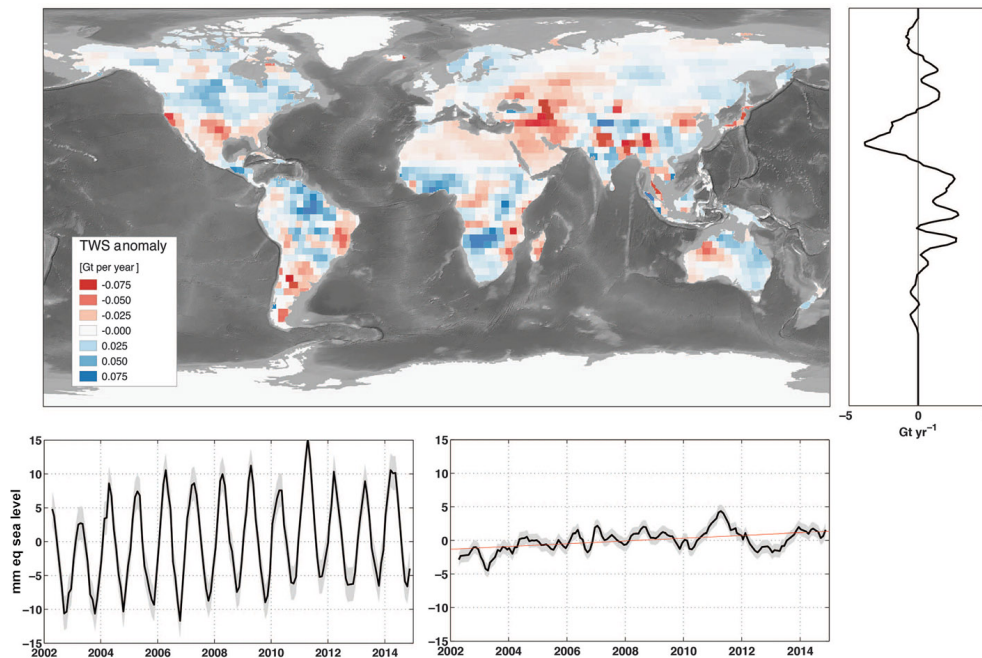


Figure 12. An example of trends in land water storage from GRACE observations, April 2002 to November 2014. Glaciers and ice sheets are excluded. Shown are the global map (gigatons per year), zonal trends and full time series of land water storage (in mm yr^{-1} SLE). Following methods detailed in Reager et al. (2016), GRACE shows a total gain in land water storage during the 2002–2014 period, corresponding to a sea-level trend of $-0.33 \pm 0.16 \text{ mm yr}^{-1}$ SLE (modified from Reager et al., 2016). These trends include all human-driven and climate-driven processes in Table 1 and can be used to close the land water budget over the study period.

constrain a global land mass budget. Note that these “top-down” estimates contain both climate-driven and direct anthropogenic driven effects, which makes them most useful in assessing the total impact of land water storage changes and closing the budget of all contributing terms. GRACE observations, when averaged over the whole land domain following Reager et al. (2016), indicate a total TWS change (including glaciers) over the 2002–2014 study period of approximately $+0.32 \pm 0.13 \text{ mm yr}^{-1}$ SLE (i.e., ocean gaining mass). Global mountain glaciers have been estimated to lose mass at a rate of $0.65 \pm 0.09 \text{ mm yr}^{-1}$ (e.g., Gardner et al., 2013; Reager et al., 2016) during that period, such that a mass balance indicates that global glacier-free land gained water at a rate of $-0.33 \pm 0.16 \text{ mm yr}^{-1}$ SLE (i.e., ocean losing mass; Fig. 12). A roughly similar estimate was found from GRACE using glacier-free river basins globally ($-0.21 \pm 0.09 \text{ mm yr}^{-1}$) (Scanlon et al., 2018). Thus, the GRACE-based net TWS estimates suggest a negative sea-level contribution from land over the GRACE period (Table 8). However, mass change estimates from GRACE incorporate uncertainty from all potential error sources that arise in processing and postprocessing of the data, including from the GIA model, and from the geocenter and mean pole corrections.

Estimates based on global hydrological models

Global land water storage can also be estimated from global hydrological models (GHMs) and global land surface models. These compute water, or water and energy balances, at the Earth’s surface, yielding time variations of water storage in response to prescribed atmospheric data (temperature, humidity and wind) and the incident water and energy fluxes from the atmosphere (precipitation and radiation). Meteorological forcing is usually based on atmospheric model re-analysis. Model uncertainties result from several factors. Recent work has underlined the large differences among different state-of-the-art precipitation datasets (Beck et al., 2017), with large impacts on model results at seasonal (Schellekens et al., 2017) and longer timescales (Felfelani et al., 2017). Another source of uncertainty is the treatment of subsurface storage in soils and aquifers, as well as dynamic changes in storage capacity due to representation of frozen soils and permafrost, the complex effects of dynamic vegetation, atmospheric vapor pressure deficit estimation and an insufficiently deep soil column. A recent study by Scanlon et al. (2018) compared water storage trends from five global land surface models and two global hydrological models to GRACE storage trends and found that models estimated the opposite trend in net land water storage to GRACE over the 2002–2014 period. These authors attributed this discrepancy to model deficiencies, in particular soil depth limitations. These

combined error sources are responsible for a range of storage trends across models of approximately $0.5 \pm 0.2 \text{ mm yr}^{-1}$ SLE. In terms of global land average, model differences can cause up to $\sim 0.4 \text{ mm yr}^{-1}$ SLE uncertainty.

2.7.3 Synthesis

Based on the different approaches to estimate the net land water storage contribution, we estimate that the corresponding sea-level rate ranges from -0.33 to 0.23 mm yr^{-1} during the period of 2002–2014/15 due to water storage changes (Table 8). According to GRACE, the net TWS change (i.e., not including glaciers) over the period 2002–2014 shows a negative contribution to sea level of -0.33 and -0.21 mm yr^{-1} by Reager et al. (2016) and Scanlon et al. (2018) respectively. Such a negative signal is not currently reproduced by hydrological models which estimate slightly positive trends over the same period (see Table 8). It is to be noted, however, that looking at trends only over periods on the order of a decade may not be appropriate due the strong interannual variability of TWS at basin and global scales. For example, Fig. 5 from Scanlon et al. (2018) (see also Fig. S9 from their Supplement), which compares GRACE TWS and model estimates over large river basins over 2002–2014, clearly shows that the discrepancies between GRACE and models occur at the end of the record for the majority of basins. This is particularly striking for the Amazon basin (the largest contributor to TWS), for which GRACE and models agree reasonably well until 2011, and then depart significantly, with GRACE TWS showing a strongly positive trend since then, unlike the models. Such a divergence at the end of the record is also noticed for several other large basins (see Scanlon et al., 2018, Fig. S9). No clear explanation can be provided yet, even though one may question the quality of the meteorological forcing used by hydrological models for the recent years. But this calls for some caution when comparing GRACE and other models on the basis of trends only because of the dominant interannual variability of the TWS component. Much more work is needed to understand differences among models, and between models and GRACE. Of all components entering in the sea-level budget, the TWS contribution currently appears to be the most uncertain one.

2.8 Glacial isostatic adjustment

The Earth's dynamic response to the waxing and waning of the late-Pleistocene ice sheets is still causing isostatic disequilibrium in various regions of the world. The accompanying slow process of GIA is responsible for regional and global fluctuations in relative and absolute sea level, 3-D crustal deformations, and changes in the Earth's gravity field (for a review, see Spada, 2017). To isolate the contribution of current climate change, geodetic observations must be corrected for the effects of GIA (King et al., 2010). These are obtained by solving the “sea-level equation” (Farrell and

Clark, 1976; Mitrovica and Milne, 2003). The sea level can be expressed as $S = N - U$, where S is the rate of change in sea level relative to the solid Earth, N is the geocentric rate of sea-level change, and U is the vertical rate of displacement of the solid Earth. The sea-level equation accounts for solid Earth deformational, gravitational and rotational effects on sea level, which are sensitive to the Earth's mechanical properties and to the melting chronology of continental ice. Forward GIA modeling, based on the solution of the sea-level equation, provides predictions of unique spatial patterns (or *fingerprints*; see Plag and Juettner, 2001) of relative and geocentric sea-level change (e.g., Milne et al., 2009; Kopp et al., 2015). During recent decades, the two fundamental components of GIA modeling have been progressively constrained from the observed history of relative sea level during the Holocene (see, e.g., Lambeck and Chappell, 2001; Peltier, 2004). In the context of climate change, the importance of GIA has been recognized since the mid-1980s, when the awareness of global sea-level rise stimulated the evaluation of the isostatic contribution to tide gauge observations (see Table 1 in Spada and Galassi, 2012). Subsequently, GIA models have been applied to the study of the pattern of sea-level change from satellite altimetry (Tamisiea, 2011), and since 2002 to the study of the gravity field variations from GRACE. Our primary goal here is to analyze GIA model outputs that have been used to infer global mean sea-level change and ice sheet volume change from geodetic datasets during the altimetry era. These outputs are the sea-level variations detected by satellite altimetry across oceanic regions (n), the ocean mass change (w) and the modern ice sheets mass balance from GRACE. We also discuss the GIA correction that needs to be applied to GRACE-based land water storage changes. The GIA correction applied to tide-gauge-based sea-level observations at the coastlines is not discussed here. Since GIA evolves on timescales of millennia (e.g., Turcotte and Schubert, 2012), the rate of change of all the isostatic signals can be considered constant on the timescale of interest.

2.8.1 GIA correction to altimetry-based sea level

Unlike tide gauges, altimeters directly sample the sea surface in a geocentric reference frame. Nevertheless, GIA contributes significantly to the rates of absolute sea-level change observed over the “altimetry era”, which require a correction N_{gia} that is obtained by solving the SLE (e.g., Spada, 2017). As discussed in detail by Tamisiea (2011), N_{gia} is sensitive to the assumed rheological profile of the Earth and to the history of continental glacial ice sheets. The variance of N_{gia} over the surface of the oceans is much reduced, being primarily determined by the change in the Earth's gravity potential, apart from a spatially uniform shift. As discussed by Spada and Galassi (2016), the GIA contribution N_{gia} is strongly affected by variations in the centrifugal potential associated with Earth's rotation, whose fingerprint is

Table 8. Estimates of TWS components due to human intervention and net TWS based on hydrological models and GRACE.

		2002–2014/15 (mm yr ⁻¹) SLE (positive values mean sea-level rise)
Estimate terrestrial water storage contribution to sea level		
Human contributions by component		
Groundwater depletion	Wada et al. (2016)	0.30 (±0.1)
Reservoir impoundment	Wada et al. (2017)	-0.24 (±0.02)
Deforestation (after 2010)	Wada et al. (2017)	0.035
Wetland loss (after 1990)	Wada et al. (2017)	0.074
Endorheic basin storage loss		
Caspian Sea	Wada et al. (2017)	0.109 (±0.004)
Aral Sea	Wada et al. (2017)	0.036 (±0.0003)
Aggregated human intervention (sum of above)	Scanlon et al. (2018)	0.15 to 0.24
Hydrological model-based estimates		
WGHM model (natural variability plus human intervention) Döll et al. (2017)		0.15 ± 0.14
ISBA-TRIP model (natural variability only; Decharme et al., 2016) + human intervention from Wada et al. (2016) (from Dieng et al., 2017)		0.23 ± 0.10
GRACE-based estimates of total land water storage (not including glaciers) (Reager et al., 2016; Rietbroek et al., 2016; Scanlon et al., 2018)		-0.20 to -0.33 (±0.09–0.16)

dominated by a spherical harmonic contribution of degree $l = 2$ and order $m = \pm 1$. Since N_{gia} has a smooth spatial pattern, the global GIA correction to altimetry data can be obtained by simply subtracting its average $n = \langle N_{\text{gia}} \rangle$ over the ocean sampled by the altimetry missions. The computation of the GIA contribution N_{gia} has been the subject of various investigations, based on different GIA models. The estimate by Peltier (2001) of $n = -0.30 \text{ mm yr}^{-1}$ is based on the ICE-4G (VM2) GIA model. Such a value has been adopted in the majority of studies estimating the GMSL rise from altimetry. Since n appears to be small compared to the global mean sea-level rise from altimetry ($\sim 3 \text{ mm yr}^{-1}$), a more precise evaluation has not been of concern until recently. However, it is important to notice that n is of comparable magnitude as the GMSL trend uncertainty, currently estimated to be $\sim 0.3 \text{ mm yr}^{-1}$ (see Sect. 2.2). In Table 9a, we summarize the values of n according to works in the literature where various GIA model models and averaging methods have been employed. Based on values in Table 9a for which a standard deviation is available, the average of n (weighted by the inverse of associated errors), assumed to represent the best estimate, is $n = (-0.29 \pm 0.02) \text{ mm yr}^{-1}$, where the uncertainty corresponds to 2σ .

2.8.2 GIA correction to GRACE-based ocean mass

GRACE observations of present-day gravity variations are sensitive to GIA, due to the sheer amount of rock material that is transported by GIA throughout the mantle and the resulting changes in surface topography, especially over the

formerly glaciated areas. The continuous change in the gravity field results in a nearly linear signal in GRACE observations. Since the gravity field is determined by global mass redistribution, GIA models used to correct GRACE data need to be global as well, especially when the region of interest is represented by all ocean areas. To date, the only global ice reconstruction publicly available is provided by the University of Toronto. Their latest product, named ICE-6G, has been published and distributed in 2015 (Peltier et al., 2015); note that the ice history has been simultaneously constrained with a specific Earth model, named VM5a. During the early period of the GRACE mission, the available Toronto model was ICE-5G (VM2) (Peltier, 2004). However, different groups have independently computed GIA model solutions based on the Toronto ice history reconstruction, by using different implementations of GIA codes and somehow different Earth models. The most widely used model is the one by Paulson et al. (2007), later updated by A et al. (2013). Both studies use a deglaciation history based on ICE-5G, but differ for the viscosity profile of the mantle: A et al. (2013) use a 3-D compressible Earth with VM2 viscosity profile and a PREM-based elastic structure used by Peltier (2004), whereas Paulson et al. (2007) use an incompressible Earth with self-gravitation, and a Maxwell 1-D multilayer mantle. Over most of the oceans, the GIA signature is much smaller than over the continents. However, once integrated over the global ocean, the signal w due to GIA is about -1 mm yr^{-1} of equivalent sea-level change (Chambers et al., 2010), which is of the same order of magnitude as the total ocean mass

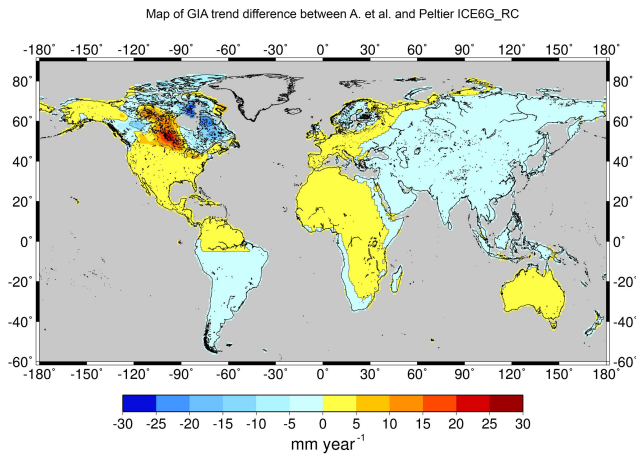


Figure 13. Difference map between two models of GIA correction to GRACE over land: A et al. (2013) versus Peltier et al. (2015). Units in millimeters per year of SLE.

change induced by increased ice melt (Leuliette and Willis, 2011). The main uncertainty in the GIA contribution to ocean mass change estimates, apart from the general uncertainty in ice history and Earth mechanical properties, originates from the importance of changes in the orientation of the Earth’s rotation axis (Chambers et al., 2010; Tamisiea, 2011). Different choices in implementing the so-called “rotational feedback” lead to significant changes in the resulting GIA contribution to GRACE estimates. The issue of properly accounting for rotational effects has not been settled yet (Mitrovica et al., 2005; Peltier and Luthcke, 2009; Mitrovica and Wahr, 2011; Martinec and Hagedoorn, 2014). Table 9b summarizes the values of the mass-rate GIA contribution w according to the literature, where various models and averaging methods are employed. The weighted average of the values in Table 9b, for which an assessment of the standard deviation is available, is $w = (-1.44 \pm 0.36) \text{ mm yr}^{-1}$ (the uncertainty is 2σ), which we assume represents the preferred estimate.

2.8.3 GIA correction to GRACE-based terrestrial water storage

As discussed in the previous section, the GIA correction to apply to GRACE over land is significant, especially in regions formerly covered by the ice sheets (Canada and Scandinavia). Over Canada, GIA models significantly differ. This is illustrated in Fig. 13, which shows difference between two models of GIA correction to GRACE over land, the A et al. (2013) and Peltier et al. (2009) models. We see that over the majority of the land areas, differences are small, except over northern Canada, in particular around the Hudson Bay, where differences larger than $\pm 20 \text{ mm yr}^{-1}$ SLE are noticed. This may affect GRACE-based TWS estimates over Canadian river basins.

When averaged over the whole land surface as done in some studies to estimate the combined effect of land water storage and glacier melting from GRACE (e.g., Reager et al., 2016; see Sect. 2.7), the GIA correction ranges from ~ 0.5 to 0.7 mm yr^{-1} (in mm yr^{-1} SLE). Values for different GIA models are given in Table 9c.

2.8.4 GIA correction to GRACE-based ice sheet mass balance

The GRACE gravity field observations allow the determination of mass balances of ice sheets and large glacier systems with inaccuracy similar or superior to the input–output method or satellite laser and radar altimetry (Shepherd et al., 2012). However, GRACE ice-mass balances rely on successfully separating and removing the apparent mass change related to GIA. While the GIA correction is small compared to the mass balance for the Greenland ice sheet (ca. $< 10\%$), its magnitude and uncertainty in Antarctica is on the order of the ice-mass balance itself (e.g., Martín-Español et al., 2016). Particularly for today’s glaciated areas, GIA remains poorly resolved due to the sparse data constraining the models, leading to large uncertainties in the climate history, the geometry and retreat chronology of the ice sheet, as well as the Earth structure. The consequences are ambiguous GIA predictions, despite fitting the same observational data. There are two principal approaches towards resolving GIA underneath the ice sheets. Empirical estimates can be derived that make use of the different sensitivities of satellite observations to ice-mass changes and GIA (e.g., Riva et al., 2009, 2010; Wu et al., 2010). Alternatively, GIA can be modeled numerically by forcing an Earth model with a fixed ice retreat scenario (e.g., Peltier, 2009; Whitehouse et al., 2012) or with output from a thermodynamic ice sheet model (Gomez et al., 2013; Konrad et al., 2015). Values of GIA-induced apparent mass change for Greenland and Antarctica as listed in the literature should be applied with caution (Table 9d) when applying them to GRACE mass balances. Each of these estimates may rely on a different GRACE postprocessing strategy and may differ in the approach used for solving the gravimetric inverse problem (mascon analysis, forward-modeling, averaging kernels). Of particular concern is the modeling and filtering of the pole tide correction caused by the rotational variations related to GIA, affecting coefficients of harmonic degree $l = 2$ and order $m = \pm 1$. As mentioned above, agreement on the modeling of the rotational feedback has not been reached within the GIA community. Furthermore, the pole tide correction applied during the determination gravity-field solutions differs between the GRACE processing centers and may not be consistent with the GIA correction listed. This inconsistency may introduce a significant bias in the ice-mass balance estimates (e.g., Sasgen et al., 2013, Supplement). Wahr et al. (2015) presented recommendations on how to treat the pole tides in GRACE analysis. However, a systematic intercomparison of the GIA predictions in terms of

their low-degree coefficients and their consistency with the GRACE processing standards still need to be done.

The GRACE-based ocean mass, Antarctica mass and terrestrial water storage changes are very model dependent. As these GIA corrections cannot be assessed from independent information, they represent a large source of uncertainties to the sea-level budget components based on GRACE.

2.9 Ocean mass change from GRACE

Since 2002, GRACE satellite gravimetry has provided a revolutionary means for measuring global mass change and redistribution at monthly intervals with unprecedented accuracy, and offered the opportunity to directly estimate ocean mass change due to water exchange between the ocean and other components of the Earth (e.g., ice sheets, mountain glaciers, terrestrial water). GRACE time-variable gravity data have been successfully applied in a series of studies of ice mass balance of polar ice sheets (e.g., Velicogna and Wahr, 2006; Luthcke et al., 2006) and mountain glaciers (e.g., Tamisiea et al., 2005; J. Chen et al., 2007) and their contributions to global sea-level change. GRACE data can also be used to directly study long-term oceanic mass change or nonsteric sea-level change (e.g., Willis et al., 2008; Leuliette and Miller, 2009; Cazenave et al., 2009), and provide a unique opportunity to study interannual or long-term TWS change and its potential impacts on sea-level change (Richey et al., 2015; Reager et al., 2016).

GRACE time-variable gravity data can be used to quantify ocean mass change from three different main approaches. One is through measuring ice mass balance of polar ice sheets and mountain glaciers and variations of TWS, and their contributions to the GMSL (e.g., Velicogna and Wahr, 2006; Schrama et al., 2014). The second approach is to directly quantify ocean mass change using ocean basin mask (kernel) (e.g., A and Chambers, 2008; Llovel et al., 2010; Johnson and Chambers, 2013). In the ocean basin kernel approach, coastal ocean areas within certain distance (e.g., 300 or 500 km) from the coast are excluded, in order to minimize contaminations from mass change signal over the land (e.g., glacial mass loss and TWS change). The third approach solves mass changes on land and over ocean at the same time via forward modeling (e.g., Chen et al., 2013; Yi et al., 2015). The forward modeling is a global inversion to reconstruct the “true” mass change magnitudes over land and ocean with geographical constraint of locations of the mass change signals, and can help effectively reduce leakage between land and ocean (Chen et al., 2013).

Estimates of ocean mass changes from GRACE are subject to a number of major error sources. These include (1) leakage errors from the larger signals over ice sheets and land hydrology due to GRACE’s low spatial resolution (of at least a few to several hundred kilometers) and the need for coastal masking, (2) spatial filtering of GRACE data to reduce spatial noise, (3) errors and biases in geophysical model correc-

tions (e.g., GIA, atmospheric mass) that need to be removed from GRACE observations to isolate oceanic mass change and/or polar ice sheets and mountain glaciers mass balance, and (4) residual measurement errors in GRACE gravity measurements, especially those associated with GRACE low-degree gravity changes. In addition, how to deal with the absent degree-1 terms, i.e., geocenter motion in GRACE gravity fields, is expected to affect estimates of GRACE-based oceanic mass rates and ice mass balances.

With a different treatment of the GRACE land–ocean signal leakage effect through global forward modeling, Chen et al. (2013) estimated ocean mass rates using GRACE RL05 time-variable gravity solutions over the period 2005–2011. They demonstrated that the ocean mass change contributes up to $1.80 \pm 0.47 \text{ mm yr}^{-1}$ (over the same period), which is significantly larger than previous estimates over about the same period. Yi et al. (2015) further confirmed that correct calibration of GRACE data and appropriate treatment of GRACE leakage bias are critical to improve the accuracy of GRACE-estimated ocean mass rates. Table 10 summarizes different estimates of GRACE ocean mass rates. The uncertainty estimates of the listed studies (Table 10) are computed from different methods, with different considerations of error sources into the error budget, and represent different confidence levels.

As demonstrated in Chen et al. (2013), different treatments of just the degree-2 spherical harmonics of the GRACE gravity solution alone can lead to substantial differences in GRACE-estimated ocean mass rates (ranging from 1.71 to 2.17 mm yr^{-1}). Similar estimates from GRACE gravity solutions from different data processing centers can also be different. In the meantime, long-term degree-1 spherical harmonics variation, representing long-term geocenter motion and neglected in some of the previous studies (due to the lack of accurate observations) are also expected to have a non-negligible effect on GRACE-derived ocean mass rates (Chen et al., 2013). Different methods for computing ocean mass change using GRACE data may also lead to different estimates (Chen et al., 2013; Johnson and Chambers, 2013; Jensen et al., 2013).

To help better understand the potential and uncertainty of GRACE satellite gravimetry in quantification of the ocean mass rate, Table 11 provides a comparison of GRACE-estimated ocean mass rates over the period January 2005 to December 2016 based on different GRACE data products and different data processing methods, including the CSR, GFZ and JPL GRACE RL05 spherical harmonic solutions (i.e., the so-called GSM solutions), as well as CSR, JPL and GSFC mascon solutions (the available GSFC mascons only cover the period up to July 2016). The three GRACE GSM results (CSR, GFZ and JPL) are updates from Johnson and Chambers (2013), with degree-2 zonal term replaced by satellite laser ranging results (Cheng and Ries, 2012), geocenter motion from Swenson et al. (2008), GIA model from A et al. (2013), an averaging kernel with a land mask

Table 9. Estimated contributions of GIA to the rate of absolute sea-level change observed by altimetry (a), to the rate of mass change observed by GRACE over the global oceans (b), to the rate of mass change observed by GRACE over land (c), and to Greenland and Antarctic ice sheets (c), during the altimetry era. The GIA corrections are expressed in millimeters per year SLE except over Greenland and Antarctica where values are given in gigatons per year (ice mass equivalent). Most of the GIA contributions are expressed as a value ± 1 standard deviation; a few others are given in terms of a plausible range, and for some the uncertainties are not specified.

(a) GIA correction to absolute sea level measured by altimetry		
Reference	GIA (mm yr ⁻¹ SLE)	Notes
Peltier (2009) (Table 3)	-0.30 \pm 0.02 -0.29 \pm 0.03 -0.28 \pm 0.02	Average of three groups of four values obtained by variants of the analysis procedure, using ICE-5G(VM2), over a global ocean, in the range of latitudes 66° S to 66° N and 60° S to 60° N, respectively.
Tamisiea (2011) (Fig. 2)	-0.15 to -0.45 -0.20 to -0.50	Simple average over the oceans for a range of estimates obtained varying the Earth model parameters, over a global ocean and between latitudes 66° S and 66° N.
Huang (2013) (Table 3.6)	-0.26 \pm 0.07 -0.27 \pm 0.08	Average from an ensemble of 14 GIA models over a global ocean and between latitude from 66° S to 66° N.
Spada (2017) (Table 1)	-0.32 \pm 0.08	Based on four runs of the sea-level equation solver SELEN (Spada and Stocchi, 2007) using model ICE-5G(VM2), with different assumptions in solving the SLE.
(b) GIA contribution to GRACE mass rate of change over the oceans		
Reference	GIA (mm yr ⁻¹ SLE)	Notes
Peltier (2009) (Table 3)	-1.60 \pm 0.30	Average of values from 12 corrections for variants of the analysis procedure, using ICE-5G (VM2).
Chambers et al. (2010) (Table 1)	-1.45 \pm 0.35	Average over the oceans for a range of estimates produced by varying the Earth models.
Tamisiea (2011) (Figs. 3 and 4)	-0.5 to -1.9 -0.9 to -1.5	Ocean average of a range of estimates varying the Earth model, and based on a restricted set, respectively.
Huang (2013) (Table 3.7)	-1.31 \pm 0.40 -1.26 \pm 0.43	Average from an ensemble of 14 GIA models over a global ocean and between latitude from 66° S to 66° N, respectively.
(c) GIA contribution to GRACE-based terrestrial water storage change		
Reference	GIA correction (mm yr ⁻¹ SLE) without Greenland, Antarctica, Iceland, Svalbard, Hudson Bay and the Black Sea	
A et al. (2013)	0.63	
Peltier ICE5G	0.68	
Peltier ICE6G_rc	0.71	
ANU_ICE6G	0.53	

that extends out 300 km, and no destriping or smoothing, as described in Johnson and Chambers (2013). An update of GRACE ocean mass rate from Chen et al. (2013) is also included for comparisons, which is based on the CSR GSM solutions using forward modeling (a global inversion approach), with similar treatments of the degree-2 zonal term, geocenter motion and GIA effects.

The JPL mascon ocean mass rate is computed from all mascon grids over the ocean, and the GSFC mascon ocean mass rate is computed from all ocean mascons, with the

Mediterranean, Black and Red seas excluded. A coastline resolution improvement (CRI) filter is already applied in the JPL mascons to reduce leakage (Wiese et al., 2016b), and in both the GSFC and JPL mascon solutions, the ocean and land are separately defined (Luthcke et al., 2013; Watkins et al., 2015). For the CSR mascon results, an averaging kernel with a land mask that extends out 200 km is applied to reduced leakage (Chen et al., 2017b). Similar treatments or corrections of degree-2 zonal term, geocenter motion and GIA effects are also applied in the three mascon solutions. When

Table 9. Continued.

(d) GIA contribution to GRACE mass rate of the ice sheets		
Reference	Greenland GIA (Gt yr ⁻¹)	Notes
Simpson et al. (2009) ^r	-3 ± 12 ^m	Thermodynamic sheet/solid Earth model, 1-D (uncoupled); constrained by geomorphology; inversion results in Sutterley et al. (2014).
Peltier (2009) (ICE-5G) ^b	-4 ^d	Ice load reconstruction/solid Earth model, 1-D (ICE-5G/similar to VM2); Greenland component of ICE-5G (13 Gt yr ⁻¹) + Laurentide component of ICE-5G (-17 Gt yr ⁻¹); inversion results in Khan et al. (2016), Discussion.
Khan et al. (2016) (GGG-1D) ^a	15 ± 10 ^f	Ice load reconstruction/solid Earth model, 1-D (uncoupled); constrained with geomorphology and GPS; Greenland component (+32 Gt yr ⁻¹) + Laurentide component of ICE-5G (-17 Gt yr ⁻¹); inversion results in Khan et al. (2016), Discussion.
Fleming and Lambeck (2004) ^a (Green1)	3 ^d	Ice load reconstruction/solid Earth model, 1-D (uncoupled); constrained with geomorphology; Greenland component (+20 Gt yr ⁻¹) + Laurentide component of ICE-5G (-17 Gt yr ⁻¹); inversion in Sasgen et al. (2012, Supplement).
Wu et al. (2010) ^b	-69 ± 19 ^m	Joint inversion estimate based on GPS, satellite laser ranging, and very long baseline interferometry, and bottom pressure from ocean model output; inversion results in Sutterley et al. (2014).
Reference	Antarctica GIA (Gt yr ⁻¹)	Notes
Whitehouse et al. (2012) (W12a) ^a	60 ^f	Thermodynamic sheet/solid Earth model, 1-D (uncoupled); constrained by geomorphology; inversion results in Shepherd et al. (2012), Supplement (Fig. S8).
Ivins et al. (2013) (IJ05_R2) ^a	40–65 ^f	Ice load reconstruction/solid Earth model, 1-D; constrained by geomorphology and GPS uplift rates; Ivins et al. (2013); inversion results in Shepherd et al. (2012), Supplement (Fig. S8).
Peltier (2009) (ICE-5G) ^b	140–180 ^f	Ice load reconstruction/solid Earth model ICE-5G(VM2); constrained by geomorphology; inversion results in Shepherd et al. (2012), Supplement (Fig. S8).
Argus et al. (2014) (ICE-6G) ^b	107 ^f	Ice load reconstruction/solid Earth model ICE-6G(VM5a); constrained by geomorphology and GPS; theory recently corrected by Purcell et al. (2016); inversion results in Argus et al. (2014), conclusion 7.8.
Sasgen et al. (2017) (REGINA) ^a	55 ± 22 ^f	Joint inversion estimate based on GRACE, altimetry, GPS and viscoelastic response functions; lateral heterogeneous Earth model parameters; inversion results in Sasgen et al. (2017), Table 1.
Gunter et al. (2014) (G14) ^a	ca. 64 ± 40 ^a (multimodel uncert.)	Joint inversion estimate based on GRACE, altimetry, GPS and regional climate model output; conversion of uplift to mass using average rock density; inversion results in, Gunter et al. (2014) Table 1.
Martín-Español et al. (2016) (RATES) ^a	55 ± 8 45 ± 7*	Joint inversion estimate based on GRACE, altimetry, GPS and regional climate model output; inversion results in Sasgen et al. (2017), * is improved for GIA of smaller spatial scales; inversion results in Martín-Español et al. (2016), Fig. 6.

^a Regional model. ^b Global model. ^c Mascon inversion. ^d Forward modeling inversion. ^e Averaging kernel inversion. ^f Inversion method not specified.

solving GRACE mascon solutions, the GRACE GAD fields (representing ocean bottom pressure changes, or combined atmospheric and oceanic mass changes) have been added back to the mascon solutions. To correctly quantify ocean mass change using GRACE mascon solutions, the means of the GAD fields over the oceans, which represents mean

atmospheric mass changes over the ocean (as ocean mass is conserved in the GAD fields) need to be removed from GRACE mascon solutions. The removal of GAD average over the ocean in GRACE mascon solutions has very minor or negligible effect (of ~ 0.02 mm yr⁻¹) on ocean mass rate

Table 10. Recently published (since 2013) estimates of GRACE-based ocean mass rates (GIA corrected). Most of the listed studies use either the A13 (A et al., 2013) or Paulson07 (Paulson et al., 2007) GIA model.

Data sources		Time period	Ocean mass trends (mm yr ⁻¹)
Chen et al. (2013)	(A13 GIA)	Jan 2005–Dec 2011	1.80 ± 0.47
Johnson and Chambers (2013)	(A13 GIA)	Jan 2003–Dec 2012	1.80 ± 0.15
Purkey et al. (2014)	(A13 GIA)	Jan 2003–Jan 2013	1.53 ± 0.36
Dieng et al. (2015a)	(Paulson07 GIA)	Jan 2005–Dec 2012	1.87 ± 0.11
Dieng et al. (2015b)	(Paulson07 GIA)	Jan 2005–Dec 2013	2.04 ± 0.08
Yi et al. (2015)	(A13 GIA)	Jan 2005–Jul 2014	2.03 ± 0.25
Rietbroek et al. (2016)		Apr 2002–Jun 2014	1.08 ± 0.30
Chambers et al. (2017)		2005–2015	2.11 ± 0.36

estimates, but is important for studying GMSL change at seasonal timescales.

Over the 12-year period (2005–2016), the three GRACE GSM solutions show pretty consistent estimates of ocean mass rate, in the range of 2.3 to 2.5 mm yr⁻¹. Greater differences are noticed for the mascon solutions. The GSFC mascons show the largest rate of 2.61 mm yr⁻¹. The CSR and JPL mascon solutions show relatively smaller ocean mass rates of 1.76 and 2.02 mm yr⁻¹, respectively, over the studied period. Based on the same CSR GSM solutions, the forward modeling and basin kernel estimates agree reasonably well (2.52 vs. 2.44 mm yr⁻¹). In addition to the degree-2 zonal term, geocenter motion, and GIA correction, the degree-2, order-1 spherical harmonics of the current GRACE RL05 solutions are affected by the definition of the reference mean pole in GRACE pole tide correction (Wahr et al., 2015). This mean pole correction, excluded in all estimates listed in Table 11 (for fair comparison), is estimated to contribute ~ -0.11 mm yr⁻¹ to GMSL. How to reduce errors from the different sources plays a critical role in estimating ocean mass change from GRACE time-variable gravity data.

GRACE satellite gravimetry has brought a completely new era for studying global ocean mass change. Owing to the extended record of GRACE gravity measurements (now over 15 years), improved understanding of GRACE gravity data and methods for addressing GRACE limitations (e.g., leakage and low-degree spherical harmonics), and improved knowledge of background geophysical signals (e.g., GIA), GRACE-derived ocean mass rates from different studies in recent years show clearly increased consistency (Table 11). Most of the results agree well with independent observations from satellite altimeter and Argo floats, although the uncertainty ranges are still large. The GRACE Follow-On (FO) mission was launched in May 2018. The GRACE and GRACE-FO together are expected to provide at least over 2 (or even 3) decades of time-variable gravity measurements. Continuous improvements of GRACE data quality (in future releases) and background geophysical models are also expected, which will help improve the accuracy GRACE observed ocean mass change.

For the sea-level budget assessment over the GRACE period, we use the ensemble mean.

3 Sea-level budget results

In Sect. 2, we have presented the different terms of the sea-level budget equation, mostly based on published estimates (and in some cases, from their updates). We now use them to examine the closure of the sea-level budget. For all terms, we only consider ensemble mean values.

3.1 Entire altimetry era (1993–present)

3.1.1 Trend estimates over 1993–present

Because it is now clear that the GMSL and some components are accelerating (e.g., Nerem et al., 2018), we propose to characterize the long-term variations of the time series by both a trend and an acceleration. We start by looking at trends. Table 12 gathers the trends estimated in Sect. 2. The end year is not always the same for all components (see Sect. 2). Thus the word “present” means either 2015 or 2016 depending on the component. As no trend estimate is available for the entire altimetry era for the terrestrial water storage contribution, we do not consider this component. The residual trend (GMSL minus sum of components trend) may then provide some constraint on the TWS contribution.

Results presented in Table 12 are discussed in detail in Sect. 4.

3.1.2 Acceleration

The GMSL acceleration estimated in Sect. 2.2 using Ablain et al.’s (2017b) TOPEX-A drift correction amounts to 0.10 mm yr⁻² for the 1993–2017 time span. This value is in good agreement with the Nerem et al. (2018) estimate (of 0.084 ± 0.025 mm yr⁻²) over nearly the same period, after removal of the interannual variability of the GMSL. In Nerem et al. (2018), acceleration of individual components are also estimated as well as acceleration of the sum of components. The latter agrees well with the GMSL acceleration.

Table 11. Ocean mass trends (in mm yr^{-1}) estimated from GRACE for the period January 2005–December 2016 (the GSFC mascon solutions cover up to July 2016). The uncertainty is based on 2 times the sigma of least-squares fitting.

Data sources	Ocean mass trend (mm yr^{-1})
GSM CSR forward modeling (update from Chen et al., 2013)	2.52 ± 0.17
GSM CSR (update from Johnson and Chambers, 2013)	2.44 ± 0.15
GSM GFZ (update from Johnson and Chambers, 2013)	2.30 ± 0.15
GSM JPL (update from Johnson and Chambers, 2013)	2.48 ± 0.16
Mascon CSR (200 km)	1.76 ± 0.16
Mascon JPL	2.02 ± 0.16
Mascon GSFC (update from Luthcke et al., 2013)	2.61 ± 0.16
Ensemble mean	2.3 ± 0.19

Table 12. Trend estimates for individual components of the sea-level budget, sum of components and GMSL minus sum of components over 1993–present. Uncertainties of the sum of components and residuals represent rooted mean squares of components errors, assuming that errors are independent.

Component	Trends (mm yr^{-1}) 1993–present
1. GMSL (TOPEX-A drift corrected)	3.07 ± 0.37
2. Thermosteric sea level (full depth)	1.3 ± 0.4
3. Glaciers	0.65 ± 0.15
4. Greenland	0.48 ± 0.10
5. Antarctica	0.25 ± 0.10
6. TWS	/
7. Sum of components (without TWS $\rightarrow 2.+3.+4.+5.$)	2.7 ± 0.23
8. GMSL minus sum of components (without TWS)	0.37 ± 0.3

Here we do not estimate the acceleration of the component ensemble means because time series are not always available. We leave this for a future assessment.

3.2 GRACE and Argo period (2005–present)

3.2.1 Sea-level budget using GRACE-based ocean mass

If we consider the ensemble mean trends for the GMSL, thermosteric and ocean mass components given in Sects. 2.2, 2.3 and 2.9 over 2005–present, we find agreement (within error bars) between the observed GMSL ($3.5 \pm 0.2 \text{ mm yr}^{-1}$) and the sum of Argo-based thermosteric plus GRACE-based ocean mass ($3.6 \pm 0.4 \text{ mm yr}^{-1}$) (see Table 13). The residual (GMSL minus sum of components) trend amounts to -0.1 mm yr^{-1} . Thus in terms of trends, the sea-level budget appears closed over this time span within quoted uncertainties.

3.2.2 Trend estimates over 2005–present from estimates of individual contributions

Table 13 gathers trends of individual components of the sea-level budget over 2005–present, as well as the trend of the sum of components and residuals (GMSL minus sum of components). As for the longer period, ensemble mean values are considered for each component.

As for Table 12, the results presented in Table 13 are discussed in detail in Sect. 4.

3.2.3 Year-to-year budget over 2005–present using GRACE-based ocean mass

We now examine the year-to-year sea-level and mass budgets. Table 14 provides annual mean values for the ensemble mean GMSL, GRACE-based ocean mass and Argo-based thermosteric component. The components are expressed as anomalies and their reference is arbitrary. So to compare with the GMSL, a constant offset for all years was applied to the thermosteric and ocean mass annual means. The reference year (where all values are set to zero) is 2003.

Figure 14 shows the sea-level budget over 2005–2015 in terms of an annual bar chart using values given in Table 14. It compares for years 2005 to 2016 the annual mean GMSL (blue bars) and annual mean sum of thermosteric and GRACE-based ocean mass (red bars). Annual residuals are also shown (green bars). These are either positive or negative depending on the years. The trend of these annual residuals is estimated to be 0.135 mm yr^{-1} .

In Fig. 15 is also shown the annual sea-level budget over 2005–2015 but now using the individual components for the mass terms. As we have no annual estimates for TWS, we ignore it, so that the total mass includes only glaciers, Greenland and Antarctica. The annual residuals thus include the TWS component in addition to the missing contributions (e.g., deep ocean warming). For years 2006 to 2011, the residuals are negative, an indication of a negative TWS to sea level as suggested by GRACE results (Reager et al., 2016; Scanlon et al., 2018). But as of 2012, the residuals become

Table 13. Trend estimates for individual components of the sea-level budget, sum of components and GMSL minus sum of components over 2005–present.

Component	Trend (mm yr ⁻¹) 2005–present
1. GMSL	3.5 ± 0.2
2. Thermosteric sea level (full depth)	1.3 ± 0.4
3. Glaciers	0.74 ± 0.1
4. Greenland	0.76 ± 0.1
5. Antarctica	0.42 ± 0.1
6. TWS from GRACE (mean of Reager et al., 2016 and Scanlon et al., 2018)	-0.27 ± 0.15
7. Sum of components (2.+3.+4.+5.+6.)	2.95 ± 0.21
8. Sum of components (thermosteric full depth + GRACE-based ocean mass)	3.6 ± 0.4
9. GMSL minus sum of components (including GRACE-based TWS → 2.+3.+4.+5.+6.)	0.55 ± 0.3
10. GMSL minus sum of components (without GRACE-based TWS → 2.+3.+4.+5.)	0.28 ± 0.2
11. GMSL minus sum of components (thermosteric full depth + GRACE-based ocean mass)	-0.1 ± 0.3

Table 14. Annual mean values for the ensemble mean GMSL and sum of components (GRACE-based ocean mass and Argo-based thermosteric, full depth). Constant offset applied to the sum of components. The reference year (where all values are set to zero) is 2003.

Year	Ensemble mean GMSL (mm)	Sum of components (mm)	GMSL minus sum of components (mm)
2005	7.00	8.78	-0.78
2006	10.25	10.78	-0.53
2007	10.51	11.35	-0.85
2008	15.33	15.07	0.25
2009	18.78	18.88	-0.10
2010	20.64	20.53	0.11
2011	20.91	21.38	-0.48
2012	31.10	29.33	1.77
2013	33.40	33.87	-0.47
2014	36.65	36.22	0.43
2015	46.34	45.69	0.65

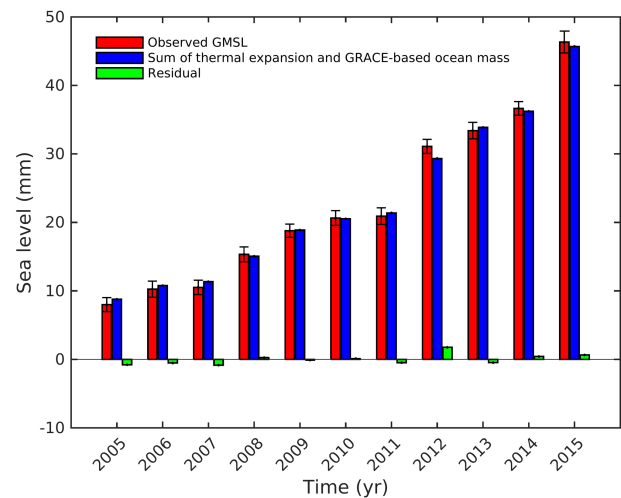


Figure 14. Annual sea level (blue bars) and sum of thermal expansion (full depth) and GRACE ocean mass component (red bars). Black vertical bars are associated uncertainties. Annual residuals (green bars) are also shown.

positive and on average over 2005–2015, the residual trend amounts to +0.28 mm yr⁻¹, a value larger than when using GRACE ocean mass.

Finally, Fig. 16 presents the mass budget. It compares annual GRACE-based ocean mass to the sum of the mass components, without TWS as in Fig. 15. The residual trend over the 2005–2015 time span is 0.14 mm yr⁻¹. It may dominantly represent the TWS contribution. From one year to another residuals can be either positive or negative, suggesting important interannual variability in the TWS or even in the deep ocean.

4 Discussion

The results presented in Sect. 2 for the components of the sea-level budget are based on syntheses of the recently pub-

lished literature. When needed, the time series have been updated. In Sect. 3, we considered ensemble means for each component to average out random errors of individual estimates. We examined the closure or nonclosure of the sea-level budget using these ensemble mean values, for two periods: 1993–present and 2005–present (Argo and GRACE period). Because of the lack of observation-based TWS estimates for the 1993–present time span, we compared the observed GMSL trend to the sum of components excluding TWS. We found a positive residual trend of 0.37 ± 0.3 mm yr⁻¹, supposed to include the TWS contribution, plus other imperfectly known contributions (deep ocean warming) and data errors.

For the 2005–present time span, we considered both GRACE-based ocean mass and the sum of individual mass

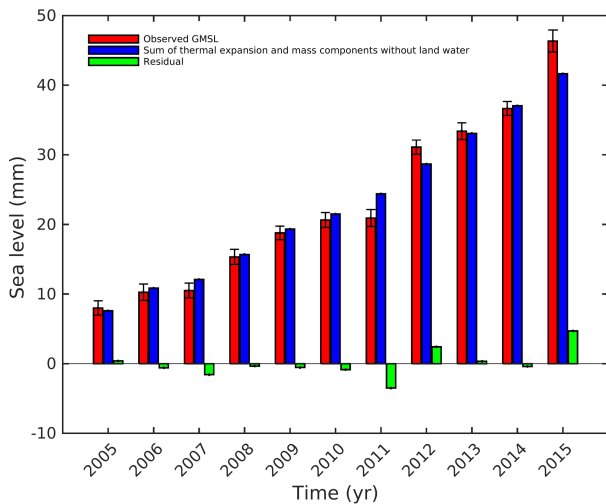


Figure 15. Annual global mean sea level (blue bars) and sum components without TWS (full depth thermal expansion + glaciers + Greenland + Antarctica) (red bars). Black vertical bars are associated uncertainties. Annual residuals (green bars) are also shown.

components, allowing us to also look at the mass budget. For TWS, as discussed in Sect. 2.7, GRACE provides a negative trend contribution to sea level over the last decade (i.e., increase on water storage on land) attributed to internal natural variability (Reager et al., 2016), unlike hydrological models that lead to a small (possibly not significantly different from zero) positive contribution to sea level over the same period. Assuming that GRACE observations are perfect, such discrepancies could be attributed to the inability of models to correctly account for uncertainties in meteorological forcing and inadequate modeling of soil storage capacity (see discussion in Sect. 2.7). However, when looking at the sea-level budget over the GRACE time span and using the GRACE-based TWS, we find a rather large positive residual trend ($> 0.5 \text{ mm yr}^{-1}$) that needs to be explained. Since GRACE-based ocean mass is supposed to represent all mass terms, one may want to attribute this residual trend to an additional contribution of the deep ocean to the abyssal contribution already taken into account here, but possibly underestimated because of incomplete monitoring by current observing systems. If such a large positive contribution from the deep ocean (meaning ocean warming) is real (which is unlikely, given the high implied heat storage), this has to be confirmed by independent approaches, e.g., using ocean reanalysis, and eventually model-based and top-of-the-atmosphere estimates of the Earth energy imbalance.

In addition to mean trends over the period, we also looked at the annual budget for all years, starting in 2005. For most components, annual mean values are provided during the Argo-GRACE era, except for the terrestrial water storage component. However, the sea-level budget based on GRACE ocean mass (plus ocean thermal expansion; Fig. 14) includes

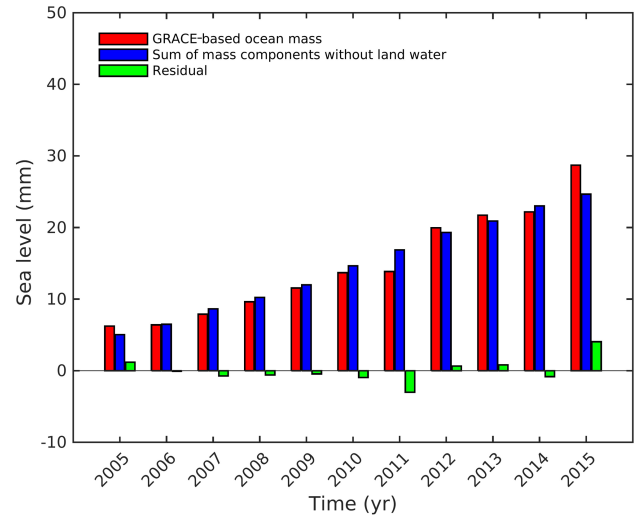


Figure 16. Annual GRACE-based ocean mass (red bars) and sum components without TWS (full depth thermal expansion + glaciers + Greenland + Antarctica) (blue bars). Annual residuals (green bars) are also shown.

the TWS contribution. As shown in Fig. 14, yearly residuals are small, suggesting near closure of the sea-level budget. The residual trend amounts to 0.13 mm yr^{-1} . It could be interpreted as an additional deep ocean contribution not accounted by the SIO estimate (see Sect. 2.3). However, when looking at Fig. 14, we note that yearly residuals are either positive or negative, an indication of interannual variability that can hardly be explained by a deep ocean contribution. The residual trend derived from the difference (GMSL minus sum of components) (Table 13) amounts $-0.1 \pm 0.3 \text{ mm yr}^{-1}$, suggesting a sea-level budget closed within 0.3 mm yr^{-1} over 2005–present, with no substantial deep ocean contribution.

Figure 16 compares GRACE ocean mass to the sum of mass components (excluding TWS, for the reasons mentioned above). In principle, this mass budget may provide a constraint on the TWS contribution. The corresponding residual trend amounts to 0.14 mm yr^{-1} over the GRACE period, a value that disagrees with the above-quoted GRACE-based TWS estimates. However, it is worth noting that the GRACE-based TWS trend is very dependent on the considered time span because of the strong interannual variability; a recent study by Palanisamy et al. (2018), based on 347 land river basins, found GRACE-based TWS trend of zero over 2005–2015. Given the remaining data uncertainties, any robust conclusion can hardly be reached so far. That being said, more work is needed to clarify the sign discrepancy between GRACE-based and model-based TWS estimates.

5 Data availability

The data sets used in this study are freely available at <https://doi.org/10.17882/54854>. We provide annual mean

time series (expressed in millimeters of equivalent sea level) between 2005 and 2015 for all components of the sea level budget: (1) global mean sea level (GMSL, GMSL.txt as data file) time series from multi-mission satellite altimetry; ensemble mean of six different sea level products (AVISO/CNES, CSIRO, University of Colorado, ESA SL_cci, NASA/GSFC, NOAA). (2) Global mean ocean thermal expansion (Steric.txt as data file) time series: ensemble mean from 10 processing groups (CORA, CSIRO, ACECRC/IMAS-UTAS, ICCES, ICDC, IPRC, JAMSTEC, MRI/JMA, NECI/NOAA, SIO). (3) Glacier contribution (Glaciers.txt) from 5 different products (update of Gardner et al., 2013, update of Marzeion et al., 2012, update of Cogley, 2009, update of Leclercq et al., 2011 and average of GRACE-based estimates of Marzeion et al., 2017). (4) Greenland ice sheet contribution (GreenlandIcesheet.txt as data file): ensemble mean from eight different products (Update from Barletta et al., 2013, Groh and Horwath, 2016, Update from Luthcke et al., 2013, Update from Sasgen et al., 2012, Update from Schrama et al., 2014, Update from van den Broeke et al., 2016, Wiese et al., 2016b, Update from Wouters et al., 2008). (5) Antarctica ice sheet contribution (AntarcticIcesheet.txt as data file): ensemble mean from 11 different products (Updated Martin-Espagnol et al., 2016, Updated Fosberg et al., 2017, Updated Groh and Horwath, 2016, Updated Luthcke et al., 2013, Updated Sasgen et al., 2013, Updated Velicogna et al., 2014, Updated Wiese et al., 2016, Updated from Wouters et al., 2013, Updated Rignot et al., 2011, Update Schrama et al., 2014 version 1, Update Schrama et al., 2014 version 2). We also provide the GRACE-based ocean mass time series that is an ensemble mean of seven different products (GSM CSR Forward Modeling (update from Chen et al., 2013), GSM CSR (update from Johnson and Chambers, 2013), GSM GFZ (update from Johnson and Chambers, 2013), GSM JPL (update from Johnson and Chambers, 2013), Mascon CSR (200 km), Mascon JPL, Mascon GSFC (update from Luthcke et al., 2013)).

6 Concluding remarks

As mentioned in the introduction, the global mean sea-level budget has been the subject of numerous previous studies, including successive IPCC assessments of the published literature. What is new in the effort presented here is that it involves the international community currently studying present-day sea level and its components. Moreover, it relies on a large variety of datasets derived from different space-based and in situ observing systems. The near closure of the sea-level budget, as reported here over the GRACE and Argo era, suggests that no large systematic errors affect these independent observing systems, including the satellite altimetry system. Study of the sea-level budget allows improved understanding of the different processes causing sea-level rise, such as ocean warming and land ice melt. When accuracy in-

creases, it will offer an integrative view of the response of the Earth system to natural and anthropogenic forcing and internal variability, and provide an independent constraint on the current Earth energy imbalance. Validation of climate models against observations is another important application of this kind of assessment (e.g., Slangen et al., 2017).

However, important uncertainties still remain, which affect several terms of the budget; for example the GIA correction applied to GRACE data over Antarctica or the net land water storage contribution to sea level. The latter results from a variety of factors but is dominated by groundwater pumping and natural climate variability. Both terms are still uncertain and accurately quantifying them remains a challenge.

Several ongoing international projects related to sea level should provide, in the near future, improved estimates of the components of the sea-level budget. This is the case, for example, of the ice sheet mass balance intercomparison exercise (IMBIE, second assessment), a community effort supported by NASA (National Aeronautics and Space Administration) and ESA, dedicated to reconciling satellite measurements of ice sheet mass balance (The IMBIE Team, 2018). This is also the case for the ongoing ESA Sea Level Budget Closure project (Horwath et al., 2018) that uses a number of space-based essential climate variables (ECVs) reprocessed during the last few years in the context of the ESA Climate Change Initiative project. The recently launched GRACE follow-on mission will lengthen the current mass component time series, with hopefully increased precision and resolution. Finally, the deep Argo project, still in an experimental phase, will provide important information on the deep ocean heat content in the coming years. Availability of this new dataset will provide new insights into the total thermosteric component of the sea-level budget, allowing other missing or poorly known contributions to be constrained from the evaluation of the budget.

The sea-level budget assessment discussed here essentially relies on trend estimates. But annual budget estimates have been proposed for the first time over the GRACE-Argo era. It is planned to provide updates of the global sea-level budget every year, as done for more than a decade for the global carbon budget (Le Queré et al., 2018). In the next assessments, updates of all components will be considered, accounting for improved evaluation of the raw data, improved processing and corrections, use of ocean reanalysis, etc. The need for additional information where gaps exist should also be considered. As a closing remark, study of the sea-level budget in terms of time series and not just trends, as done here, will be required.

Author contributions. This community assessment was initiated by AC and BM as a contribution to the Grand Challenge “Regional Sea Level and Coastal Impacts” of the World Climate Research Programme (WCRP). The results presented in this paper were prepared by nine different teams dedicated to the various terms of the sea-

level budget (i.e., altimetry-based sea level, tide gauges, thermal expansion, glaciers, Greenland, Antarctica, terrestrial water storage, glacial isostatic adjustment, ocean mass from GRACE). Thanks to the team leaders (in alphabetic order) MA, JB, NC, JC, CD, SJ, JTR, KvS, GS, IV and RvdW, who interacted with their team members, collected all needed information, provided a synthesized assessment of the literature and when needed, updated the published results. The coordinators AC and BM collected those materials and prepared a first draft of the paper, but all authors contributed to its refinement and to the discussion of the results. Special thanks are addressed to JB, EB, GC, JC, GJ (PMEL Contribution Number 4776), BM, FP, RP and ES for improving the successive versions of the paper, and to HP for providing all figures presented in Sect. 3.

The views, opinions and findings contained in this paper are those of the authors and should not be construed as an official position, policy or decision of the NOAA, US Government or other institutions.

Competing interests. The authors declare that they have no conflict of interest.

Acknowledgements. We are grateful to the anonymous reviewer for his/her thorough comments that helped to improve the paper.

Edited by: Giuseppe M. R. Manzella
Reviewed by: one anonymous referee

References

- A. G. and Chambers, D. P.: Calculating trends from GRACE in the presence of large changes in continental ice storage and ocean mass, *Geophys. J. Int.*, 272, <https://doi.org/10.1111/j.1365-246X.2008.04012.x>, 2008.
- A. G., Wahr, J., and Zhong, S.: Computations of the viscoelastic response of a 3-D compressible Earth to surface loading: an application to Glacial Isostatic Adjustment in Antarctica and Canada, *Geophys. J. Int.*, 192.2, 557–572, 2013.
- Ablain, M., Cazenave, A., Valladeau, G., and Guinehut, S.: A New Assessment of the Error Budget of Global Mean Sea Level Rate Estimated by Satellite Altimetry over 1993–2008, *Ocean Sci.*, European Geosciences Union, 2009, 5, 193–201, <https://doi.org/10.5194/os-5-193-2009>, 2009.
- Ablain, M., Philipps, S., Urvoy, M., Tran, N., and Picot, N.: Detection of Long-Term Instabilities on Altimeter Backscatter Coefficient Thanks to Wind Speed Data Comparisons from Altimeters and Models, *Mar. Geod.*, 35 (sup1), 258–75, <https://doi.org/10.1080/01490419.2012.718675>, 2012.
- Ablain, M., Cazenave, A., Larnicol, G., Balmaseda, M., Cipollini, P., Faugère, Y., Fernandes, M. J., Henry, O., Johannessen, J. A., Knudsen, P., and Andersen, O.: Improved Sea Level Record over the Satellite Altimetry Era (1993–2010) from the Climate Change Initiative Project, *Ocean Sci.*, 11, 67–82, <https://doi.org/10.5194/os-11-67-2015>, 2015.
- Ablain, M., Legeais, J. F., Prandi, P., Marcos, M., Fenoglio-Marc, L., Dieng, H. B., Benveniste, J., and Cazenave, A.: Satellite Altimetry-Based Sea Level at Global and Regional Scales, *Surv. Geophys.*, 38, 7–31, <https://doi.org/10.1007/s10712-016-9389-8>, 2017a.
- Ablain, M., Jugier, R., Zawadki, L., and Taburet, N.: The TOPEX-A Drift and Impacts on GMSL Time Series, AVISO Website, October 2017, available at: https://meetings.aviso.altimetry.fr/fileadmin/user_upload/tx_ausyclsseminar/files/Poster_OSTST17_GMSL_Drift_TOPEX-A.pdf, last access: October 2017b.
- Abraham, J. P., Baringer, M., Bindoff, N. L., Boyer, T., Cheng, L. J., Church, J. A., Conroy, J. L., Domingues, C. M., Fasullo, J. T., Gilson, J., and Goni, G.: A review of global ocean temperature observations: Implications for ocean heat content estimates and climate change, *Rev. Geophys.*, 51, 450–483, <https://doi.org/10.1002/rog.20022>, 2013.
- Argus, D. F., Peltier, W. R., and Drummond, R.: The Antarctica component of postglacial rebound model ICE-6G_C (VM5a) based on GPS positioning, exposure age dating of ice thicknesses, and relative sea level histories, *Geophys. J. Int.*, 198, 537–563, 2014.
- Bahr, D. B. and Radić, V.: Significant contribution to total mass from very small glaciers, *The Cryosphere*, 6, 763–770, <https://doi.org/10.5194/tc-6-763-2012>, 2012.
- Bahr, D., Pfeffer, W., Sassolas, C., and Meier, M.: Response time of glaciers as a function of size and mass balance: 1. Theory, *J. Geophys. Res.-Solid Earth*, 103, 9777–9782, 1998.
- Bamber, J. L., Westaway, R. M., Marzeion, B., and Wouters, B.: The land ice contribution to sea level during the satellite era, *Environ. Res. Lett.*, 13, 063008, <https://doi.org/10.1088/1748-9326/aac2f0>, 2018.
- Barletta, V. R., Sørensen, L. S., and Forsberg, R.: Scatter of mass changes estimates at basin scale for Greenland and Antarctica, *The Cryosphere*, 7, 1411–1432, <https://doi.org/10.5194/tc-7-1411-2013>, 2013.
- Barnett, T. P.: The estimation of “global” sea level change: A problem of uniqueness, *J. Geophys. Res.*, 89, 7980–7988, 1984.
- Beck, H. E., van Dijk, A. I. J. M., de Roo, A., Dutra, E., Fink, G., Orth, R., and Schellekens, J.: Global evaluation of runoff from 10 state-of-the-art hydrological models, *Hydrol. Earth Syst. Sci.*, 21, 2881–2903, <https://doi.org/10.5194/hess-21-2881-2017>, 2017.
- Beckley, B. D., Callahan, P. S., Hancock, D. W., Mitchum, G. T., and Ray, R. D.: On the ‘Cal-Mode’ Correction to TOPEX Satellite Altimetry and Its Effect on the Global Mean Sea Level Time Series, *J. Geophys. Res.-Oceans*, 122, 8371–8384, <https://doi.org/10.1002/2017jc013090>, 2017.
- Belward, A. S., Estes, J. E., and Kline, K. D.: The IGBP-DIS global 1-km land-cover data set DISCover: A project overview, *Photogramm. Eng. Remote Sens.*, 65, 1013–1020, 1999.
- Bolch, T., Sandberg Sørensen, L., Simonsen, S. B., Mölg, N., Machguth, H., Rastner, P., and Paul, F.: Mass loss of Greenland’s glaciers and ice caps 2003–2008 revealed from ICESat laser altimetry data, *Geophys. Res. Lett.*, 40, 875–881, 2013.
- Bosmans, J. H. C., van Beek, L. P. H., Sutanudjaja, E. H., and Bierkens, M. F. P.: Hydrological impacts of global land cover change and human water use, *Hydrol. Earth Syst. Sci.*, 21, 5603–5626, <https://doi.org/10.5194/hess-21-5603-2017>, 2017.
- Boyer, T., Domingues, C., Good, S., Johnson, G. C., Lyman, J. M., Ishii, M., Gouretski, V., Antonov, J., Bindoff, N., Church, J. A., Cowley, R., Willis, J., and Wijffels, S.: Sensitivity of global ocean heat content estimates to mapping methods, XBT bias cor-

- rections, and baseline climatology, *J. Climate*, 29, 4817–4842, <https://doi.org/10.1175/JCLI-D-15-0801.1>, 2016.
- Box, J. E. and Colgan, W. T.: Sea level rise contribution from Arctic land ice: 1850–2100, *Snow, Water, Ice and Permafrost in the Arctic (SWIPA) 2017*, Oslo, Norway: Arctic Monitoring and Assessment Programme (AMAP), 2017.
- Brun, F., Berthier, E., Wagnon, P., Käab, A., and Treichler, D.: A spatially resolved estimate of High Mountain Asia mass balances from 2000 to 2016, *Nat. Geosci.*, 10, 668–673, <https://doi.org/10.1038/NGEO2999>, 2017.
- Butt, N., de Oliveira, P. A., and Costa, M. H.: Evidence that deforestation affects the onset of the rainy season in Rondonia, Brazil, *J. Geophys. Res.-Atmos.*, 116, D11120, <https://doi.org/10.1029/2010jd015174>, 2011.
- Calafat, F. M., Chambers, D. P., and Tsimplis, M. N.: On the ability of global sea level reconstructions to determine trends and variability, *J. Geophys. Res.*, 119, 1572–1592, 2014.
- Cazenave, A., Dominh, K., Guinehut, S., Berthier, E., Llovel, W., Ramillien, G., Ablain, M., and Larnicol, G.: Sea level budget over 2003–2008: A reevaluation from GRACE space gravimetry, satellite altimetry and Argo, *Global Planet. Change*, 65, 83–88, <https://doi.org/10.1016/j.gloplacha.2008.10.004>, 2009.
- Cazenave, A., Dieng, H. B., Meyssignac, B., von Schuckmann, K., Decharme, B., and Berthier, E.: The Rate of Sea-Level Rise, *Nat. Clim. Change*, 4, 358–361, <https://doi.org/10.1038/nclimate2159>, 2014.
- Cazenave, A., Champollion, N., Paul, F., and Benveniste, J.: *Integrative Study of the Mean Sea Level and Its Components*, Space Science Series of ISSI, Springer, 416 pp., Vol. 58, 2017.
- Chagnon, F. J. F. and Bras, R. L.: Contemporary climate change in the Amazon, *Geophys. Res. Lett.*, 32, L13703, <https://doi.org/10.1029/2005gl022722>, 2005.
- Chambers, D. P., Wahr, J., Tamisiea, M. E., and Nerem, R. S.: Ocean mass from GRACE and glacial isostatic adjustment, *J. Geophys. Res.-Solid Earth*, 115, L11415, <https://doi.org/10.1029/2010JB007530>, 2010.
- Chambers, D. P., Cazenave, A., Champollion, N., Dieng, H. B., Llovel, W., Forsberg, R., von Schuckmann, K., and Wada, Y.: Evaluation of the Global Mean Sea Level Budget between 1993 and 2014, *Surv. Geophys.* 38, 309–327, <https://doi.org/10.1007/s10712-016-9381-3>, 2017.
- Chao, B. F., Wu, Y. H., and Li, Y. S.: Impact of artificial reservoir water impoundment on global sea level, *Science*, 320, 212–214, <https://doi.org/10.1126/science.1154580>, 2008.
- Chen, J. L., Wilson, C. R., Tapley, B. D., Blankenship, D. D., and Ivins, E. R.: Patagonia Icefield Melting Observed by GRACE, *Geophys. Res. Lett.*, 34, L22501, <https://doi.org/10.1029/2007GL031871>, 2007.
- Chen, J. L., Wilson, C. R., and Tapley, B. D.: Contribution of ice sheet and mountain glacier melt to recent sea level rise, *Nat. Geosci.*, 9, 549–552, <https://doi.org/10.1038/NGEO1829>, 2013.
- Chen, J. L., Wilson, C. R., Tapley, B. D., Save, H., and Cretaux, J.-F.: Long-term and seasonal Caspian Sea level change from satellite gravity and altimeter measurements, *J. Geophys. Res.-Solid Earth*, 122, 2274–2290, <https://doi.org/10.1002/2016JB013595>, 2017a.
- Chen, J., Famiglietti, J. S., Scanlon, B. R., and Rodell, M.: Groundwater Storage Changes: Present Status from GRACE Observations, *Surv. Geophys.*, 37, 397–417, <https://doi.org/10.1007/s10712-015-9332-4>, 2017b.
- Chen, X., Zhang, X., Church, J. A., Watson, C. S., King, M. A., Monselesan, D., Legresy, B., and Harig, C.: The Increasing Rate of Global Mean Sea-Level Rise during 1993–2014, *Nat. Clim. Change*, 7, 492–95, <https://doi.org/10.1038/nclimate3325>, 2017.
- Cheng, L., Trenberth, K., Fasullo, J., Boyer, T., Abraham, J., and Zhu, J.: Improved estimates of ocean heat content from 1960–2015, *Sci. Adv.*, 3, e1601545, <https://doi.org/10.1126/sciadv.1601545>, 2017.
- Cheng, M. K. and Ries, J. R.: Monthly estimates of C20 from 5 SLR satellites based on GRACE RL05 models, GRACE Technical Note 07, The GRACE Project, Center for Space Research, University of Texas at Austin, 2012.
- Choblet, G., Husson, L., and Bodin, T.: Probabilistic surface reconstruction of coastal sea level rise during the twentieth century, *J. Geophys. Res.*, 119, 9206–9236, 2014.
- Church, J. A. and White, N. J.: A 20th century acceleration in global sea-level rise, *Geophys. Res. Lett.*, 33, L01602, <https://doi.org/10.1029/2005GL024826>, 2006.
- Church, J. A. and White, N. J.: Sea-Level Rise from the Late 19th to the Early 21st Century, *Surv. Geophys.*, 32, 585–602, <https://doi.org/10.1007/s10712-011-9119-1>, 2011.
- Church, J. A., Gregory, J., White, N. J., Platten, S., and Mitrovica, J. X.: Understanding and Projecting Sea Level Change, *Oceanography*, 24, 130–143, <https://doi.org/10.5670/oceanog.2011.33>, 2011.
- Church, J. A., Clark, P. U., Cazenave, A., Gregory, J. M., Jevrejeva, S., Levermann, A., Merrifield, M. A., Milne, G. A., Nerem, R. S., Nunn, P. D., Payne, A. J., Pfeffer, W. T., Stammer, D., and Unnikrishnan, A. S.: Sea level change, in: *Climate Change 2013: The Physical Science Basis*, edited by: Stocker, T. F., Qin, D., Plattner, G.-K., Tignor, M., Allen, S. K., Boschung, J., Nauels, A., Xia, Y., Bex, V., and Midgley, P. M., Contribution of Working Group I to the Fifth Assessment Report of the Intergovernmental Panel on Climate Change (Cambridge University Press, Cambridge, United Kingdom and New York, NY, USA), 2013.
- Cogley, J.: Geodetic and direct mass-balance measurements: comparison and joint analysis, *Ann. Glaciol.*, 50, 96–100, 2009.
- Couhert, A., Cerri, L., Legeais, J. F., Ablain, M., Zelensky, N. P., Haines, B. J., Lemoine, F. G., Bertiger, W. I., Desai, S. D., and Otten, M.: Towards the 1mm/y Stability of the Radial Orbit Error at Regional Scales.” *Advances in Space Research: The Official J. Committ. Space Res.*, 55, 2–23, <https://doi.org/10.1016/j.asr.2014.06.041>, 2015.
- Dangendorf, S., Marcos, M., Müller, A., Zorita, E., Riva, R., Berk, K., and Jensen, J.: Detecting anthropogenic footprints in sea level rise, *Nat. Commun.*, 6, 7849, <https://doi.org/10.1038/ncomms8849>, 2015.
- Dangendorf, S., Marcos, M., Wöppelmann, G., Conrad, C. P., Frederikse, T., and Riccardo Riva, R.: Reassessment of 20th Century Global Mean Sea Level Rise, *Proc. Natl. Acad. Sci. USA*, 114, 5946–5951, <https://doi.org/10.1073/pnas.1616007114>, 2017.
- Darras, S.: IGBP-DIS wetlands data initiative, a first step towards identifying a global delineation of wetlands, IGBP-DIS Office, Toulouse, France, 1999.
- Davidson, N.C.: How much wetland has the world lost? Long-term and recent trends in global wetland area, *Mar. Freshw. Res.*, 65, 934–941 <https://doi.org/10.1071/Mf14173>, 2014.

- Decharme, B., Brun, E., Boone, A., Delire, C., Le Moigne, P., and Morin, S.: Impacts of snow and organic soils parameterization on northern Eurasian soil temperature profiles simulated by the ISBA land surface model, *The Cryosphere*, 10, 853–877, <https://doi.org/10.5194/tc-10-853-2016>, 2016.
- Dieng, H. B., Champollion, N., Cazenave, A., Wada, Y., Schrama, E. J. O., and Meyssignac, B.: Total land water storage change over 2003–2013 estimated from a global mass budget approach, *Environ. Res. Lett.*, 10, 124010, <https://doi.org/10.1088/1748-9326/10/12/124010>, 2015a.
- Dieng, H. B., Cazenave, A., von Schuckmann, K., Ablain, M., and Meyssignac, B.: Sea level budget over 2005–2013: missing contributions and data errors, *Ocean Sci.*, 11, 789–802, <https://doi.org/10.5194/os-11-789-2015>, 2015b.
- Dieng, H. B., Palanisamy, H., Cazenave, A., Meyssignac, B., and von Schuckmann, K.: The Sea Level Budget Since 2003: Inference on the Deep Ocean Heat Content, *Surv. Geophys.*, 36, 209–229, <https://doi.org/10.1007/s10712-015-9314-6>, 2015c.
- Dieng, H. B., Cazenave, A., Meyssignac, B., and Ablain, M.: New estimate of the current rate of sea level rise from a sea level budget approach, *Geophys. Res. Lett.*, 44, 3744–3751, <https://doi.org/10.1002/2017GL073308>, 2017.
- Döll, P., Fritsche, M., Eicker, A., and Mueller, S. H.: Seasonal water storage variations as impacted by water abstractions: Comparing the output of a global hydrological model with GRACE and GPS observations, *Surv. Geophys.*, 35, 1311–1331, <https://doi.org/10.1093/gji/ggt485>, 2014a.
- Döll, P., Müller, S. H., Schuh, C., Portmann, F. T., and Eicker, A.: Global-scale assessment of groundwater depletion and related groundwater abstractions: Combining hydrological modeling with information from well observations and GRACE satellites, *Water Resour. Res.*, 50, 5698–5720, <https://doi.org/10.1002/2014WR015595>, 2014b.
- Döll, P., Douville, H., Güntner, A., Müller Schmied, H., and Wada, Y.: Modelling freshwater resources at the global scale: Challenges and prospects, *Surv. Geophys.*, 37, 195–221, Special Issue: ISSI Workshop on Remote Sensing and Water Resources, 2017.
- Domingues, C., Church, J., White, N., Gleckler, P. J., Wijffels, S. E., Barker, P. M., and Dunn, J. R.: Improved estimates of upper ocean warming and multidecadal sea level rise, *Nature*, 453, 1090–1093, <https://doi.org/10.1038/nature07080>, 2008.
- Douglas, B.: Global sea level rise, *J. Geophys. Res.-Oceans*, 96, 6981–6992, 1991.
- Douglas, B.: Global sea rise: a redetermination, *Surv. Geophys.*, 18, 279–292, 1997.
- Douglas, B. C.: Sea level change in the era of recording tide gauges, in: *Sea Level Rise, History and Consequences*, 37–64, edited by: Douglas, B. C., Kearney, M. S., and Leatherman, S. P., Academic Press, San Diego, CA, 2001.
- Dutrieux, P., De Rydt, J., Jenkins, A., Holland, P. R., Ha, H. K., Lee, S. H., Steig, E. J., Ding, Q., Abrahamsen, E. P., and Schröder, M.: Strong sensitivity of Pine Island ice shelf melting to climatic variability, *Science*, 343, 174–178, <https://doi.org/10.1126/science.1244341>, 2014.
- Escudier, P., Ablain, M., Amarouche, L., Carrère, L., Couhert, A., Dibarboure, G., Dorandeu, J., Dubois, P., Mallet, A., Mercier, F., and Picard, B.: Satellite radar altimetry: principle, accuracy and precision, in: *Satellite altimetry over oceans and land surfaces*, edited by: Stammer, D. L. and Cazenave, A., 617 pp., CRC Press, Taylor and Francis Group, Boca Raton, New York, London, ISBN:13:978-1-4987-4345-7, 2018.
- FAO: Global forest resources assessment 2015: how have the world's forests changed?, Rome, 2015.
- Farinotti, D., Brinkerhoff, D. J., Clarke, G. K. C., Fürst, J. J., Frey, H., Gantayat, P., Gillet-Chaulet, F., Girard, C., Huss, M., Leclercq, P. W., Linsbauer, A., Machguth, H., Martin, C., Mausson, F., Morlighem, M., Mosbeux, C., Pandit, A., Portmann, A., Rabatel, A., Ramsankaran, R., Reerink, T. J., Sanchez, O., Stentoft, P. A., Singh Kumari, S., van Pelt, W. J. J., Anderson, B., Benham, T., Binder, D., Dowdeswell, J. A., Fischer, A., Helfricht, K., Kutuzov, S., Lavrentiev, I., McNabb, R., Gudmundsson, G. H., Li, H., and Andreassen, L. M.: How accurate are estimates of glacier ice thickness? Results from ITMIX, the Ice Thickness Models Intercomparison eXperiment, *The Cryosphere*, 11, 949–970, <https://doi.org/10.5194/tc-11-949-2017>, 2017.
- Farrell, W. and Clark, J.: On postglacial sea level, *Geophys. J. Int.*, 46.3, 647–667, 1976.
- Fasullo, J. T., Boening, C., Landerer, F. W., and Nerem, R. S.: Australia's unique influence on global sea level in 2010–2011, *Geophys. Res. Lett.*, 40, 4368–4373, <https://doi.org/10.1002/grl.50834>, 2013.
- Felfelani, F., Wada, Y., Longuevergne, L., and Pokhrel, Y. N.: Natural and human-induced terrestrial water storage change: A global analysis using hydrological models and GRACE, *J. Hydrol.*, 553, 105–118, 2017.
- Fleming, K. and Lambeck, K.: Constraints on the Greenland Ice Sheet since the Last Glacial Maximum from sea-level observations and glacial-rebound models, *Quatern. Sci. Rev.*, 23, 1053–1077, 2004.
- Forsberg, R., Sørensen, L., and Simonsen, S.: Greenland and Antarctica Ice Sheet Mass Changes and Effects on Global Sea Level, *Surv. Geophys.*, 38, 89–104, <https://doi.org/10.1007/s10712-016-9398-7>, 2017.
- Foster, S. and Loucks, D. P. (Eds.): *Non-Renewable Groundwater Resources: A guidebook on socially-sustainable management for water-policy makers*, IHP-VI, Series on Groundwater No. 10, UNESCO, Paris, France, 2006.
- Frederikse, T., Jevrejeva, S., Riva, R. E., and Dangendorf, S.: A consistent sea-level reconstruction and its budget on basin and global scales over 1958–2014, *J. Climate*, 31.3, 1267–1280, <https://doi.org/10.1175/JCLI-D-17-0502.1>, 2017.
- Frey, H., Machguth, H., Huss, M., Huggel, C., Bajracharya, S., Bolch, T., Kulkarni, A., Linsbauer, A., Salzmann, N., and Stoffel, M.: Estimating the volume of glaciers in the Himalayan-Karakoram region using different methods, *The Cryosphere*, 8, 2313–2333, <https://doi.org/10.5194/tc-8-2313-2014>, 2014.
- Gardner, A. S., Moholdt, G., Cogley, J. G., Wouters, B., Arendt, A. A., Wahr, J., Berthier, E., Hock, R., Pfeffer, W. T., Kaser, G., Ligtenberg, S. R. M., Bolch, T., Sharp, M. J., Hagen, J. O., van den Broeke, M. R., and Paul, F.: A reconciled estimate of glacier contributions to sea level rise: 2003 to 2009, *Science*, 340, 852–857, <https://doi.org/10.1126/science.1234532>, 2013.
- Gomez, N., Pollard, D., and Mitrovica, J. X.: A 3-D coupled ice sheet–sea level model applied to Antarctica through the last 40 ky, *Earth Planet. Sci. Lett.*, 384, 88–99, 2013.

- Gornitz, V.: Sea-level rise: A review of recent past and near-future trends, *Earth Surf. Process. Landf.*, 20, 7–20, <https://doi.org/10.1002/esp.3290200103>, 1995.
- Gornitz, V.: *Sea Level Rise: History and Consequences*, edited by: Douglas, B. C., Kearney, M. S., and Leatherman, S. P., 97–119, Academic Press, San Diego, CA, USA, 2001.
- Gornitz, V., Lebedeff, S., and Hansen, J.: Global sea level trend in the past century, *Science*, 215, 1611–1614, 1982.
- Gornitz, V., Rosenzweig, C., and Hillel, D.: Effects of anthropogenic intervention in the land hydrologic cycle on global sea level rise, *Global Planet. Change*, 14, 147–161, [https://doi.org/10.1016/s0921-8181\(96\)00008-2](https://doi.org/10.1016/s0921-8181(96)00008-2), 1997.
- Gouretski, V. and Koltermann, K.P.: How much is the ocean really warming?, *Geophys. Res. Lett.*, 34, L01610, <https://doi.org/10.1029/2006GL027834>, 2007.
- Gregory, J. M. and Lowe, J. A.: Predictions of global and regional sea-level rise using AOGCMs with and without flux adjustment, *Geophys. Res. Lett.*, 27, 3069–3072, 2000.
- Gregory, J. M., White, N. J., Church, J. A., Bierkens, M. F. P., Box, J. E., van den Broeke, M. R., Cogley, J. G., Fettweis, X., Hanna, E., Huybrechts, P., Konikow, L. F., Leclercq, P. W., Marzeion, B., Oerlemans, J., Tamisiea, M. E., Wada, Y., Wake, L. M., and van de Wal, R. S. W.: Twentieth-Century Global-Mean Sea Level Rise: Is the Whole Greater than the Sum of the Parts?, *J. Climate*, 26, 4476–4499, <https://doi.org/10.1175/JCLI-D-12-00319.1>, 2013.
- Grinsted, A.: An estimate of global glacier volume, *The Cryosphere*, 7, 141–151, <https://doi.org/10.5194/tc-7-141-2013>, 2013.
- Groh, A. and Horwath, M.: The method of tailored sensitivity kernels for GRACE mass change estimates, *Geophys. Res. Abstract.*, 18, EGU2016–12065, 2016.
- Gunter, B. C., Didova, O., Riva, R. E. M., Ligtenberg, S. R. M., Lenaerts, J. T. M., King, M. A., van den Broeke, M. R., and Urban, T.: Empirical estimation of present-day Antarctic glacial isostatic adjustment and ice mass change, *The Cryosphere*, 8, 743–760, <https://doi.org/10.5194/tc-8-743-2014>, 2014.
- Haerberli, W. and Linsbauer, A.: Brief communication “Global glacier volumes and sea level – small but systematic effects of ice below the surface of the ocean and of new local lakes on land”, *The Cryosphere*, 7, 817–821, <https://doi.org/10.5194/tc-7-817-2013>, 2013.
- Hamlington, B. D., Leben, R. R., Nerem, R. S., Han, W., and Kim, K. Y.: Reconstructing sea level using cyclostationary empirical orthogonal functions, *J. Geophys. Res.*, 116, C12015, <https://doi.org/10.1029/2011JC007529>, 2011.
- Hamlington, B. D., Thompson, P., Hammond, W. C., Blewitt, G., and Ray, R. D.: Assessing the impact of vertical land motion on twentieth century global mean sea level estimates, *J. Geophys. Res.-Oceans*, 121, 4980–4993, <https://doi.org/10.1002/2016JC011747>, 2016.
- Hay, C. C., Morrow, E., Kopp, R. E., and Mitrovica, J. X.: Probabilistic Reanalysis of Twentieth-Century Sea-Level Rise, *Nature* 517, 481–484, <https://doi.org/10.1038/nature14093>, 2015.
- Henry, O., Ablain, M., Meyssignac, B., Cazenave, A., Masters, D., Nerem, S., and Garric, G.: Effect of the Processing Methodology on Satellite Altimetry-Based Global Mean Sea Level Rise over the Jason-1 Operating Period, *J. Geod.*, 88, 351–361, <https://doi.org/10.1007/s00190-013-0687-3>, 2014.
- Horwath, M., Novotny, K., Cazenave, A., Palanisamy, H., Marzeion, B., Paul, F., Döll, P., Cáceres, D., Hogg, A., Shepherd, A., Forsberg, R., Sørensen, L., Barletta, V. R., Andersen, O. B., Rannal, H., Johannessen, J., Nilsen, J. E., Gutknecht, B. D., Merchant, Ch. J., MacIntosh, C. R., and von Schuckmann, K.: ESA Climate Change Initiative (CCI) Sea Level Budget Closure (SLBC_cci) Sea Level Budget Closure Assessment Report D3.1, Version 1.0, 2018.
- Hosoda, S., Ohira, T., and Nakamura, T.: A monthly mean dataset of global oceanic temperature and salinity derived from Argo float observations, *JAMSTEC Rep. Res. Dev.*, 8, 47–59, 2008.
- Huang, Z.: The Role of glacial isostatic adjustment (GIA) process on the determination of present-day sea level rise, Report no 505, Geodetic Science, The Ohio State University, 2013.
- Hurkmans, R. T. W. L., Bamber, J. L., Davis, C. H., Joughin, I. R., Khvorostovsky, K. S., Smith, B. S., and Schoen, N.: Time-evolving mass loss of the Greenland Ice Sheet from satellite altimetry, *The Cryosphere*, 8, 1725–1740, <https://doi.org/10.5194/tc-8-1725-2014>, 2014.
- Huss, M. and Hock, R.: A new model for global glacier change and sea-level rise, *Front Earth Sci.*, 3, 54, <https://doi.org/10.3389/feart.2015.00054>, 2015.
- IMBIE Team (the): Mass balance of the Antarctic ice sheet from 1992 to 2017, *Nature*, 558, 219–222, <https://doi.org/10.1038/s41586-018-0179-y>, 2018.
- IPCC: Climate Change 2013: The Physical Science Basis, Contribution of Working Group I to the Fifth Assessment Report of the Intergovernmental Panel on Climate Change, edited by: Stocker, T. F., Qin, D., Plattner, G.-K., Tignor, M., Allen, S. K., Boschung, J., Nauels, A., Xia, Y., Bex, V., and Midgley, P. M., Cambridge University Press, Cambridge, United Kingdom and New York, NY, USA, 1535 pp., 2013.
- Ishii, M. and Kimoto, M.: Reevaluation of Historical Ocean Heat Content Variations with Time-varying XBT and MBT Depth Bias Corrections, *J. Oceanogr.*, 65, 287–299, <https://doi.org/10.1007/s10872-009-0027-7>, 2009.
- Ishii, M., Fukuda, Y., Hirahara, S., Yasui, S., Suzuki, T., and Sato, K.: Accuracy of Global Upper Ocean Heat Content Estimation Expected from Present Observational Data Sets, *SOLA*, 2017, 13, 163–167, <https://doi.org/10.2151/sola.2017-030>, 2017.
- Ivins, E. R., James, T. S., Wahr, J., Schrama, E. J. O., Landerer, F. W., and Simon, K. M.: Antarctic contribution to sea level rise observed by GRACE with improved GIA correction, *J. Geophys. Res.-Solid Earth*, 118, 3126–3141, <https://doi.org/10.1002/jgrb.50208>, 2013.
- Jacob, T., Wahr, J., Pfeffer, W. T., and Swenson, S.: Recent contributions of glaciers and ice caps to sea level rise, *Nature*, 482, 514–518, <https://doi.org/10.1038/nature10847>, 2012.
- Jensen, L., Rietbroek, R., and Kusche, J.: Land water contribution to sea level from GRACE and Jason-1 measurements, *J. Geophys. Res.-Oceans*, 118, 212–226, <https://doi.org/10.1002/jgrc.20058>, 2013.
- Jevrejeva, S., Grinsted, A., Moore, J. C., and Holgate, S.: Nonlinear trends and multi-year cycle in sea level records, *J. Geophys. Res.*, 111, 2005JC003229, <https://doi.org/10.1029/2005JC003229>, 2006.
- Jevrejeva, S., Moore, J. C., Grinsted, A., Matthews, A. P., and Spada, G.: Trends and Acceleration in Global and Regional

- Sea Levels since 1807, *Global Planet. Change J.C.*, 113, 11–22, <https://doi.org/10.1016/j.gloplacha.2013.12.004>, 2014.
- Johannesson, T., Raymond, C., and Waddington, E.: Time-Scale for Adjustment of Glaciers to Changes in Mass Balance, *J. Glaciol.*, 35, 355–369, 1989.
- Johnson, G. C. and Chambers, D. P.: Ocean bottom pressure seasonal cycles and decadal trends from GRACERelease-05: Ocean circulation implications, *J. Geophys. Res.-Oceans*, 118, 4228–4240, <https://doi.org/10.1002/jgrc.20307>, 2013.
- Johnson, G. C. and Birnbaum, A. N.: As El Niño builds, Pacific Warm Pool expands, ocean gains more heat, *Geophys. Res. Lett.*, 44, 438–445, <https://doi.org/10.1002/2016GL071767>, 2017.
- Kääb, A., Treichler, D., Nuth, C., and Berthier, E.: Brief Communication: Contending estimates of 2003–2008 glacier mass balance over the Pamir-Karakoram-Himalaya, *The Cryosphere*, 9, 557–564, <https://doi.org/10.5194/tc-9-557-2015>, 2015.
- Kaser, G., Cogley, J., Dyurgerov, M., Meier, M., and Ohmura, A.: Mass balance of glaciers and ice caps: Consensus estimates for 1961–2004, *Geophys. Res. Lett.*, 33, L19501, <https://doi.org/10.1029/2006GL027511> 2006.
- Keenan, R. J., Reams, G. A., Achard, F., de Freitas, J. V., Grainger, A., and Lindquist, E.: Dynamics of global forest area: Results from the FAO Global Forest Resources Assessment 2015, *Forest Ecol. Manag.*, 352, 9–20 <https://doi.org/10.1016/j.foreco.2015.06.014>, 2015.
- Kemp, A. C., Horton, B., Donnelly, J. P., Mann, M. E., Vermeer, M., and Rahmstorf, S.: Climate related sea level variations over the past two millennia, *Proc. Natl. Acad. Sci. USA*, 108, 11017–11022, 2011.
- Khan, S. A., Sasgen, I., Bevis, M., Van Dam, T., Bamber, J. L., Wahr, J., Willis, M., Kjær, K. H., Wouters, B., Helm, V., Csatho, B., Fleming, K., Björk, A. A., Aschwanden, A., Knudsen, P., and Munneke, P. K.: Geodetic measurements reveal similarities between post – Last Glacial Maximum and present-day mass loss from the Greenland ice sheet, *Sci. Adv.*, 2, 465–507, <https://doi.org/10.1007/s10712-010-9100-4>, 2016.
- King, M. A., Altamimi, Z., Boehm, J., Bos, M., Dach, R., Elosegui, P., Fund, F., Hernández-Pajares, M., Lavallee, D., Cervera, P. J. M., and Penna, N.: Improved constraints on models of glacial isostatic adjustment: a review of the contribution of ground-based geodetic observations, *Surv. Geophys.*, 31, 465–507, <https://doi.org/10.1007/s10712-010-9100-4>, 2010.
- Konikow, L. F.: Contribution of global groundwater depletion since 1900 to sea-level rise, *Geophys. Res. Lett.*, 38, L17401, <https://doi.org/10.1029/2011GL048604>, 2011.
- Konrad, H., Sasgen, I., Pollard, D., and Klemann, V.: Potential of the solid-Earth response for limiting long-term West Antarctic Ice Sheet retreat in a warming climate, *Earth Planet. Sci. Lett.*, 432, 254–264, 2015.
- Lambeck, K.: Sea-level change from mid-Holocene to recent time: An Australian example with global implications, in: *Ice Sheets, Sea Level and the Dynamic Earth*, edited by: Mitrovica, J. X. and Vermeersen, L. L. A., *Geodynam. Series*, 29, 33–50, 2002.
- Lambeck, K. and Chappell, J.: Sea Level Change Through the Last Glacial Cycle, *Science*, 292, 679–686, <https://doi.org/10.1126/science.1059549>, 2001.
- Lambeck, K., Woodroff, C. D., Antonioli, F., Anzidei, M., Gehrels, W. R., Laborel, J., and Wright, A. J.: Paleoenvironmental records, geophysical modelling and reconstruction of sea level trends and variability on centennial and longer time scales, in: *Understanding sea level rise and variability*, edited by: Church, J. A., Woodworth, P. L., Aarup, T., and Wilson, W. S., Wiley-Blackwell, 2010.
- Leclercq, P., Oerlemans, J., and Cogley, J.: Estimating the glacier contribution to sea-level rise for the period 1800–2005, *Surv. Geophys.*, 32, 519–535, 2011.
- Legeais, J.-F., Ablain, M., Zawadzki, L., Zuo, H., Johannessen, J. A., Scharffenberg, M. G., Fenoglio-Marc, L., Fernandes, M. J., Andersen, O. B., Rudenko, S., Cipollini, P., Quartly, G. D., Passaro, M., Cazenave, A., and Benveniste, J.: An improved and homogeneous altimeter sea level record from the ESA Climate Change Initiative, *Earth Syst. Sci. Data*, 10, 281–301, <https://doi.org/10.5194/essd-10-281-2018>, 2018.
- Le Quéré, C., Andrew, R. M., Friedlingstein, P., Sitch, S., Pongratz, J., Manning, A. C., Korsbakken, J. I., Peters, G. P., Canadell, J. G., Jackson, R. B., Boden, T. A., Tans, P. P., Andrews, O. D., Arora, V. K., Bakker, D. C. E., Barbero, L., Becker, M., Betts, R. A., Bopp, L., Chevallier, F., Chini, L. P., Ciais, P., Cosca, C. E., Cross, J., Currie, K., Gasser, T., Harris, I., Hauck, J., Haverd, V., Houghton, R. A., Hunt, C. W., Hurtt, G., Ilyina, T., Jain, A. K., Kato, E., Kautz, M., Keeling, R. F., Klein Goldewijk, K., Körtzinger, A., Landschützer, P., Lefèvre, N., Lenton, A., Lienert, S., Lima, I., Lombardozi, D., Metzl, N., Millero, F., Monteiro, P. M. S., Munro, D. R., Nabel, J. E. M. S., Nakaoka, S.-I., Nojiri, Y., Padin, X. A., Peregón, A., Pfeil, B., Pierrot, D., Poulter, B., Rehder, G., Reimer, J., Rödenbeck, C., Schwinger, J., Séférian, R., Skjelvan, I., Stocker, B. D., Tian, H., Tilbrook, B., Tubiello, F. N., van der Laan-Luijkx, I. T., van der Werf, G. R., van Heuven, S., Viovy, N., Vuichard, N., Walker, A. P., Watson, A. J., Wiltshire, A. J., Zaehle, S., and Zhu, D.: Global Carbon Budget 2017, *Earth Syst. Sci. Data*, 10, 405–448, <https://doi.org/10.5194/essd-10-405-2018>, 2018.
- Lettenmaier, D. P. and Milly, P. C. D.: Land waters and sea level, *Nat. Geosci.*, 2, 452–454, <https://doi.org/10.1038/ngeo567>, 2009.
- Leuliette, E. W. and Miller, L.: Closing the sea level rise budget with altimetry, Argo, and GRACE, *Geophys. Res. Lett.*, 36, L04608, <https://doi.org/10.1029/2008GL036010>, 2009.
- Leuliette, E. W. and Willis, J. K.: Balancing the sea level budget, *Oceanography*, 24, 122–129, <https://doi.org/10.5670/oceanog.2011.32>, 2011.
- Leuschen, C.: IceBridge Geolocated Radar Echo Strength Profiles, Boulder, Colorado, NASA DAAC at the National Snow and Ice Data Center, <https://doi.org/10.5067/FAZTWP500V70>, last access: 15 June 2014.
- Levitus, S., Antonov, J. I., Boyer, T. P., Baranova, O. K., Garcia, H. E., Locarnini, R. A., Mishonov, A. V., Reagan, J. R., Seidov, D., Yarosh, E. S., and Zweng, M. M.: World ocean heat content and thermosteric sea level change (0–2000 m), 1955–2010, *Geophys. Res. Lett.*, 39, L10603, <https://doi.org/10.1029/2012GL051106>, 2012.
- Llovel, W., Becker, M., Cazenave, A., Crétaux, J. F., and Ramillien, G.: Global land water storage change from GRACE over 2002–2009; Inference on sea level, *C. R. Geosci.*, 342, 179–188, <https://doi.org/10.1016/j.crte.2009.12.004>, 2010.
- Llovel, W., Willis, J. K., Landerer, F. W., and Fukumori, I.: Deep-ocean contribution to sea level and energy budget not de-

- tectable over the past decade, *Nat. Clim. Change* 4, 1031–1035, <https://doi.org/10.1038/nclimate2387>, 2014.
- Lo, M. H. and Famiglietti, J. S.: Irrigation in California’s Central Valley strengthens the southwestern U.S. water cycle, *Geophys. Res. Lett.*, 40, 301–306, <https://doi.org/10.1002/grl.50108>, 2013.
- Loriaux, T. and Casassa, G.: Evolution of glacial lakes from the Northern Patagonia Icefield and terrestrial water storage in a sea-level rise context, *Global Planet. Change*, 102, 33–40, 2013.
- Lovel, T. R. and Belward, A. S.: The IGBP-DIS global 1 km land cover data set, DISCover: first results, *Int. J. Remote Sens.*, 18, 3291–3295, 1997.
- Luthcke, S. B., Zwally, H. J., Abdalati, W., Rowlands, D. D., Ray, R. D., Nerem, R. S., Lemoine, F. G., McCarthy, J. J., and Chinn, D. S.: Recent Greenland Ice Mass Loss by Drainage System from Satellite Gravity Observations, *Science*, 314, 1286–1289, <https://doi.org/10.1126/science.1130776>, 2006.
- Luthcke, S. B., Sabaka, T., Loomis, B., Arendt, A., McCarthy, J., and Camp, J.: Antarctica, Greenland and Gulf of Alaska land-ice evolution from an iterated GRACE global mascon solution, *J. Glaciol.*, 59, 613–631, 2013.
- MacDicken, K. G.: Global Forest Resources Assessment, What, why and how?, *Forest Ecol. Manage.*, 352, 3–8, <https://doi.org/10.1016/j.foreco.2015.02.006>, 2015.
- Martinec, Z. and Hagedoorn, J.: The rotational feedback on linear-momentum balance in glacial isostatic adjustment, *Geophys. J. Int.*, 199, 1823–1846, 2014.
- Martín-Español, A., Zammit-Mangion, A., Clarke, P. J., Flament, T., Helm, V., King, M. A., and Wouters, B.: Spatial and temporal Antarctic Ice Sheet mass trends, glacio-isostatic adjustment, and surface processes from a joint inversion of satellite altimeter, gravity, and GPS data, *J. Geophys. Res.-Earth Surf.*, 121, 182–200, 2016.
- Marzeion, B., Jarosch, A. H., and Hofer, M.: Past and future sea-level change from the surface mass balance of glaciers, *The Cryosphere*, 6, 1295–1322, <https://doi.org/10.5194/tc-6-1295-2012>, 2012.
- Marzeion, B., Cogley, J., Richter, K., and Parkes, D.: Attribution of global glacier mass loss to anthropogenic and natural causes, *Science*, 345, 919–920, 2014.
- Marzeion, B., Champollion, N., Haeberli, W., Langley, K., Leclercq, P., and Paul, F.: Observation-Based Estimates of Global Glacier Mass Change and Its Contribution to Sea-Level Change, *Surv. Geophys.*, 28, 105–130, 2017.
- Marzeion, B., Kaser, G., Maussion, F., and Champollion, N.: Limited influence of climate change mitigation on short-term glacier mass loss, *Nat. Clim. Change*, 8, 305–308, <https://doi.org/10.1038/s41558-018-0093-1>, 2018.
- Masters, D., Nerem, R. S., Choe, C., Leuliette, E., Beckley, B., White, N., and Ablain, M.: Comparison of Global Mean Sea Level Time Series from TOPEX/Poseidon, Jason-1, and Jason-2, *Mar. Geod.*, 35 (sup1), 20–41, <https://doi.org/10.1080/01490419.2012.717862>, 2012.
- Matthews, E. and Fung, I.: Methane emission from natural wetlands: Global distribution, area, and environmental characteristics of sources, *Global Biogeochem. Cy.*, 1, 61–86, 1987.
- Maussion, F., Butenko, A., Eis, J., Fourteau, K., Jarosch, A. H., Landmann, J., Oesterle, F., Recinos, B., Rothenpieler, T., Vlug, A., Wild, C. T., and Marzeion, B.: The Open Global Glacier Model (OGGM) v1.0, *Geosci. Model Dev. Discuss.*, <https://doi.org/https://doi.org/10.5194/gmd-2018-9>, in review, 2018.
- McMillan, M., Shepherd, A., Sundal, A., Briggs, K., Muir, A., Ridout, A., Hogg, A., and Wingham, D.: Increased ice losses from Antarctica detected by Cryosat-2, *Geophys. Res. Lett.*, 41, 3899–3905, 2014.
- Merrifield, M. A., Merrifield, S. T., and Mitchum, G. T.: An anomalous recent acceleration of global sea level rise, *J. Climate*, 22, 5772–5781, <https://doi.org/10.1175/2009JCLI2985.1>, 2009.
- Meyssignac, B., Becker, M., Llovel, W., and Cazenave, A.: An Assessment of Two-Dimensional Past Sea Level Reconstructions Over 1950–2009 Based on Tide-Gauge Data and Different Input Sea Level Grids, *Surv. Geophys.*, 33, 945–972, <https://doi.org/10.1007/s10712-011-9171-x>, 2011.
- Milly, P. C. D., Cazenave, A., and Gennero, M.C.: Contribution of climate-driven change in continental water storage to recent sea-level rise, *Proc. Natl. Acad. Sci. USA*, 100, 13158–13161, 2003.
- Milly, P. C. D., Cazenave, A., Famiglietti, J. S., Gornitz, Vivien, Laval, Katia, Lettenmaier, D. P., Sahagian, D. L., Wahr, J. M., and Wilson, C. R.: Terrestrial water-storage contributions to sea-level rise and variability, in: *Understanding Sea-Level Rise and Variability*, 226–255, 2010.
- Milne, G. A., Gehrels, W. R., Hughes, C. W., and Tamisiea, M. E.: Identifying the causes of sea-level change, *Nat. Geosci.*, 2.7, 471–478, 2009.
- Mitrovica, J. X. and Milne, G. A.: On post-glacial sea level: I. General theory, *Geophys. J. Int.*, 154, 253–267, 2003.
- Mitrovica, J. X. and Wahr, J.: Ice age Earth rotation, *Annu. Rev. Earth Planet. Sci.*, 39, 577–616, 2011.
- Mitrovica, J. X., Wahr, J., Matsuyama, I., and Paulson, A.: The rotational stability of an ice-age earth, *Geophys. J. Int.*, 161.2, 491–506, 2005.
- Mitrovica, J. X., Wahr, J., Matsuyama, I., Paulson, A., and Tamisiea, M. E.: Reanalysis of ancient eclipse, astronomic and geodetic data: A possible route to resolving the enigma of global sea-level rise, *Earth Planet. Sci. Lett.*, 243, 390–399, <https://doi.org/10.1016/j.epsl.2005.12.029>, 2006.
- Mouginot, J., Rignot, E., and Scheuchl, B.: Sustained increase in ice discharge from the Amundsen Sea Embayment, West Antarctica, from 1973 to 2013, *Geophys. Res. Lett.*, 41, 1576–1584, 2014.
- Munk, W.: Twentieth century sea level: An enigma, *Proc. Natl. Acad. Sci. USA*, 99, 6550–6555, <https://doi.org/10.1073/pnas.092704599>, 2002.
- Natarov, S. I., Merrifield, M. A., Becker, J. M., and Thompson, P. R.: Regional influences on reconstructed global mean sea level, *Geophys. Res. Lett.*, 44, 3274–3282, 2017.
- Nerem, R. S., Chambers, D. P., Choe, C., and Mitchum, G. T.: “Estimating Mean Sea Level Change from the TOPEX and Jason Altimeter Missions.”, *Mar. Geod.*, 33 (sup1), 435–446, <https://doi.org/10.1080/01490419.2010.491031>, 2010.
- Nerem, R. S., Beckley, B. D., Fasullo, J., Hamlington, B. D., Masters, D., and Mitchum, G. T.: Climate Change Driven Accelerated Sea Level Rise Detected In The Altimeter Era, *Proc. Natl. Acad. Sci. USA*, 115, 2022–2025, <https://doi.org/10.1073/pnas.1717312115>, 2018.
- Nghiem, S., Hall, D., Mote, T., Tedesco, M., Albert, M., Keegan, K., Shuman, C., Digirolamo, N., and Neumann, G.: The extreme melt across the Greenland ice sheet in 2012, *Geophys. Res. Lett.*, 39, L20502, <https://doi.org/10.1029/2012GL053611>, 2012.

- Nobre, P., Malagutti, M., Urbano, D. F., de Almeida, R. A. F., and Giarolla, E.: Amazon Deforestation and Climate Change in a Coupled Model Simulation, *J. Climate*, 22, 5686–5697, <https://doi.org/10.1175/2009jcli2757.1>, 2009.
- Oki, T. and Kanae, S.: Global hydrological cycles and world water resources, *Science*, 313, 1068–1072, <https://doi.org/10.1126/science.1128845>, 2006.
- Ozyavas, A., Khan, S. D., and Casey, J. F.: A possible connection of Caspian Sea level fluctuations with meteorological factors and seismicity, *Earth Planet. Sci. Lett.*, 299, 150–158, <https://doi.org/10.1016/j.epsl.2010.08.030>, 2010.
- Palanisamy, H., Cazenave, A., Blazquez, A., Döll, P., Caceres, D., and Decharme, B.: Land water storage changes over world river basins from GRACE and global hydrological models, LEGOS internal report, August, 2018.
- Paul, F., Huggel, C., and Kääb, A.: Combining satellite multispectral image data and a digital elevation model for mapping of debris-covered glaciers, *Remote Sens. Environ.*, 89, 510–518, 2004.
- Paulson, A., Zhong, S., and Wahr, J.: Inference of mantle viscosity from GRACE and relative sea level data, *Geophys. J. Int.*, 171, 497–508, <https://doi.org/10.1111/j.1365-246X.2007.03556.x>, 2007.
- Peltier, W. R.: Global glacial isostatic adjustment and modern instrumental records of relative sea level history, in: *Sea-Level Rise: History and Consequences*, edited by: Douglas, B. C., Kearney, M. S., and Leatherman, S. P., Vol. 75, Academic Press, San Diego, 65–95, 2001.
- Peltier, W. R.: Global glacial isostasy and the surface of the ice-age Earth: the ICE-5G (VM2) model and GRACE, *Annu. Rev. Earth Planet. Sci.*, 32, 111–149, 2004.
- Peltier, W. R.: Closure of the budget of global sea level rise over the GRACE era: the importance and magnitudes of the required corrections for global glacial isostatic adjustment, *Quatern. Sci. Rev.*, 28, 1658–1674, 2009.
- Peltier, W. R. and Luthcke, S. B.: On the origins of Earth rotation anomalies: New insights on the basis of both “paleogeodetic” data and Gravity Recovery and Climate Experiment (GRACE) data, *J. Geophys. Res.-Solid Earth*, 114, B11405, <https://doi.org/10.1029/2009JB006352>, 2009.
- Peltier, W. R., Argus, D. F., and Drummond, R.: Space geodesy constrains ice age terminal deglaciation: The global ICE-6G_C (VM5a) model, *J. Geophys. Res.-Solid Earth*, 120, 450–487, 2015.
- Perera, J.: A Sea Turns to Dust, *New Sci.*, 140, 24–27, 1993.
- Pfeffer, W., Arendt, A., Bliss, A., Bolch, T., Cogley, J., Gardner, A., Hagen, J.-O., Hock, R., Kaser, G., Kienholz, C., Miles, E., Moholdt, G., Mölg, N., Paul, F., Radić, V., Rastner, P., Raup, B., Rich, J., and Sharp, M.: The Randolph Glacier Inventory: a globally complete inventory of glaciers, *J. Glaciol.*, 60, 537–552, 2014.
- Plag, H. P. and Juetner, H. U.: Inversion of global tide gauge data for present-day ice load changes, *Memoir. Natl. Inst. Polar Res.*, 54, 301–317, 2001.
- Pokhrel, Y. N., Hanasaki, N., Yeh, P. J. F., Yamada, T., Kanae, S., and Oki, T.: Model estimates of sea level change due to anthropogenic impacts on terrestrial water storage, *Nat. Geosci.*, 5, 389–392, <https://doi.org/10.1038/ngeo1476>, 2012.
- Purcell, A. P., Tregoning, P., and Dehecq, A.: An assessment of the ICE6G_C (VM5a) glacial isostatic adjustment model, *J. Geophys. Res.-Solid Earth* 121, 3939–3950, 2016.
- Purkey, S. and Johnson, G. C.: Warming of global abyssal and deep southern ocean waters between the 1990s and 2000s: Contributions to global heat and sea level rise budget, *J. Climate*, 23, 6336–6351, <https://doi.org/10.1175/2010JCLI3682.1>, 2010.
- Purkey, S. G., Johnson, G. C., and Chambers, D. P.: Relative contributions of ocean mass and deep steric changes to sea level rise between 1993 and 2013, *J. Geophys. Res.-Oceans*, 119, 7509–7522, <https://doi.org/10.1002/2014JC010180>, 2014.
- Radic, V. and Hock, R.: Regional and global volumes of glaciers derived from statistical upscaling of glacier inventory data, *J. Geophys. Res.-Earth Surf.*, 115, F01010, <https://doi.org/10.1029/2009JF001373>, 2010.
- Ray, R. D. and Douglas, C.: Experiments in reconstructing twentieth-century sea levels, *Prog. Oceanogr.* 91, 495–515, 2011.
- Reager, J. T., Thomas, B. F., and Famiglietti, J. S.: River basin flood potential inferred using GRACE gravity observations at several months lead time, *Nat. Geosci.*, 7, 588–592, <https://doi.org/10.1038/ngeo2203>, 2014.
- Reager, J. T., Gardner, A. S., Famiglietti, J. S., Wiese, D. N., Eicker, A., and Lo, M. H.: A decade of sea level rise slowed by climate-driven hydrology, *Science*, 351, 699–703, <https://doi.org/10.1126/science.aad8386>, 2016.
- Rhein, M. A., Rintoul, S. R., Aoki, S., Campos, E., Chambers, D., Feely, R. A., Gulev, S., Johnson, G. C., Josey, S. A., Kostianoy, A., and Mauritzen, C.: Observations: Ocean, in: *Climate Change 2013: The Physical Science Basis. Contribution of Working Group I to the Fifth Assessment Report of the Intergovernmental Panel on Climate Change*, edited by: Stocker, T. F., Qin, D., Plattner, G.-K., Tignor, M., Allen, S. K., Boschung, J., Nauels, A., Xia, Y., Bex, V., and Midgley, P. M., Cambridge University Press, Cambridge, United Kingdom and New York, NY, USA, 2013.
- Richey, A. S., Thomas, B. F., Lo, M. H., Reager, J. T., Famiglietti, J. S., Voss, K., Swenson, S., and Rodell, M.: Quantifying renewable groundwater stress with GRACE, *Water Resour. Res.*, 51, 5217–5238, <https://doi.org/10.1002/2015WR017349>, 2015.
- Rietbroek, R., Brunnabend, S. E., Kusche, J., Schröter, J., and Dahle, C.: Revisiting the contemporary sea-level budget on global and regional scales, *Proc. Natl. Acad. Sci. USA*, 113, 1504–1509, <https://doi.org/10.1073/pnas.1519132113>, 2016.
- Rignot, E. J., Velicogna, I., van den Broeke, M. R., Monaghan, A. J., and Lenaerts, J. T. M.: Acceleration of the contribution of the Greenland and Antarctic ice sheets to sea level rise, *Geophys. Res. Lett.*, 38, L05503, <https://doi.org/10.1029/2011GL046583>, 2011a.
- Rignot, E., Mouginot, J., and Scheuchl, B.: Ice flow of the Antarctic Ice Sheet, *Science*, 333, 1427–1430, <https://doi.org/10.1126/science.1208336>, 2011b.
- Riser, S. C., Freeland, H. J., Roemmich, D., Wijffels, Troisi, S. A., Belbéoch, M., Gilbert, D., Xu, J., Pouliquen, S., Thresher, A., Le Traon, P. Y., Maze, G., Klein, B., M Ravichandran, M., Grant, F., Poulain, P. M., Suga, T., Lim, B., Sterl, A., Sutton, P., Mork, K. A., Vélez-Belchí, P. J., Anson, I., King, B., Turton, J., Baringer, M., and Jayne, S. R.: Fifteen years of ocean observations with the global Argo array, *Nat. Clim. Change*, 6, 145–153, <https://doi.org/10.1038/NCLIMATE2872>, 2016.

- Riva, R. E., Gunter, B. C., Urban, T. J., Vermeersen, B. L., Lindenbergh, R. C., Helsen, M. M., Bamber, J. L., van de Wal, R. S., van den Broeke, M. R. and Schutz, B. E.: Glacial isostatic adjustment over Antarctica from combined ICESat and GRACE satellite data, *Earth Planet. Sci. Lett.*, 288, 516–523, 2009.
- Riva, R. E. M., Bamber, J. L., Lavallée, D. A., and Wouters, B.: Sea-level fingerprint of continental water and ice mass change from GRACE, *Geophys. Res. Lett.*, 37, L19605, <https://doi.org/10.1029/2010GL044770>, 2010.
- Rodell, M., Velicogna, I., and Famiglietti, J. S.: Satellite-based estimates of groundwater depletion in India, *Nature*, 460, 999–1002, <https://doi.org/10.1038/nature08238>, 2009.
- Roemmich, D. and Gilson, J.: The 2004–2008 mean and annual cycle of temperature, salinity, and steric height in the global ocean from the Argo Program, *Prog. Oceanogr.*, 82, 81–100, 2009.
- Roemmich, D. and Gilson, J.: The global ocean imprint of ENSO, *Geophys. Res. Lett.*, 38, L13606, <https://doi.org/10.1029/2011GL047992>, 2011.
- Roemmich, D., Gould, W. J., and Gilson, J.: 135 years of global ocean warming between the Challenger expedition and the Argo Programme, *Nat. Clim. Change*, 2, 425–428, <https://doi.org/10.1038/nclimate1461>, 2012.
- Roemmich, D., Church, J., Gilson, J., Monselesan, D., Sutton, P., and Wijffels, S.: Unabated planetary warming and its ocean structure since 2006, *Nat. Clim. Change*, 5, 240–245, <https://doi.org/10.1038/NCLIMATE2513>, 2015.
- Roemmich, D., Gilson, J., Sutton, P., and Zilberman, N.: Multi-decadal change of the South Pacific gyre circulation, *J. Phys. Oceanography*, 46, 1871–1883, <https://doi.org/10.1175/jpo-d-15-0237.1>, 2016.
- Sahagian, D.: Global physical effects of anthropogenic hydrological alterations: sea level and water redistribution, *Global Planet. Change*, 25, 39–48, [https://doi.org/10.1016/S0921-8181\(00\)00020-5](https://doi.org/10.1016/S0921-8181(00)00020-5), 2000.
- Sahagian, D. L., Schwartz, F. W., and D. K. Jacobs, D. K.: Direct anthropogenic contributions to sea level rise in the twentieth century, *Nature*, 367, 54–57, <https://doi.org/10.1038/367054a0>, 1994.
- Sasgen, I., Van Den Broeke, M., Bamber, J. L., Rignot, E., Sørensen, L. S., Wouters, B., Martinec, Z., Velicogna, I., and Simonsen, S. B.: Timing and origin of recent regional ice-mass loss in Greenland, *Earth Planet. Sci. Lett.*, 333, 293–303, 2012.
- Sasgen, I., Konrad, H., Ivins, E. R., Van den Broeke, M. R., Bamber, J. L., Martinec, Z., and Klemann, V.: Antarctic ice-mass balance 2003 to 2012: regional reanalysis of GRACE satellite gravimetry measurements with improved estimate of glacial-isostatic adjustment based on GPS uplift rates, *The Cryosphere*, 7, 1499–1512, <https://doi.org/10.5194/tc-7-1499-2013>, 2013.
- Sasgen, I., Martín-Español, A., Horvath, A., Klemann, V., Petrie, E. J., Wouters, B., and Konrad, H.: Joint inversion estimate of regional glacial isostatic adjustment in Antarctica considering a lateral varying Earth structure (ESA STSE Project REGINA), *Geophys. J. Int.*, 211, 1534–1553, 2017.
- Scanlon, B. R., Jolly, I., Sophocleous, M., and Zhang, L.: Global impacts of conversions from natural to agricultural ecosystems on water resources: Quantity versus quality, *Water Resour. Res.*, 43, W03437, <https://doi.org/10.1029/2006WR005486> 2007.
- Scanlon, B. R., Zhang, Z., Save, H., Sun, A. Y., Schmied, H. M., van Beek, L. P., and Longuevergne, L.: Global models underestimate large decadal declining and rising water storage trends relative to GRACE satellite data, *Proc. Natl. Acad. Sci. USA*, <https://doi.org/10.1073/pnas.1704665115>, 2018.
- Schellekens, J., Dutra, E., Martínez-de la Torre, A., Balsamo, G., van Dijk, A., Sperna Weiland, F., Minvielle, M., Calvet, J.-C., Decharme, B., Eisner, S., Fink, G., Flörke, M., Peßenteiner, S., van Beek, R., Polcher, J., Beck, H., Orth, R., Calton, B., Burke, S., Dorigo, W., and Weedon, G. P.: A global water resources ensemble of hydrological models: the earth2Observe Tier-1 dataset, *Earth Syst. Sci. Data*, 9, 389–413, <https://doi.org/10.5194/essd-9-389-2017>, 2017.
- Schrama, E. J., Wouters, B., and Rietbroek, R.: A mascon approach to assess ice sheet and glacier mass balances and their uncertainties from GRACE data, *J. Geophys. Res.-Solid Earth*, 119, 6048–6066, 2014.
- Schwatke, C., Dettmering, D., Bosch, W., and Seitz, F.: DAHITI – an innovative approach for estimating water level time series over inland waters using multi-mission satellite altimetry, *Hydrol. Earth Syst. Sci.*, 19, 4345–4364, <https://doi.org/10.5194/hess-19-4345-2015>, 2015.
- Shamsudduha, M., Taylor, R. G., and Longuevergne, L.: Monitoring groundwater storage changes in the highly seasonal humid tropics: Validation of GRACE measurements in the Bengal Basin, *Water Resour. Res.*, 48, W02508, <https://doi.org/10.1029/2011WR010993>, 2012.
- Shepherd, A., Ivins, E. R., A. G., Barletta, V. R., Bentley, M. J., Bettadpur, S., Briggs, K. H., Bromwich, D. H., Forsberg, R., Galin, N., Horvath, M., Jacob, S., Joughin, I., King, M. A., Lenaerts, J. T. M., Li, J., Ligtenberg, S. R. M., Luckman, A., Luthcke, S. B., McMillan, M., Meister, R., Milne, G., Mouginot, J., Muir, A., Nicolas, J. P., Paden, J., Payne, A. J., Pritchard, H., Rignot, E., Rott, H., Sandberg Sørensen, L., Scambos, T. A., Scheuchl, B., Schrama, E. J. O., Smith, B., Sundal, A. V., van Angelen, J. H., van de Berg, W. J., van den Broeke, M. R., Vaughan, D. G., Velicogna, I., Wahr, J., Whitehouse, P. L., Wingham, D. J., Yi, D., Young, D., Zwally, H. J.: A reconciled estimate of ice-sheet mass balance, *Science*, 338, 1183–1189, <https://doi.org/10.1126/science.1228102>, 2012.
- Shukla, J., Nobre, C., and Sellers, P.: Amazon Deforestation and Climate Change, *Science*, 247, 1322–1325, <https://doi.org/10.1126/science.247.4948.1322>, 1990.
- Slangen, A. B. A., Meyssignac, B., Agosta, C., Champollion, N., Church, J. A., Fettweis, X., Ligtenberg, S. R. M., Marzeion, B., Melet, A., Palmer, M. D., Richter, K., Roberts, C. D., and Spada, G.: Evaluating model simulations of 20th century sea-level rise. Part 1: global mean sea-level change, *J. Climate*, 30, 8539–8563, <https://doi.org/10.1175/jcli-d-17-0110.1>, 2017.
- Sloan, S. and Sayer, J. A.: Forest Resources Assessment of 2015 shows positive global trends but forest loss and degradation persist in poor tropical countries, *Forest Ecol. Manage.*, 352, 134–145, <https://doi.org/10.1016/j.foreco.2015.06.013>, 2015.
- Solomon, S., Qin, D., Manning, M., Averyt, K., and Marquis, M. (Eds.): *Climate Change 2007: The Physical Science Basis. Contribution of Working Group I to the Fourth Assessment Report of the Intergovernmental Panel on Climate Change*, Cambridge Univ. Press, Cambridge, UK, 2007.
- Spada, G.: Glacial isostatic adjustment and contemporary sea level rise: An overview, *Surv. Geophys.*, 38, 153–185, 2017.

- Spada, G. and Galassi, G.: New estimates of secular sea level rise from tide gauge data and GIA modelling, *Geophys. J. Int.*, 191, 1067–1094, 2012.
- Spada, G. and Galassi, G.: Spectral analysis of sea level during the altimetry era, and evidence for GIA and glacial melting fingerprints, *Global Planet. Change*, 143, 34–49, 2016.
- Spada, G. and Stocchi, P.: SELEN: A Fortran 90 program for solving the “sea-level equation”, *Comput. Geosci.*, 33.4, 538–562, 2007.
- Spracklen, D. V., Arnold, S. R., and Taylor, C. M.: Observations of increased tropical rainfall preceded by air passage over forests, *Nature*, 489, 282–U127, <https://doi.org/10.1038/nature11390>, 2012.
- Stammer, D. and Cazenave, A.: *Satellite Altimetry Over Oceans and Land Surfaces*, 617 pp., CRC Press, Taylor and Francis Group, Boca Raton, New York, London, ISBN:13:978-1-4987-4345-7, 2018.
- Strassberg, G., Scanlon, B. R., and Rodell, M.: Comparison of seasonal terrestrial water storage variations from GRACE with groundwater-level measurements from the High Plains Aquifer (USA), *Geophys. Res. Lett.*, 34, L14402, <https://doi.org/10.1029/2007GL030139>, 2007.
- Sutterley, T. C., Velicogna, I., Csatho, B., van den Broeke, M., Rezan-Behbahani, S., and Babonis, G.: Evaluating Greenland glacial isostatic adjustment corrections using GRACE, altimetry and surface mass balance data, *Environ. Res. Lett.*, 9, 014004, <https://doi.org/10.1088/1748-9326/9/1/014004>, 2014.
- Swenson, S., Chambers, D., and Wahr, J.: Estimating geocenter variations from a combination of GRACE and ocean model output, *J. Geophys. Res.*, 113, B08410, <https://doi.org/10.1029/2007JB005338>, 2008.
- Tamisiea, M. E.: Ongoing glacial isostatic contributions to observations of sea level change, *Geophys. J. Int.*, 186, 1036–1044, 2011.
- Tamisiea, M. E., Leuliette, E. W., Davis, J. L., and Mitrovica, J. X.: Constraining hydrological and cryospheric mass flux in southeastern Alaska using space-based gravity measurements, *Geophys. Res. Lett.*, 32, L20501, <https://doi.org/10.1029/2005GL023961>, 2005.
- Tapley, B. D., Bettadpur, S., Ries, J. C., Thompson, P. F., and Watkins, M. M. L.: GRACE measurements of mass variability in the Earth system, *Science*, 305, 503–505, <https://doi.org/10.1126/science.1099192>, 2004a.
- Tapley, B. D., Bettadpur, S., Ries, J. C., Thompson, P. F., and Watkins, M. M. L.: The Gravity Recovery and Climate Experiment: Mission Overview and Early Results, *Geophys. Res. Lett.*, 31, L09607, <https://doi.org/10.1029/2004GL019920>, 2004b.
- Taylor, R. G., Scanlon, B., Döll, P., Rodell, M., van Beek, R., Wada, Y., Longuevergne, L., LeBlond, M., Famiglietti, J. S., Edmunds, M., Konikow, L., Green, T. R., Chen, J., Taniguchi, M., Bierkens, M. F. P., MacDonald, A., Fan, Y., Maxwell, R. M., Yechieli, Y., Gurdak, J. J., Allen, D. M., Shamsuduha, M., Hiscock, K., Yeh, P. J. F., Holman, I., and Treidel, H.: Groundwater and climate change, *Nat. Clim. Change*, 3, 322–329, <https://doi.org/10.1038/nclimate1744>, 2013.
- Thompson, P. R. and Merrifield, M. A.: A unique asymmetry in the pattern of recent sea level change, *Geophys. Res. Lett.*, 41, 7675–7683, 2014.
- Tiwari, V. M., Wahr, J., and Swenson, S.: Dwindling groundwater resources in northern India, from satellite gravity observations, *Geophys. Res. Lett.*, 36, L18401, <https://doi.org/10.1029/2009GL039401>, 2009.
- Turcotte, D. L. and Schubert, G.: *Geodynamics*. Cambridge University Press, Cambridge, 2014, Mar. Geode., 35 (sup1), 42–60, <https://doi.org/10.1080/01490419.2012.718226>, 2012.
- Valladeau, G., Legeais, J. F., Ablain, M., Guinehut, S., and Picot, N.: Comparing Altimetry with Tide Gauges and Argo Profiling Floats for Data Quality Assessment and Mean Sea Level Studies, *Mar. Geodesy.*, 35, 42–60, <https://doi.org/10.1080/01490419.2012.718226>, 2012.
- van den Broeke, M. R., Enderlin, E. M., Howat, I. M., Kuipers Munneke, P., Noël, B. P. Y., van de Berg, W. J., van Meijgaard, E., and Wouters, B.: On the recent contribution of the Greenland ice sheet to sea level change, *The Cryosphere*, 10, 1933–1946, <https://doi.org/10.5194/tc-10-1933-2016>, 2016.
- van Wessem, J. M., van de Berg, W. J., Noël, B. P. Y., van Meijgaard, E., Amory, C., Birnbaum, G., Jakobs, C. L., Krüger, K., Lenaerts, J. T. M., Lhermitte, S., Ligtenberg, S. R. M., Medley, B., Reijmer, C. H., van Tricht, K., Trusel, L. D., van Uffrt, L. H., Wouters, B., Wuite, J., and van den Broeke, M. R.: Modelling the climate and surface mass balance of polar ice sheets using RACMO2 – Part 2: Antarctica (1979–2016), *The Cryosphere*, 12, 1479–1498, <https://doi.org/10.5194/tc-12-1479-2018>, 2018.
- Velicogna, I.: Increasing rates of ice mass loss from the Greenland and Antarctic ice sheets revealed by GRACE, *Geophys. Res. Lett.*, 36, L19503, <https://doi.org/10.1029/2009GL040222>, 2009.
- Velicogna, I. and Wahr, J.: Measurements of Time-Varying Gravity Show Mass Loss in Antarctica, *Science*, 311, 1754–1756, <https://doi.org/10.1126/science.1123785>, 2006.
- Velicogna, I., Sutterley, T. C., and Van Den Broeke, M. R.: Regional acceleration in ice mass loss from Greenland and Antarctica using GRACE time-variable gravity data, *Geophys. Res. Lett.*, 41, 8130–8137, 2014.
- von Schuckmann, K., Palmer, M. D., Trenberth, K. E., Cazenave, A., Chambers, D., Champollion, N., Hansen, J., Josey, S. A., Loeb, N., Mathieu, P. P., Meyssignac, B., and Wild, M.: Earth’s energy imbalance: an imperative for monitoring, *Nat. Clim. Change*, 26, 138–144, <https://doi.org/10.1038/NCLIMATE2876>, 2016.
- Vörösmarty, C. J. and Sahagian, D.: Anthropogenic disturbance of the terrestrial water cycle, *Biosci.*, 50, 753–765, [https://doi.org/10.1641/0006-3568\(2000\)050\[0753:Adottw\]2.0.Co;2](https://doi.org/10.1641/0006-3568(2000)050[0753:Adottw]2.0.Co;2), 2000.
- Voss, K. A., Famiglietti, J. S., Lo, M., de Linage, C., Rodell, M., and Swenson, S. C.: Groundwater depletion in the Middle East from GRACE with implications for transboundary water management in the Tigris-Euphrates-Western Iran region, *Water Resour. Res.*, 49, 904–914, <https://doi.org/10.1002/wrcr.20078>, 2013.
- Wada, Y., Reager, J. T., Chao, B. F., Wang, J., Lo, M. H., Song, C., and Gardner, A. S.: Modelling groundwater depletion at regional and global scales: Present state and future prospects, *Surv. Geophys.*, 37, 419–451, <https://doi.org/10.1007/s10712-015-9347-x>, Special Issue: ISSI Workshop on Remote Sensing and Water Resources, 2017.
- Wada, Y., van Beek, L. P. H., and Bierkens, M. F. P.: Nonsustainable groundwater sustaining irrigation: A global assessment, *Water Resour. Res.*, 48, W00L06,

- <https://doi.org/10.1029/2011WR010562>, Special Issue: Toward Sustainable Groundwater in Agriculture, 2012a.
- Wada, Y., van Beek, L. P. H., Sperna Weiland, F. C., Chao, B. F., Wu, Y. H., and Bierkens, M. F. P.: Past and future contribution of global groundwater depletion to sea-level rise, *Geophys. Res. Lett.*, 39, L09402, <https://doi.org/10.1029/2012GL051230>, 2012b.
- Wada, Y., Lo, M. H., Yeh, P. J. F., Reager, J. T., Famiglietti, J. S., Wu, R. J., and Tseng, Y. H.: Fate of water pumped from underground causing sea level rise, *Nat. Clim. Change*, 6, 777–780, <https://doi.org/10.1038/nclimate3001>, 2016.
- Wahr, J., Nerem, R. S., and Bettadpur, S. V.: The pole tide and its effect on GRACE time-variable gravity measurements: Implications for estimates of surface mass variations, *J. Geophys. Res.-Solid Earth*, 120, 4597–4615, 2015.
- Wang, J., Sheng, Y., Hinkel, K. M., and Lyons, E. A.: Drained thaw lake basin recovery on the western Arctic Coastal Plain of Alaska using high-resolution digital elevation models and remote sensing imagery, *Remote Sens. Environ.*, 119, 325–336, <https://doi.org/10.1016/j.rse.2011.10.027>, 2012.
- Watkins, M. M., Wiese, D. N., Yuan, D.-N., Boening, C., and Landerer, F. W.: Improved methods for observing Earth's time variable mass distribution with GRACE using spherical cap mascons, *J. Geophys. Res.-Solid Earth*, 120, 2648–2671, <https://doi.org/10.1002/2014JB011547>, 2015.
- Watson, C. S., White, N. J., Church, J. A., King, M. A., Burgette, R. J., and Legresy, B.: Unabated Global Mean Sea-Level Rise over the Satellite Altimeter Era, *Nat. Clim. Change*, 5, 565–568, <https://doi.org/10.1038/nclimate2635>, 2015.
- Wenzel, M. and Schroter, J.: Reconstruction of regional mean sea level anomalies from tide gauges using neural networks, *J. Geophys. Res.*, 115, C08013, <https://doi.org/10.1029/2009JC005630>, 2010.
- Whitehouse, P. L., Bentley, M. J., Milne, G. A., King, M. A., and Thomas, I. D.: A new glacial isostatic adjustment model for Antarctica: calibrating the deglacial model using observations of relative sea-level and present-day uplift rates, *Geophys. J. Int.*, 190, 1464–1482, 2012.
- Wiese, D. N., Landerer, F. W., and Watkins, M. M.: Quantifying and reducing leakage errors in the JPL RL05M GRACE mascon solution, *Water Resour. Res.*, 52, 7490–7502, <https://doi.org/10.1002/2016WR019344>, 2016a.
- Wiese, D., Yuan, D., Boening, C., Landerer, F., and Watkins, M.: JPL GRACE Mascon Ocean, Ice, and Hydrology Equivalent Water Height RL05M. 1 CRI Filtered, Ver. 2, PO. DAAC, CA, USA. Dataset provided by Wiese in Nov/Dec 2017, 2016b.
- Wijffels, S. E., Roemmich, D., Monselesan, D., Church, J., and Gilson, J.: Ocean temperatures chronicle the ongoing warming of Earth, *Nat. Clim. Change*, 6, 116–118, <https://doi.org/10.1038/nclimate2924>, 2016.
- Willis, J. K., Chambers, D. T., and Nerem, R. S.: Assessing the globally averaged sea level budget on seasonal to interannual time scales, *J. Geophys. Res.*, 113, C06015, <https://doi.org/10.1029/2007JC004517>, 2008.
- Wöppelmann, G. and Marcos, M.: Vertical land motion as a key to understanding sea level change and variability, *Rev. Geophys.*, 54, 64–92, <https://doi.org/10.1002/2015RG000502>, 2016.
- Wouters, B., Chambers, D., and Schrama, E.: GRACE observes small-scale mass loss in Greenland, *Geophys. Res. Lett.*, 35, L20501, <https://doi.org/10.1029/2008GL034816>, 2008.
- Wouters, B., Bamber, J. Á., Van den Broeke, M. R., Lenaerts, J. T. M., and Sasgen, I.: Limits in detecting acceleration of ice sheet mass loss due to climate variability, *Nat. Geosci.*, 6, 613–616, 2013.
- Wu, X., Heflin, M. B., Schotman, H., Vermeersen, B. L., Dong, D., Gross, R. S., Ivins, E. I., Moore, A. W., and Owen, S.: Simultaneous estimation of global present-day water transport and glacial isostatic adjustment, *Nat. Geosci.*, 39, 642–646, 2010.
- Yi, S., Sun, W., Heki, K., and Qian, A.: An increase in the rate of global mean sea level rise since 2010, *Geophys. Res. Lett.*, 42, 3998–4006, <https://doi.org/10.1002/2015GL063902>, 2015.
- Zawadzki, L. and Ablain, M.: Estimating a drift in TOPEX-A Global Mean Sea Level using Poseidon-1 measurements, paper presented at the OSTST meeting, October 2016, La Rochelle, 2016.
- Zemp, M., Frey, H., Gärtner-Roer, I., Nussbaumer, S., Hoelzle, M., Paul, F., Haeblerli, W., Denzinger, F., Ahlström, A., Anderson, B., Bajracharya, S., Baroni, C., Braun, L., Cáceres, B., Casassa, G., Cobos, G., Dávila, L., Delgado Granados, H., Demuth, M., Espizua, L., Fischer, A., Fujita, K., Gadek, B., Ghazanfar, A., Hagen, J., Holmlund, P., Karimi, N., Li, Z., Pelto, M., Pitte, P., Popovnin, V., Portocarrero, C., Prinz, R., Sangewar, C., SeverSKIY, I., Sigurdsson, O., Soruco, A., Usabaliyev, R., and Vincent, C.: Historically unprecedented global glacier decline in the early 21st century, *J. Glaciol.*, 61, 745–762, 2015.
- Zwally, J. H., Li, J., Robbins, J. W., Saba, J. L., Yi, D. H., and Brenner, A. C.: Mass gains of the Antarctic ice sheet exceed losses, *J. Glaciol.*, 61, 1013–1036, <https://doi.org/10.3189/2015JoG15J071>, 2016.

Team list. Anny Cazenave (LEGOS, France, and ISSI, Switzerland), Benoit Meyssignac (LEGOS, France), Michael Ablain (CLS, France), Magdalena Balmaseda (ECMWF, UK), Jonathan Bamber (U. Bristol, UK), Valentina Barletta (DTU-SPACE, Denmark), Brian Beckley (SGT Inc./NASA GSFC, USA), Jérôme Benveniste (ESA/ESRIN, Italy), Etienne Berthier (LEGOS, France), Alejandro Blazquez (LEGOS, France), Tim Boyer (NOAA, USA), Denise Caceres (Goethe U., Germany), Don Chambers (U. South Florida, USA), Nicolas Champollion (U. Bremen, Germany), Ben Chao (IES-AS, Taiwan), Jianli Chen (U. Texas, USA), Lijing Cheng (IAP-CAS, China), John A. Church (U. New South Wales, Australia), Stephen Chuter (U. Bristol, UK), J. Graham Cogley (Trent U., Canada), Soenke Dangendorf (U. Siegen, Germany), Damien Desbryères (IFREMER, France), Petra Döll (Goethe U., Germany), Catia Domingues (CSIRO, Australia), Ulrike Falk (U. Bremen, Germany), James Famiglietti (JPL/Caltech, USA), Luciana Fenoglio-Marc (U. Bonn, Germany), Rene Forsberg (DTU-SPACE, Denmark), Gaia Galassi (U. Urbino, Italy), Alex Gardner (JPL/Caltech, USA), Andreas Groh (TU-Dresden, Germany), Benjamin Hamlington (Old Dominion U., USA), Anna Hogg (U. Leeds, UK), Martin Horwath (TU-Dresden, Germany), Vincent Humphrey (ETHZ, Switzerland), Laurent Husson (U. Grenoble, France), Masayoshi Ishii (MRI-JMA, Japan), Adrian Jaeggi (U. Bern, Switzerland), Svetlana Jevrejeva (NOC, UK), Gregory Johnson (NOAA/PMEL, USA), Nicolas Kolodziejczyk (LOPS, France), Jür-

gen Kusche (U. Bonn, Germany), Kurt Lambeck (ANU, Australia, and ISSI, Switzerland), Felix Landerer (JPL/Caltech, USA), Paul Leclercq (UIO, Norway), Benoit Legresy (CSIRO, Australia), Eric Leuliette (NOAA, USA), William Llovel (LEGOS, France), Laurent Longueuevigne (U. Rennes, France), Bryant D. Loomis (NASA GSFC, USA), Scott B. Luthcke (NASA GSFC, USA), Marta Marcos (UIB, Spain), Ben Marzeion (U. Bremen, Germany), Chris Merchant (U. Reading, UK), Mark Merrifield (UCSD, USA), Glenn Milne (U. Ottawa, Canada), Gary Mitchum (U. South Florida, USA), Yara Mohajerani (UCI, USA), Maeva Monier (Mercator-Ocean, France), Didier Monselesan (CSIRO, Australia), Steve Nerem (U. Colorado, USA), Hindumathi Palanisamy (LEGOS, France), Frank Paul (UZH, Switzerland), Begoña Perez (Puerros del Estados, Spain), Christopher G. Piecuch (WHOI, USA), Rui M. Ponte (AER inc., USA), Sarah G. Purkey (SIO/UCSD, USA), John T. Reager (JPL/Caltech, USA), Roelof Rietbroek (U. Bonn, Germany), Eric Rignot (UCI and JPL, USA), Riccardo Riva (TU Delft, The Netherlands), Dean H. Roemmich (SIO/UCSD USA), Louise Sandberg Sørensen (DTU-SPACE, Denmark), Ingo Sasgen (AWI, Germany), E.J.O. Schrama (TU Delft, The Netherlands), Sonia I. Seneviratne (ETHZ, Switzerland), C.K. Shum (Ohio State U., USA), Giorgio Spada (U. Urbino, Italy), Detlef Stammer (U. Hamburg, Germany), Roderic van de Wal (U. Utrecht, The Netherlands), Isabella Velicogna (UCI and JPL, USA), Karina von Schuckmann (Mercator-Océan, France), Yoshihide Wada (U. Utrecht, The Netherlands), Yiguo Wang (NERSC/BCCR, Norway), Christopher Watson (U. Tasmania, Australia), David Wiese (JPL/Caltech, USA), Susan Wijffels (CSIRO, Australia), Richard Westaway (U. Bristol, UK), Guy Woppelmann (U. La Rochelle, France), Bert Wouters (U. Utrecht, The Netherlands).